The effect of complex feed on Bioelectrochemical systems (BESs) performance

Thesis submitted to Newcastle University for the degree of Doctor of Philosophy

Author: Fei Zhao

Supervisor: Professor Tom Curtis

Co-Supervisor: Dr Jan Dolfing

Co-Supervisor: Dr Elizabeth Heidrich

Date: Jan 2018

Abstract

Bioelectrochemical systems (BESs) are being widely proposed as an energy neutral or even positive alternatives to current aerobic wastewater treatment technologies. However, to achieve this goal their electrogenic performance will need to be substantially improved. In particular, the disparity of the performance of acetate-fed BESs and complex wastes-fed BESs needs to be understood.

In order to obtain rationale of the strategy of this improvement, this study sought to investigate the complex composition of wastewater in BESs by peeling off this effect into two major parts: the effect of the complex pathway in electron donor and the effect of the presence of alternative electron acceptor. In particular, glucose and sulphate was used as the model of complex electron donor and alternative electron acceptor respectively. In addition, this study investigated the effect of anode potential/carbon:sulphate (C:S) ratio on the major electrogenic pathways of these two components in BESs.

This study found that the observed low current production and low coulombic efficiency of glucose-fed BESs was attributed to the low acetate availability (<6.24mM acetate) and the electron loss in the degradation pathway of glucose, formate and ethanol. In addition, the low abundance of the electrogenic microorganism *Geobacteraceae* was also associated with the low current production in the glucose-fed BESs. Increasing of anode potential improved the abundance of the electrogenic microorganism *Geobacteraceae* in the glucose-fed BESs but did not improve the acetate availability.

The low current production in the BESs in the presence of sulphate was also attributed to the low abundance of the electrogenic microorganism *Geobacteraceae*. This was attributed to the toxicity of the by-products of sulphate presumably sulphide. The BESs reactors with a higher acetate concentration in their feed had a higher tolerance to this toxicity and were able to support a higher *Geobacteraceae* population. On the other hand, lower coulombic efficiency in the BESs in the presence of sulphate was largely attributed to the electron accumulation in the anodic sulphur deposit. Moreover, the negative impact of sulphate on the electrogenic performance in BESs was generally lower than the negative impact of complex organics such as glucose, sucrose and starch. Increasing anode potential increased the coulombic efficiency in the BESs in presence of sulphate in

the short term, however this was caused by higher acetate consumption rather than lower sulphate reduction.

In summary, this study provides detailed information of the effect of the complex components on the electrogenic performance of BESs and effect of anode potential/C:S ratio on the major electrogenic pathways of these complex components in BESs. This can be used to adjust anode potential in BESs to optimize the electrogenic performance based on the type of influent and to determine the role of BESs in wastewater treatment in terms of energy and valuable products recovery based on the upstream effluent.

Acknowledgement

To participate in science research and to learn the objective reality of this world by my own hands have always been my dream since I was a child. It is a great fortune to actually have the chance to endeavour this PhD research in Newcastle University in the last four years.

I want to thank my supervisor Tom Curtis for offering this great chance to let me make my dream come true and giving me great support for my PhD with his incredible passion, optimism and scope. I also want to thank Jan Dolfing for giving me great support on the scientific details and logic of my research with his fabulous intelligence, discernment and patience. I also want to thank Elizabeth Heidrich for giving me great support especially on the proposal build up and lab practise with her marvellous thoughts and practise skills.

I want to thank all the technician stuffs for offering me great help in the lab. I want to particularly thank Dave Race for his instruction and help on lab details. I also want to thank Sarah Smith for offering my help on molecular lab practises. I also want to thank research stuffs for their kind help and guide in the lab. I want to particularly thank Stephen Edwards for the great help on the reactor set up at my PhD early stage and Matt Brown for wastewater samplings.

I want to thanks all my friends and colleagues (long list of names). To do PhD research thousands miles away from home was tough. My friends and colleagues gave me strong support in and off the works to make me feel warm. I will always miss those sparkling time working with my friends and colleagues in the lab and office days and nights. Especially the ‘2:00pm lunch club’ and ‘Spanish time dinner’ before and after the exhausting lab work!

I want to especially thank to my parents for financially support me for my PhD without hesitation to let me pursue my dream as always. They are always my strongest support in this world!

And last but not least, I want to thank my dear love for the company during the thesis correction and the company in our fantastic future!

Table of Contents

List of figures

List of tables

Chapter 1 Introduction

1.1. Literature review

Current wastewater treatment is energy costly (~ 0.914KJ/L for urban wastewater treatment) (Smith and Liu, 2017). However, wastewater contains high enough internal chemical energy (~7.6KJ/L in domestic wastewater) to compensate this cost or even recover extra energy for other commercial utilizations (Heidrich et al., 2011). Therefore, energy recovery-wastewater treatment technology is needed. Bioelectrochemical systems (BESs) have received much attention in the last decade due to the potential ability to revolutionize wastewater treatment by recovering the energy from waste (Li et al., 2013; Rozendal et al., 2008). A normal BES contains two electrodes, where one side is connected by an external circuit, and the other side is connected to electrolyte (Verstraete and Rabaey, 2006). The working mechanism of BESs is as follows: electrogenic microorganisms are deployed on anode to capture the electrons from the electron donors such as organic and inorganic wastes, then electrons are transferred by electrogenic microorganisms via anode to cathode. This process is powered by the difference of the redox potential between anodic oxidation and cathodic reduction, and the anions and the cations from each side are exchanged via electrolyte in order to accomplish desired redox reaction for either energy generation or creation of a product of value (Figure 1-1).

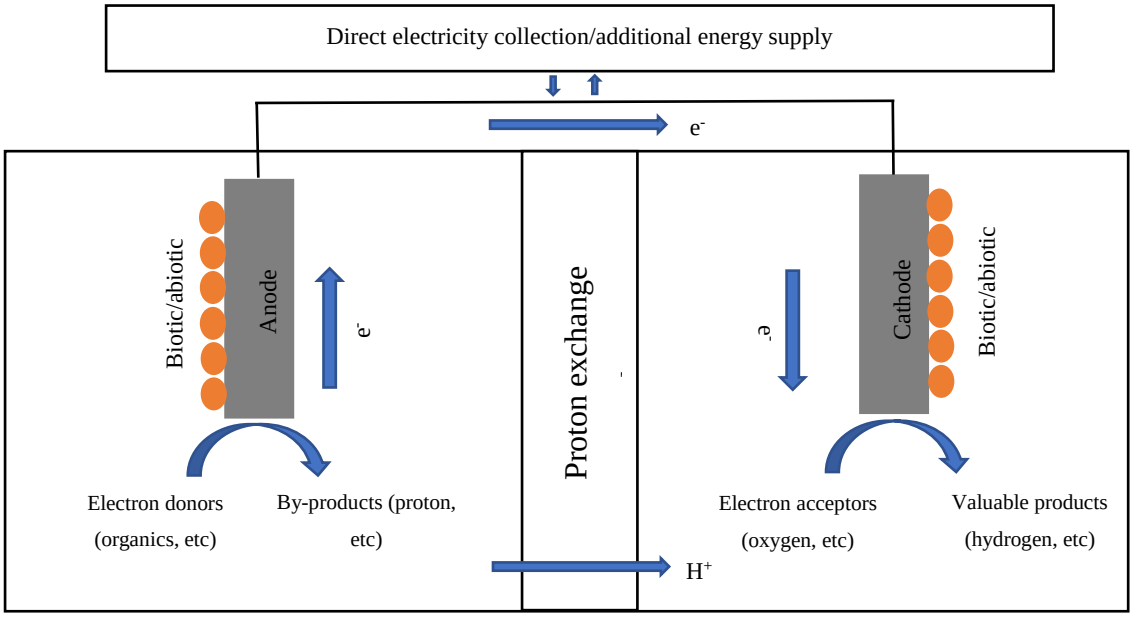

Figure 1-1 The configuration and the working mechanism of a typical bioelectrochemical system (BES).

Redox reactions are some of the most important reactions in conventional wastewater treatment because virtually all wastes are degraded by the combination of oxidation and reduction reaction. One distinguishing feature of BES in wastewater treatment application is the physical separation of oxidizing and reducing half reaction. This allows BESs to undertake redox reaction in two different environments. For instance, microbial fuel cells (MFCs), as pioneering BESs, oxidize waste at anaerobic anode and transfer electrons via external circuit to aerobic cathode to facilitate the reduction of oxygen (Logan et al., 2006). This can therefore result anaerobic oxidation by aerobic driving force because the terminal electron acceptor of anaerobic oxidation is oxygen in such condition. Moreover, the energy generated from redox reaction can be largely facilitated by anaerobic microorganisms. Consequently, the energy that is normally wasted in the aerobic microbial redox reaction in wastewater treatment can be recovered as electricity by MFCs. In addition, the cost of aeration and excessive sludge generation are avoided. The subsequent development of biocathodes to replace expensive chemical catalysts at the cathode has improved the prospects for more sustainable wastewater treatment and energy recovery using MFCs (Milner et al., 2016).

Moreover, the separation of two halves of a redox reaction can also make the overall microbial redox reactions in BESs amenable to generate desired products. For instance, microbial electrolysis cells (MECs) can accomplish microbial anodic oxidation and abiotic cathodic hydrogen production with small energy supply (>0.2V when acetate oxidation is anodic reaction). The supplied energy is theoretically much lower than water electrolysis hydrogen generation, which was about ~1.8V under standard conditions. Moreover, MECs can produce 4 times more hydrogen production from glucose ($molH_2$/mol of glucose) than microbial dark fermentation (Lee and Rittmann, 2010).

Other valuable products can also be produced by cathodic microbial electrosynthesis in BESs (Rabaey and Rozendal, 2010a). Instead of using anodic microbial driving oxidation, these microbial electrosynthesis technologies can provide electron donor via water electrolysis by renewable energy (for example: solar). This design not only encourages more diverse and sustainable reducing reactions at cathode, but also redirects the cathodic intracellular electron pathways towards more desirable cathodic products. In which case, BESs provide exciting opportunity for the regulation of electron transfer routes in conventional anaerobic reactions by so called “electro-fermentation” (Moscoviz et al.,

2016). The migration of ion is an indispensable aspect of BESs whenever redox reactions occur. This ion migration in BESs can be harnessed to separate or direct anions and cations to achieve particular purposes such as seawater desalination in microbial desalination cells (MDCs) or ammonia removal in MFCs (Cao et al., 2009; Jung et al., 2008).

Electrogenic redox reaction is important to wastewater-fed BESs since this reaction directly relates to both waste removal and energy recovery. The movement of electron in BESs is particular important because it determines the rate and the efficiency of electrogenic redox reaction. Current production and coulombic efficiency are key parameters for assessing the electrogenic electron transfer in BES. In particular, current production is described as the electron transfer rate in electrogenic process. On the other hand, coulombic efficiency represents the proportion of the electrogenic electrons against the total consumed electrons of substrates (Logan et al., 2006). Other parameters of BESs (e.g. power density, energy efficiency, cathodic production rate) are also used to describe the performance of specific BESs such as MFCs and MECs and these parameters are partially derived from current production and coulombic efficiency in combination with the others features of BESs (e.g. external resistance, the type of substrates and cathodic products) (Cheng et al., 2008; Logan et al., 2006). When treating domestic wastewater and alleviating economic cost are the goals for BESs, ~150A/m^3 of current density from ~1kgCOD/m^3d of wastewater is proposed as target in order to meet commercial requirement (Dhar and Lee, 2014). However, the current density from the wastewater-fed BESs in laboratory was only ~40A/m^3 and the current density in scale-up BESs was even lower (Dhar and Lee, 2014; Min and Logan, 2004). On the other hand, although part of the electrons was indispensably used for biomass synthesis, most of the electrons from initial substrates were supposed to be used by anode reduction in BESs for achieving high coulombic efficiency in such BESs (Rittmann and McCarty, 2012). However, the coulombic efficiency in the wastewater-fed BESs in laboratory was as low as 3% to 57% since large part of the electrons from initial substrates in such BESs was trapped by non-electrogenic redox reactions (Karra et al., 2013; Min and Logan, 2004). In which case, low current production and low coulombic efficiency are considered as the major constraints to hinder the utilization of BESs for commercial wastewater treatment.

Abiotic resistances account for part of these electrogenic constraints in BESs since they can hinder the movement of electrons and ions in BESs, and therefore cause low current production and low coulombic efficiency. Generally, the electron transfer resistance of redox reaction from organism to electrode is negligible (Malvankar et al., 2011; Torres et al., 2008). However, electrodes, electrolyte and membrane have considerable resistance because they physically extend the electron transfer route of microbial redox reactions in BESs. These resistances resulted the constraints of electrogenic processes in BESs such as ohmic losses, low conductivity of electrolyte and slow transportation of ions, potential loss by pH gradient (Rozendal et al., 2008). Additionally, these resistances could be substantially increased when scaling up the system (Logan, 2010).

However, these abiotic electrochemical resistances are not the only obstacles to the electrogenic electron transfer processes in BESs for treating wastewater as the biotic characters can also significantly influence such electron transfer processes. For example, in a series BESs with same abiotic resistances and initial substrates, the BESs with higher abundance of electrogenic microorganisms can better electrogenically catalyze anode and achieve higher current production and high coulombic efficiency. Moreover, previous studies suggest that electrogenic microorganisms can only use a few substrates to conduct efficient electrogenic processes (Kiely, Regan, et al., 2011). Therefore, BESs require both high abundance of electrogenic microorganism and appropriate type of electrogenic substrates to achieve high current production. For example, acetate-fed BESs with anodic microbial communities that contain high proportion of *Geobacter* could achieve high current production and high coulombic efficiency (Kiely, Regan, et al., 2011). However, high electroactive microorganisms such as *Geobacter* in BESs were normally unable to directly utilize those complex organics in wastewater. Consequently, non-electrogenic degradation partners were often developed in anodic microbial communities to degrade the complex matters into electrogenic preferred products (Kiely, Regan, et al., 2011). In which case, considerable electrons and energy in initial electron donors potentially lose in non-electrogenic pathways rather than be recovered by anode in BESs. This can cause the decrease of the energy for the growth and the metabolism of electrogenic microorganisms in BESs and therefore decline the electrogenic performance. Moreover, inorganic ions (e.g. nitrite, sulphate) and carbon dioxide are widely present in wastewater (Heidrich et al., 2014; Kelly and He, 2014). The anaerobic anodic condition in BESs however

encourages the reduction of these inorganic ions combined with the oxidation of electrogenic electron donors to create competitive electron sinks alongside with anode in BESs. It is known that the energy for the metabolism of microorganism in a redox reaction is the difference of the redox potentials of initial electron donors and the redox potentials of final electron acceptors (Rittmann and McCarty, 2012). In the case of BESs, the redox potentials of initial electron donors and final electron acceptors are defined as the redox potentials of initial substrates and anode potentials respectively. In which case, when final anode potential in BESs is below the redox potentials of such electron sinks, the available energy for the electrogenic microorganisms is therefore lower than the energy for the engaged microorganisms of these alternative electron sinks. Therefore, these alternative electron sinks can compete with anodic electrogenic process for the electrons and the energy in electrogenic electron donors, and hence cause the decline of the electrogenic performance in wastewater-fed BESs.

The negative effect of complex feed on the electrogenic performance of BESs therefore needs to be attenuated for the optimization of the realistic applications of BESs. In particular, anode potentials is considered as a major factor to affect the extent of anode reduction in BESs (Wagner et al., 2010). Moreover, the availabilities of competitive electron acceptor can influence the extent of the reduction of competitive electron acceptor, which therefore also affect the extent of anode reduction (Omil et al., 1998). In which case, to alter both of the anode potential and the availabilities of competitive electron acceptor in BESs has been attempted in previous studies, which have been selectively listed in Table 1. In particular, some studies demonstrated that to alter anode potentials in the BESs in the presence of complex organics regulated the anodic microbial communities. This therefore introduced various degradation intermediates and products, which consequently influenced the electrogenic performance of such BESs (Hari et al., 2016; Ishii et al., 2014). On the other hand, to alter both of the anode potentials and the ratios of initial substrate and competitive electron acceptors (mole/L/mole/L) also made effect on the electrogenic performance of the BESs in the presence of the competitive electron acceptors because the extent of the reduction of both competitive electron acceptors and anode in BESs were regulated by such conditions (Kashima and Regan, 2015; Srinivasan and Butler, 2017). However, the effect of these engineered parameters have yet to be quantitively associated with the microbial electrogenic constraints in BESs

in the presence of complex feed. This is because the key microbial electrogenic processes in such BESs are yet to be identified. In particular, the electrogenic processes of the BESs fed with complex feed are composed by those individual electrogenic processes of electrogenic molecules. However, the microbial electrogenic constraints of those major individual electrogenic processes in the BESs in the presence of complex feed were yet to be identified, and consequently the relationship between the individual electrogenic performance of these major electrogenic pathways and the engineered conditions in such BESs was unknown. This hinders the rational design of BESs for treating complex feed such as wastewater. Therefore, it is necessary to individually identify the major electrogenic pathways and their corresponding microbial electrogenic constraints in the BESs in the presence of complex feed. Moreover, the quantative relationship between those engineered parameters and the electrogenic constraints of the major electrogenic pathways in such BESs needs to be investigated.

Glucose and sulphate are common organic degradation intermediate and anion in wastewater respectively (Rittmann and McCarty, 2012). Moreover, the pathways of these two molecules in conventional anaerobic system are well studied. In which case, the identification of the major electrogenic pathways in BESs in the presence of these two molecules is promising (Hoelzle et al., 2014a; Liang et al., 2013). Therefore, this study used glucose and sulphate as the model of complex organic electron donor and competitive electron acceptor respectively.

Initial electron donor	Initial competitive electron acceptor	Anode potential (mV vs SHE)	The raio of initial carbon feed : initial competitive electron acceptor feed (mol/L:mol/L)	Major electrogenic pathways	Reference
Propionate	n/a	-250, 0, +250	n/a	Propionate→acetate→current	(Hari et al., 2016)
Sucrose	n/a	-200, -50, +100	n/a	Surcose→acetate/unknown intermediates →current	(Ishii et al., 2014)
Xylose	n/a	0, +200, +400	n/a	Unknown	(Kokko et al., 2015)
Glucose	n/a	-189, -70, -7	n/a	Unknown	(Jung and Regan, 2011)
Lactate	Sulfate	-300, +300	Unknown	n/a	(Chou et al., 2014)
Acetate	Carbon dioxide	-300, -250, -200, -150, -50	n/a	Acetate→current	(Sleutels et al., 2011)
Acetate	Nitrite	n/a	1.8, 3.7, 7.4	Acetate→current	(Srinivasan and Butler, 2017)
Glucose	n/a	-150, 0, +200	n/a	Glucose→acetate/formate→current	This study
Acetate	Sulphate	-250, -150, 0, 200, 500, 700	1.33, 0.67, 4, 2, 1, 0.5	Acetate→current, Acetate→sulfide→current	This study
Glucose, sucrose, starch	Sulphate	0	4	Glucose/surcose/starch→ Acetate→sulfide→current Glucose/surcose/starch→ Acetate →current	This study

Table 1-1 Summary of previous studies about the effect of engineered parameters on the electrogenic performance of the BESs in the presence of relative complex substrates or competitive electron acceptors.

1.2. Aims and objectives

This study is aiming to understand the effect of complex feed on the electrogenic performance in BESs in response to anode potential and the ratio of carbon:sulphate (C:S) (mole/L:mole/L). The hypothesis of this study was that there is a quantative relationship between anode potential/C:S ratio and the individual electrogenic performance of the major electrogenic pathways/the electrogenic constraints in the BESs in the presence of complex feed. Consequently, this study firstly identified the major electrogenic pathways and electrogenic constraints in the BESs in the presence of complex feed. Secondly, this study investigated in the quantative relationship between the electrogenic performance of the major electrogenic pathways and either anode potential or C:S ratio in the BESs in the presence of complex feed.

In which case, the objectives of this study are as following:

1. To identify the major electrogenic pathways and the electrogenic constraints in glucose-fed BESs

2. To investigate the relationship between the electrogenic performance and the major electrogenic pathways in the glucose-fed BESs at different anode potentials

3. To identify the major sulphur pathways and the electrogenic constraints in the BESs in the presence of sulphate

4. 2. To investigate the relationship between the electrogenic performance and the major sulphur pathways in the BESs in the presence of sulphate in response to anode potentials and C/S ratio

5. To identify the relationship between the electrogenic constraints and the electrogenic performance of the BESs in the presence of both complex organics and sulphate

Chapter 2 Materials and Methods

2.1. Reactors set up

H-type two-chambers BESs reactors were constructed by combining two 300mL borosilicate glass bottles with 250mL individual working volume (Duran group, Germany) as anodic and cathodic chambers. The chambers were structurally connected with two glass flange arms and spatially separated by a Nafion membrane (Sigma-Aldrich, USA) to exchange ions. Three glass screw threads joints were attached to the anodic chamber to provide one sampling port, one reference electrode port and one media replacement port. Nafion membranes were pretreated by soaking in 2% H_2O_2 for 1hours before use. 5cm×2.5cm×1cm graphic plates (Olmec, UK) were used as anode and they were polished with sandpaper and then soaked in 10%HCl overnight and rinsed with deionized water to remove the residuals. 5cm×2.5cm platinum meshes (Ti-shop. UK) were used as cathode. The cathodes were rinsed with deionized water to remove residuals. Anode and cathode in each reactor were connected via a 10mm diameter stainless steel wire (Goodfellow, UK). The ohmic resistance of each electrode set up was tested with a voltmeter to ensure that the resistance was <5Ω. All H-type reactors were sterilized by autoclaving for 6 minutes at 121°C before the experiments. The schematic description of the H-type two-chambers BESs reactors was described below (Figure 2-1).

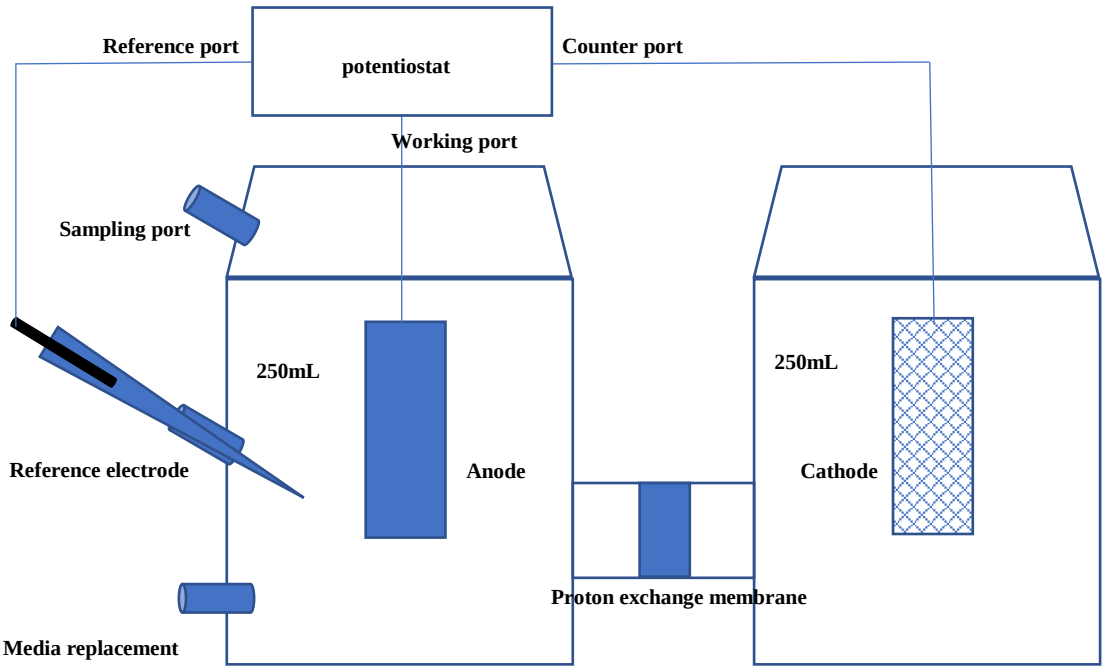

Figure 2-1 The schematic description of H-type two-chambers BESs reactors.

Tubular two-chamber reactors were constructed by combining two 78.5mL tubular fabricated perspex vessels with 78.5mL individual working volume as both anodic and cathodic chambers. Nafion membrane (Sigma-Aldrich, USA) was used to spatially separated the chambers and allow for ion exchange. Nafion membranes were pretreated by soaking in 2% H_2O_2 for 1hours before use. 2.5cm×2.5cm×1cm carbon felt (Olmec, UK) was used as anode. 2.5cm×2.5cm platinum mesh (Ti-shop. UK) was used as cathode. All the electrodes were rinsed with deionized water to remove residuals. Anode and cathode were connected via a 10mm diameter stainless steel wire (Goodfellow, UK). The ohmic resistance of each electrode set up was tested with a voltmeter to ensure that the resistance was <5Ω. The perspex reactors were sterilized by ultraviolet light (UV) for 60 minutes in a UV-cabinet (Labcaire, UK) before the experiments. The schematic description of the tubular two-chambers BESs reactors was described below (Figure 2-2).

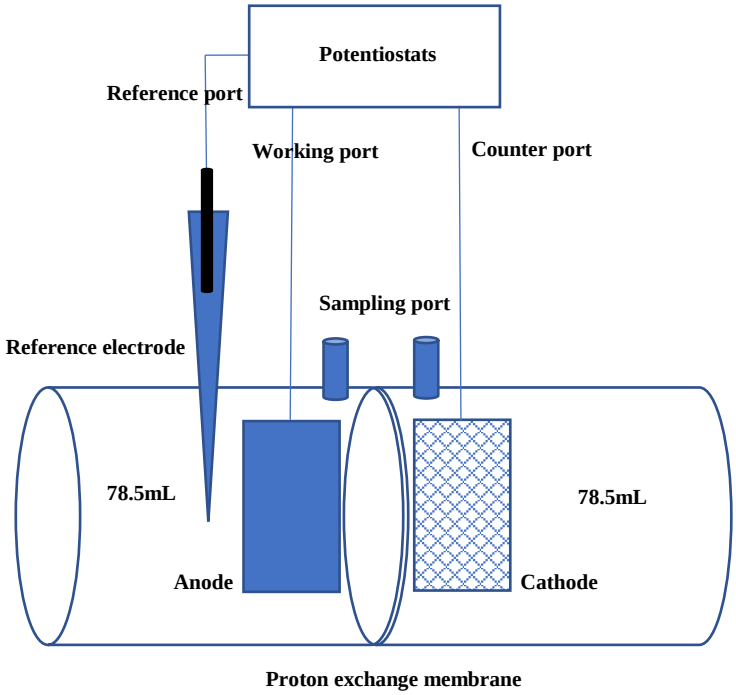

Figure 2-2 The schematic description of the tubular two-chambers BESs reactors.

2.2. Media and buffer

Settled sewage from Tudhoe mill domestic wastewater treatment plant (Durham, UK) was used as inoculum in anodic chamber unless indicated otherwise. Other inocula, included activated sludge collected from Tudhoe mill domestic wastewater treatment plant (Durham, UK), settled sewage was collected from Howden wastewater treatment

plant (North shields, UK), arctic biomass originally collected from the soil at Svalbard (N78^{o}, E11, 15,16^{o}, Norway). Sewage inocula and anodic media were used in the ratio of 1:5 for the initial acclimation. Alternatively, sludge or arctic resource and anodic media were used in the ratio of 1:20 for the initial acclimation. Anodic media contained monosodium phosphate ($NaHPO_4$, 4.58g/L), sodium dihydrogen phosphate ($NaH_2PO_4 \cdot 2H_2O$, 2.77g/L), ammonia chlorine NH_4Cl (1g/L). Trace element solution (10mL/L) and vitamin solution (10mL/L) were used as described in (Gimkiewicz and Harnisch, 2013). The detailed recipe is given in Table 8-6. Cathodic buffer contained monosodium phosphate **(**$NaHPO_4$, 4.58g/L), sodium dihydrogen phosphate ($NaH_2PO_4 \cdot 2H_2O$, 2.77g/L). The final pH in both anodic media and cathodic buffer was 7.0. Both solutions were sparged with nitrogen (99%) before use. Sodium acetate ($C_2H_3NaO_2$), sodium formate (HCOONa), ethanol (C_2H_6O), sodium propionate ($C_3H_5NaO_2$), sodium pyruvate ($C_3H_3NaO_3$), sodium butyrate ($C_4H_7NaO_2$), glucose ($C_6H_{12}O_6$), sucrose ($C_{12}H_{22}O_{11}$), starch (($C_6H_{10}O_5)_n$), sodium sulphide nonahydrate ($Na_2S \cdot 9H_2O$), hydrogen (H_2:CO_2 (80%:20%)), sodium sulphate (Na_2SO_4) and sodium chlorine (NaCl) was applied before the tests as indicated in chapter 3, chapter 4 and chapter 5.

2.3. Reactor operation

In the tests with controlled anode potentials, quad potentiostats (Whistonbrook, UK) were used to control the anode potential of each reactor. The applied anode potentials were indicated in chapter 3, chapter 4 and chapter 5. AgCl/Cl electrodes (+197mV vs Standard Hydrogen Electrode)) (MF-2052, BASi, USA) were used as reference electrode. Each reference electrode was connected with the media in the reactor via a salt bridge in order to protect the reference electrode and minimize the potential draft of reference electrode. The salt bridges were built by 10mL pipette tips filled with mixture of 3M NaCl and 5% agar at the bottom and extra 3M NaCl solution to soak the tip of reference electrode. The top of the salt bridges was sealed with a rubber stopper in order to prevent evaporation and leakage of NaCl solution. Salt bridges were replaced once a month in order to prevent the increase of ohmic loss. The potential of each reference electrode with salt bridge was tested to ensure the potential draft was <10mV. The distance of reference electrode and anode was ~10mm in order to minimize the potential loss. Current production was

measured by Version 3 data logging software (Whistonbrook, UK) once per min unless indicated otherwise.

In the test without controlled anode potentials, power units (PSM2/2A, Caltek, Hong Kong) were used to provide extra energy to the reactors across anode and cathode. The amount of supplied energy was 800mV in all these reactors. 10Ω resistor (TE Connectivity, UK) was used to connect the anode with the power unit in each reactor. The voltage between anode and power unit was measured with a data logger (ADC-20,Picotech, UK) once per min. All the experiments were run under room temperature at (23℃ to 25℃). A data logger (Omega, UK) was used to monitor the temperature.

2.4. Chemical analysis

TC (Total carbon), TOC (Total organic carbon) and IC (Inorganic carbon) was determined with a total carbon analyser combined ASI-5000A autosampler (TOC-5050A, Shimadzu, Japan). All the samples were filtered with polyethersulphone syringe filters (0.2 μm nylon membrane, VWR, USA) before the measurement to remove the particulates. Each sample was measured in duplicate. COD (Chemical Oxygen Demand) of each sample was measured with COD kits (25mg/L ~ 1500mg/L, Merck & Co. Inc, USA) according to the manufacturer's protocol. Each sample was measured in triplicate. VFAs (Volatile Fatty Acids) such as formate, acetate, propionate and butyrate were determined by ion exchange method (Manning and Bewsher, 1997). In particular, all the samples were filtered through syringe filters (0.2 μm nylon membrane, VWR, UK) after the samples had been taken from the reactors. Then all the samples were diluted with oxysulfonic acid (1:1;v:v) and sonicated for 40 minutes in order to remove the dissolved carbonate. The treated samples were measured on Ion Chromatography (IC, Dionex ICS-1000, thermofisher, USA). The column of 4×250mm Ionpac ICE-AS1 with eluent of 1.0mM heptafluorobutyric acid was applied for the IC. The injection was conducted by a loop with volume of 10mL and flow rate of 0.16mL/min. 5mM tetrabutylammonium hydroxide was applied as cation regenerant solution in the Dionex Anion Micro Membrane Suppressor (AMMS-ICE II). Each sample was measured in duplicate. Glucose, pyruvate, ethanol and lactate were determined by assay kits (Megazyme, Ireland) according to the manufacturer's protocol. All the samples were filtered with syringe filters (0.2 μm nylon membrane, VWR, USA) after sampled from reactors. The quantitative reactions of both standards calibration and the reactor samples were done in

microwell solid plates (96 multiwell polystyrene plates, Sigma-aldrich, UK). After the reactions, the absorbance of the samples was read on a microplate reader of multi-mode, molecular devices with absorbance of 340nm (SpectraMax M3, USA). The calculation of the final concentration of each organic was determined by the method provided by manufacturer's protocol. Each sample was measured in duplicate. Anions (sulphate (SO_4^{2-}), nitrite (NO_2^-), nitrate (NO_3^-), phosphate (PO_4^{3-}) and chloride (Cl^-)) was determined by ion chromatography (IC, Dionex ICS-1000, Thermofisher, USA) applied with a column of ionpack AS 14A with carbonate as the eluent. All the samples were filtered through syringe filters (0.2 µm nylon membrane, VWR, UK) before the measurement to remove the particulates. Each sample was measured in duplicate. Sulphide was measured with a sulphide cuvette kit (Hach, USA) according to the manufacturer's protocol. All the samples were read on spectrophotometer (DR1900, Hach, USA). Each sample was measured in duplicate.

All the gas samples in the headspace of the reactors were taken by 100 µl gas tight syringes (SGE Analytical Science, Australia). Hydrogen was determined by Trace Ultra GC (Thermo Scientific, USA) applied with a Restek Micropacked 2m Shin carbon column with argon as the carrier gas was applied in the Trace Ultra GC. The detection procedure was to heat up the oven to 40°C following with ramping from 110°C with a interval of 30°C per min until 200°C for 1.5min. The standard calibration curves was built by injection of the standard gas with 80% of hydrogen (Calgaz, USA) in the portions of 20ul, 40ul, 60ul, 80ul and 100ul. Both standard calibration gas and sample gas were injected in triplicate. The methane (CH_4) in the headspace of the reactors was determined by a Carlo Erba HRGC S160 GC applied with an FID detector and a HP-PLOTQ column with size of 0.32 mm diameter and 30 m length. The temperature of oven was set at 35°C. The standard calibration curves was built by injection of the standard gas of methane (Calgaz, USA) in the portions of 20ul, 40ul, 60ul, 80ul and 100ul. The gas sample was injected after the standard calibration gas. Both standard calibration gas and sample gas were injected in triplicate.

The pH value of each sample was measured by pH meter (HQ11D, Hach, USA). The conductivity of media was measured with a conductivity meter (EC300, VWR, UK). The chemical elements on the surface of anode were analysed by energy-dispersive X-ray spectroscopy (EDX) and scanning electron microscope (SEM) (TM3030 benchtop,

Hitachi, Japan). All the anode samples were rinsed with deionized water and preserved in 100mL serum vials individually, which were then sparged with N_2 (99%) for 10mins and sealed with butyl rubber caps and aluminium crimp seals to prevent the oxidation.

2.5. Microbial community analysis

The microorganisms on the graphite plate anode were sampled and extracted with a sterilized stainless steel scratcher and preserved in 50% ethanol at -20℃. The microorganisms on the carbon felt anode were extracted by cutting the anode felt into small 250mg±3mg pieces with a sterilized tweezer, and preserved in tubes containing a lysing matrix. The DNA of the anodic microbial communities was extracted by the QBiogene FastDNA spin soil kit (MP Biomedicals, UK).

To sequence the microbial communities, the V4 and V5 regions of 16S rRNA gene of the extracted DNA samples were amplified by polymerase chain reaction (PCR), using the forward primer 515f :5'-*GTGNCAGCMG CCGCGGTAA*-3' and the reverse primer 926r :5'-*CCGYCAATTYMTTTRAGTTT*-3' using the Roche Fast Start High Fidelity PCR system (Roche, UK). All the samples were labelled with barcodes. The PCR programme was initial denaturation at 95°C for 2 minutes, then 30 cycles for denaturation at 95°C for 30 seconds, annealing at 55°C for 30 seconds and extension at 72°C for 45 seconds, terminated by a final extension at 72°C for 7 minutes. The DNA amplicons were then cleaned by AMPure bead purification reagent (Beckmancoulter, UK) to remove the residue of primers, enzymes and nucleotides. The cleaned DNA amplicons were individually quantified by dsDNA HS Assay Kit (Thermofisher, USA) on a fluorometer (Qubit 2.0, Thermofisher, USA). All the amplicons were diluted to equimolar 10pM for building one pooled library. Template was prepared (includes amplification and enrichment) on Ion OneTouch™ 2 System (Life Technologies, UK).The templated Ion Sphere™ Particles obtained from template preparation was combined with an Ion 316™ Chip Kit v2 with 2 million to 3millon reads pre run for sequencing. The sequencing was conducted by Ion PGM™ Sequencing 200 Kit v2 (Life Technologies, UK) according to the manufacturer's protocol. The data was generated as FASTQ file from ion serve. QIIME denoiser was then used to filter the sequencing data at a minimum length of 200bp and to select the targeted gene according to the barcode. The operational taxonomic unit (OTU) table of anodic microbial communities was produced by QIIME pipeline at 97% similarity level using Greengenes database. All the sequence data were

then rarified to a minimum sequencing read of 13880 for the beta diversity analysis. Principal component analysis (PCA) was conducted on the OTU table at the family level was performed with STAMP (Parks et al., 2014). The post-hoc test was used Tukey-Kramer method (at 95% confidence level) because of the relative small group size of the targeting samples in this study, and this method can therefore include all the pairs of means while avoid the computationally expensive.

To quantify the abundance of *Geobacteraceae*, quantitative PCR (qPCR) was used. The primers (forward primer *Geobacteraceae* 494f: 5'-*AGGAAGCACCGGCTAACTCC*-3', reverse primer *Geobacteraceae* 825r: 5'-*TACCCGCRACACCTAGT*-3') were used according to (Holmes et al., 2002). All the extracted DNA samples were diluted with nuclease-free water 1:10, to minimize inhibition. 3µl of either diluted samples, negative controls (nuclease-free water) or *Geobacteraceae* standards (1×10^8 copies/ul to 1×10^2 copies/ul) were individually reacted with a mixture of 5µl of ssofast EvaGreen supermix (Biorad, UK), 0.5µl forward primer, 0.5µl reverse primer and 1µl of nuclease-free water. Each sample was measured in triplicate. The qPCR programme used was: initial denaturation at 98°C for 3 minutes, then 39 cycles for denaturation at 98°C for 5 seconds, annealing at 51°C for 10 seconds. Melting curve was generated by temperature increasing stepwise with 0.5°C increment every 5 seconds. The optimal annealing temperature was selected based on ten trial qPCR runs with annealing temperature between 50°C and 60°C. The qPCR was carried out on real-time PCR system (CFX96, Biorad, UK). A calibration curve of the cycle number (cq value) against the copy number of standards was generated at the end of the programme. The copy number in each DNA sample was calculated based on this calibration curve. To estimate the final cells numbers of *Geobacteraceae* in each sample, the copy number was assumed to be 2 per cell of *Geobacteraceae* (Methé et al., 2003).

2.6. Calculations and data analysis

The electron equivalent of molecules (e^-mmol/L) represent the amount of electron released from the substrate after completely oxidation and fully converted to carbon dioxide. The value of the electron equivalent of molecules was based on:

The electron equivalent of molecules (e^-mmol/L) was based on:

$$\text{The electron equivalent of molecules} = \text{The concentration of the molecules} \times \text{The number of electrons released per molecule when the molecule is mineralised to } CO2, \text{protons and electrons}$$

The number of electrons released per molecule when the molecule is mineralised to CO2, protons and electrons was shown in Appendix A Table 8-5.

Current production in reactors operated with additional voltage supply was calculated by the equation:

$$I = V/R \quad (1)$$

Where I is the current in the reactors (mA); V is the voltage measured across the resistors (mV); R is the resistance of the resistor (Ω).

Coulombic efficiency was calculated based on the equation:

$$\text{CE} = \frac{M \int_0^t I dt}{FbV\Delta COD} \quad (2)$$

CE is the coulombic efficiency (%); M= 32, which is the molecular weight of O_2; t is the period of the test; I is the measured current (mA); F is the Faraday constant (9.65×10^4 C/mole e^-); b= 4, which is the numbers of the electrons transferred when reducing O_2; V is the anodic working volume in the reactors. ΔCOD is the consumption of chemical oxygen demand.

Analysis of variance (ANOVA), linear regression, nonlinear regression and T-test was carried out by using Minitab 17 (Minitab Inc, USA).

Chapter 3 The effect of the degradation pathway of glucose on bioelectrochemical systems

3.1. Introduction

Bioelectrochemical system (BESs) have been proposed as an energy neutral wastewater treatment technology (Li et al., 2013). Various organics in wastewater can be utilized as electron donors for the growth and metabolism of electrogenic microorganisms, which can be harnessed by BESs to recover energy via electricity generation by microbial fuel cells (MFCs), or via cathodic hydrogen production by microbial electrolysis cells (MECs) (Call and Logan, 2008; Logan et al., 2006). The ideal scenario for the use of BESs in wastewater treatment is to remove waste while to completely and rapidly recover the energy from wastewater. This however has yet to be realized. In particular, when those complex wastes such as carbohydrates in wastewater are used as electron donors in BESs, syntrophic processes are required to convert complex wastes into electrogenic molecules such as acetate, which can be utilized by electrogenic microorganisms to conduct electrogenic processes. However, the electrogenic performance of the BESs acclimated to complex wastes is often reported to be inferior to the BESs acclimated with those simple molecules favoured by electrogenic bacteria (Kiely, Regan, et al., 2011). Therefore, understanding how the degradation pathways of those complex wastes affect the electrogenic performance of BESs is of great interest.

Glucose, a type of monosaccharide from polysaccharide decomposition, is an important degradation intermediate in anaerobic wastewater treatment system. It is therefore matter to complex-fed BESs because the anodic chambers of BESs are normally anaerobic (Call and Logan, 2008; Logan et al., 2006; Rittmann and McCarty, 2012). Although glucose is considered as a relative simple substrate for BESs, it can be used to simulate the degradation pathways of complex. This is because similar to other complex, glucose-based electrogenic processes in BESs also rely on the syntrophic electrogenic network and they are typically converted to pyruvate via glycolysis, and then degraded to various carboxylic acid, alcohol, dicarboxylic acid to produce current. (Freguia et al., 2008; Lee and Rittmann, 2009; Temudo et al., 2007). Moreover, similar to other complex-fed BESs, the electrogenic performance of glucose-fed BESs was often inferior than the simple molecules-fed BESs (e.g. acetate-fed BESs). For instant, the power density of glucose-fed

BESs was similar to wastewater-acclimated BESs (~0.12 to 0.17 kWh/kgCOD), but lower than acetate-fed controls (~0.40 kWh/kgCOD) (Ge et al., 2014). Likewise, glucose-acclimated BES produced lower current (~0.12A/m^2 to 0.58A/m^2) than paralleled acetate-fed controls (~0.65A/m^2 to 0.76A/m^2) (Ishii et al., 2014; Lee et al., 2008). On the other hand, it frequently reported that glucose-fed BESs had lower coulombic efficiency (15% to 49%,) than acetate-fed controls (20% to 72%) (Ishii et al., 2014; Kiely, Regan, et al., 2011; Lee, Parameswaran, et al., 2008). More importantly, the concentration of most of the intermediates and products from glucose degradation were easily to be measured in laboratory (Lee and Rittmann, 2009). Therefore, glucose is a good model of complex substrate to be used to identify the electrogenic role of degradation intermediates and products and to study the effect of the degradation pathways of substrates on the electrogenic performance of BESs.

The current production of BESs depends on the electrogenic kinetics of electrogenic microorganisms. Some authors (Escapa et al., 2012; Torres, Marcus, Parameswaran, et al., 2008) suggest that the electrogenic kinetics of BESs is subjected to Monod equation, where microbial growth is a non-linear function of the substrate concentration:

$$\frac{1}{V} = \frac{K_S + [S]}{V_{max}\,[S]} \tag{4}$$

Where V is the reaction rate/current production here, [S] is the substrate availability of electrogenic molecules in the complex-fed BESs, V_{max} is the maximum reaction rate/saturated current production, Ks is the substrate availability when reaction rate reach half of the maximum rate (V_{max})/saturated current production. In which case, the current production in complex-fed BESs is possibly determined by the availabilities of electrogenic molecules. On the other hand, that at least some electrogenic microorganisms have different electrogenic kinetics when utilizing different electron donors (Cheng and Logan, 2008; Speers and Reguera, 2012). This implies that the availability and the type of electrogenic electron donors are important to the current production of glucose-fed BESs. It is thought that electrogenic processes in glucose-fed BESs occurred via the direct oxidation of both glucose and the glucose degradtion intermiediates and products (GDIPs) such as acetate. However, the electrogenic contribution of glucose was normally minor (Freguia et al., 2008; de los Ángeles Fernandez et al., 2016). Consequently, the availabilities of those electrogenic preferred

GDIPs will dictate the current production of glucose-fed BESs and minimum availabilities of these electrogenic molecules for saturated current production in glucose-fed BESs need to be achieved. Moreover, since coulombic efficiency is the assessment of the electron distribution of the initial electron donor, the coulombic efficiency of glucose-fed BESs is determined by the electron distribution of each glucose degradation pathway. Consequently, identifying the electrogenic GDIPs and evaluating the minimum availability of electrogenic preferred GDIPs for saturated current production in glucose-fed BESs is essential to understand the effect of the degradation pathways of glucose on the electrogenic performance and the electrogenic constraints in glucose-fed BESs.

It has observed that the availabilities of GDIPs varied with the current production during the glucose degradation processes in glucose-fed BESs (Selembo *et al.*, 2009; Lu *et al.*, 2012). Moreover, the final electron distribution of glucose degradation processes in glucose-fed BESs have been well described and current, residue organics such as propinate, methane and biomass were often recognized as the major terminal electron sinks (Freguia et al., 2007, 2008; Lee et al., 2008). However, it was difficult to understand electrogenic role of each GDIP in glucose-fed BESs as these GDIPs co-existed and interacted in the same glucose-fed system. In particular, the electrogenic contribution and the non-electrogenic electron loss the degradation pathway of each GDIP in glucose-fed BESs are not clear. Moreover, the effect of the degradation of GDIPs on the availabilities of electrogenic preferred GDIPs was not well understood. In which case, it was difficult to identify electrogenic GDIPs and the non-electrogenic pathway in glucose-fed BESs. This hinders the recognition of the electrogenic constraints in the glucose degradation pathway in glucose-fed BESs.

Consequently, this study investigated the electrogenic role of glucose and the major GDIPs in electrogenic processes in glucose-fed BESs individually. In particular, the degradation pathway of glucose and the electrogenic molecules in glucose-fed BESs were identified. Moreover, the minimum availabilities of electrogenic preferred GDIPs for saturated current production in glucose-fed BESs was evaluated. In addition, the constraints the glucose degradation pathway placed on the production of the major electrogenic GDIPs and the non-electrogenic electron loss were identified. Therefore, this study aimed to:

1. To identify the major electrogenic molecules and the major electrogenic pathways in glucose-fed BESs.

2. To measure the minimum availabilities of the major electrogenic molecules for saturated current production in the glucose-fed BESs

3. To identify and the constraints to achieve the minimum availabilities of the major electrogenic molecules for saturated current production in the glucose-fed BESs.

4. To evaluate the electron loss in non-electrogenic degradation pathways of glucose in glucose-fed BESs

3.2. Method

3.2.1. Reactors start up

H-type reactors were used in this chapter and the configuration of these reactors were described in 2.1 and Figure 2-1. The anodic media and cathodic media used in these reactors were described in 2.2. The glucose-fed BESs and the acetate-fed controls were initially fed with either 20Cmeq/L glucose (0.61g/L) or 20Cmeq/L acetate (0.88g/L) respectively. The conversion equations between the carbon equivalent of substrates and the real concentration of substrates were shown in 2.6. All the reactors were inoculated with the settled sewage from Tudhoe mill domestic wastewater treatment plant (Durham, UK). The treatment of media and inoculum was described in 2.2. All the reactors were operated in microbial electrolysis cells (MECs) mode and the anode potentials of them were stabilized at -150mV vs standard hydrogen electrode (SHE) through all the tests. The details of operation were described in 2.3.

3.2.2. Experiment design

The test of glucose degradation profile in glucose-fed BESs and acetate degradation profile in acetate-fed controls

After stable current production was achieved, the glucose degradation profile and the acetate degradation profile was tested in the glucose-fed BESs and the acetate-fed controls respectively. Either 20Cmeq/L glucose or 20Cmeq/L acetate was used as the initial composition of influent. The tests was run until the current production <1mA. Current production in these reactors was monitored as described in 2.3. The coulombic efficiency of the tests was evaluated by the method in 2.6. The variation of the concentration of the GDIPs (glucose degradation intermediates and products) in these reactors were sampled and monitored by the method in 2.4.

To identify the major electrogenic molecules and the major electrogenic pathways in the glucose-fed BESs

In order to investigate whether glucose is the major electrogenic molecules in the glucose-fed BESs, the current production at 9^{th} hour and 15^{th} hour in the glucose-fed BESs initially fed with 40Cmeq/L (1.2g/L) glucose were tested. This current production was then compared with the current production in the tests with 20Cmeq/L glucose.

In order to investigate whether GDIPs were the major electrogenic molecules in the glucose-fed BESs, 20Cmeq/L of acetate, propionate, ethanol, pyruvate, formate, butyrate was individually fed in the glucose-fed BESs for a 9 hours test. Moreover, hydrogen ($80\%H_2/20\%CO_2$) was continuously injected in hydrogen test rather than dosing at the beginning of the test, and these hydrogen-fed tests were run for 2 hours. All these tests with open circuit was operated as non-electrogenic controls. Current production was monitored in these tests and the coulombic efficiency was calculated at the end of the tests based on the method in 2.6. Moreover, in order to investigate the electrogenic pathway of GDIPs in the glucose-fed BESs, the concentration of the GDIPs in the effluent of these tests was measured. Additionally, in order to investigate whether the current in each individual GDIPs tests was directly produced from itself, rather than the other degradation products, the anode potential was stepwise altered from -300mV to +600mV in the glucose-acclimated BESs individually fed with formate/acetate/ethanol/propionate to thermodynamically suspend or favour the electrogenic effort of them.

To calculate the conversion rate of the individual pathway of glucose degradation in the glucose-fed BESs, it was assumed that the reactions in the glucose-fed BESs were in first order, which subjected to the relation of that $r=k[R]$, where r is the rate of reaction, R is the concentration of reactant, k is the rate constant. k was obtained based on the equation:

$$\ln R=-kt+\ln R_0 \quad (5)$$

where t was the reaction time (Velasquez-Orta et al., 2011).

To investigate the quantative relationship between current production and the availabilities of acetate/formate in the glucose-fed BESs

In order to investigate the quantative relationship between current production and the availabilities of acetate/formate in the glucose-fed BESs, the initial concentration of acetate and formate was increased stepwise in ten (3.4Cmeq/L; 8.8 Cmeq/L; 14.1 Cmeq/L; 15.5 Cmeq/L; 17.0 Cmeq/L; 19.2 Cmeq/L; 23.1 Cmeq/L; 26.6 Cmeq/L; 32.2 Cmeq/L; 40.0 Cmeq/L) and seven (2.5Cmeq/L; 5Cmeq/L; 10Cmeq/L; 15Cmeq/L; 20Cmeq/L; 30Cmeq/L; 40Cmeq/L) individual cycles respectively in the glucose-fed BESs. In particular, the *Ks* value of acetate/formate in equation 3-1 was evaluated by the

non-linear regression between the initial concentration and corresponding current production.

To investigated the electrogenic constraints on the current production of the glucose-fed BESs other than low availabilities of acetate and formate.

1. The tests-fed with a mixture of 12.48Cmeq/L of acetate and 7.60Cmeq/L formate, 2. The tests fed with 12.48Cmeq/L, 3. The tests fed with 7.60Cmeq/L formate in glucose-fed BESs for 9 hours. Current production was monitored in per min. The coulombic efficiency of each test was evaluated based on the method in 2.6.

To investigate the presence of ethanol/propionate on the electrogenic performance of glucose-fed BESs.

In order to investigate whether the presence of ethanol and propionate suppressed the current production in the glucose-fed BESs, the cycles initially feed with the composition of 8.8Cmeq/L acetate + 5.1Cmeq/L formate +5.3 Cmeq/L ethanol + 2.5 Cmeq/L propionate in glucose-fed BESs were tested. In particular, the concentration of acetate and formate here equals to the *Ks* value of them in glucose-fed BESs. The concentration of ethanol and propionate here equals to peak accumulation in the glucose-fed cycle in Figure 3-1

The effect of the availabilities of acetate and the accumulation of hydrogen on the derivative reactions in the glucose-fed BESs was investigated based on the method in (Dolfing et al., 2008). The effect of anode potential on the electrogenic degradation of ethanol and propionate in the glucose was also investigated based on the method in (Dolfing et al., 2008).

Microbial communities analysis

In order to investigate the electrogenic microorganisms in the glucose-fed BESs and the acetate-fed controls, the anodic microbial communities of the glucose-fed BESs and the acetate-fed controls was investigated at the end of the experiment based on the method described in 2.5.

3.3.Results

3.3.1. The comparison of the electrogenic performance between the glucose-fed BESs and the acetate-fed controls

The glucose-fed BESs were first produced <30mA of current in 48 hours after inoculation and stable current of ~2.3mA was achieved at ~500 hours. Current was produced from acetate-acclimated controls at ~120 hours and reached to stable at ~6.6mA at ~600 hours. After stable current was produced, the glucose-fed cycle in the glucose-fed BESs and the acetate-fed cycle in the acetate-fed controls was operated. A comparison between the electrogenic performance of the glucose-fed BESs and acetate-fed controls was shown in (Table 3-1). In a selected cycle, maximum current production in acetate-fed controls was 6.6±0.2mA, which was much higher than the maximum current production of 2.4±0.2mA in the glucose-fed BESs (Table 3-1). No organic GDIPs other than acetate were observed in the entire acetate degradation process in the acetate-fed controls. The coulombic efficiency of the acetate-fed controls in first 9 hours was 80.1±4.9% and slightly decreased to 78.5±1.1% at the end of the test. The coulombic efficiency of the glucose-fed BESs in the first 9 hours was only 14.8±2.1%, and increased to 45.3±5.9% at 102nd hour at the end of the test (Table 3-1).

	Maximum current	**Coulombic efficiency in 9hrs**	**Coulombic efficiency when current production <1mA**
Acetate-fed	6.6±0.2mA	80.1±4.9%	78.5±1.1%
Glucose-fed	2.4±0.2mA	14.8±2.1%	45.3±5.9%

Table 3-1 Summary of electrogenic performance in acetate-fed controls and glucose-fed BESs.

3.3.2. The glucose degradation profile in the glucose-fed BESs

In a representative glucose-fed cycle in a glucose-fed BES, >93% of glucose was degraded in the first 9 hours. Acetate, formate, ethanol and propionate were observed as major organic GDIPs (Figure 3-1). In particular, acetate and ethanol accumulations reached ~5.9Cmeq/L and ~5.3Cmeq/L respectively at 9th hour and both were removed in similar rate until 102nd hour (Figure 3-1). Formate accumulation reached ~3.2Cmeq/L at 9th hour and it was completely removed at 30th hour (Figure 3-1). Propionate accumulation was ~2.2Cmeq/L at 9th hour and it further increased to ~2.5Cmeq/L at 102nd hour (Figure 3-1). Other common organic GDIPs such as pyruvate, lactate and butyrate were negligible in the entire glucose degradation process. Neither hydrogen nor methane was detected in the headspace of the anodic chamber of glucose-fed BESs at 9th hour. However, hydrogen accumulation of 19.0% was observed in the head space at 24th hour and then increased to ~22.1% at 102nd hour. Additionally, <1% of Methane was detected at the end of the102 hours in glucose-fed BESs.

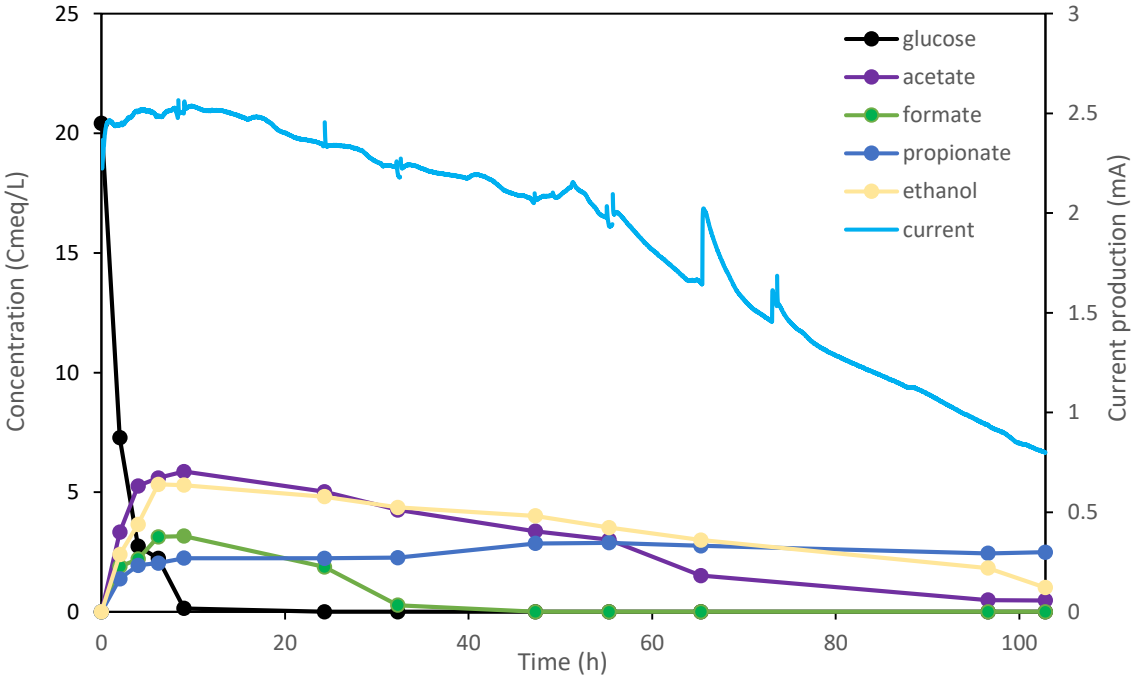

Figure 3-1 A selected glucose degradation pattern in 102 hours in glucose-fed BES.

3.3.3. Identifying the major electrogenic molecules and the major electrogenic pathway in the glucose-fed BESs.

Whether glucose were major electrogenic molecules in the glucose-fed BESs?

The current production at the 9th hour and at the 15th hour in the 40Cmeq/L glucose-fed cycles was ~2.4mA, which was similar to the 20Cmeq/L-fed cycle (Figure 3-2). This indicated that the current production was barely affected by the absence of glucose in the glucose-fed BESs. Therefore, rather than glucose, GDIPs are the major substrates to produce current in these glucose-fed BESs.

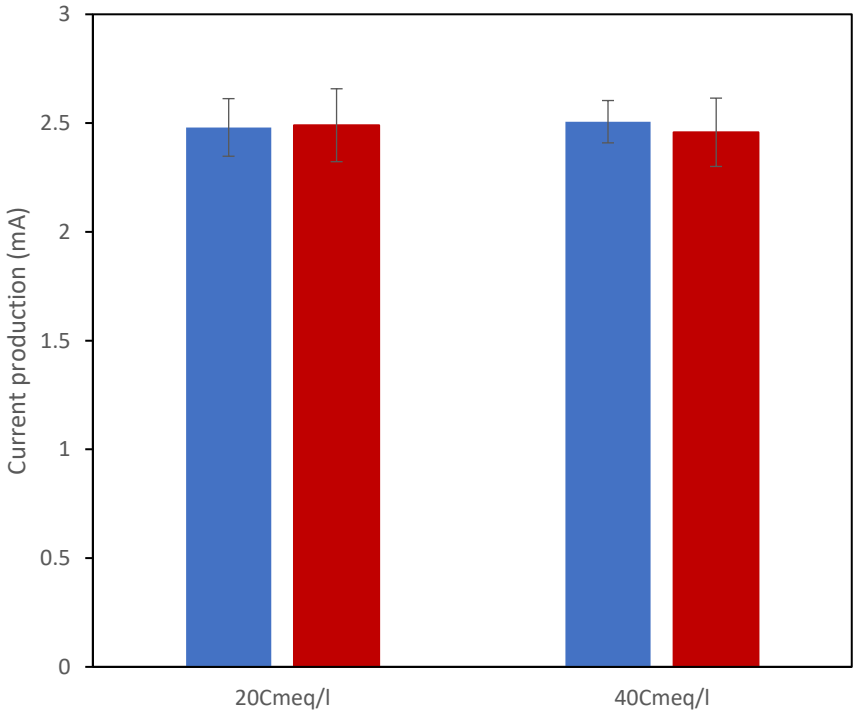

Figure 3-2 The current production at 9th hour and 15th hour in the 20Cmeq/L glucose-fed cycles and 40Cmeq/L glucose-fed cycles in the glucose-fed BESs.

Whether GDIPs were major electrogenic molecules in the glucose-fed BESs?

High current production of 3.9±0.1 mA and 2.4±0.7mA in the acetate-fed tests and the formate-fed tests in the glucose-fed BESs was observed respectively (Table 3-2). The current production was low (0.8±0.2 mA) in the ethanol cycles. The propionate-fed tests produced the lowest current of 0.4±0.0mA (Table 3-2). Since tests without any feed produced ~0.2mA in first 5 hours, which possibly due to the organics residues from previous tests and self-decay of the biofilm, the current production in the propionate-fed tests was negligible. The current production in the hydrogen-fed tests was 1.3±0.2mA, whereas the current production vanished instantly when suspending the hydrogen injection. The current production in the butyrate-fed tests was only 0.6±0.1mA (Table 3-2). Therefore, acetate and formate were the major electrogenic GDIPs to engage the current production in the glucose-fed BESs.

The coulombic efficiency with acetate and ethanol was 75.2±6.4% and 55.9±21.5% respectively, whereas the coulombic efficiency with formate was only 26.9±2.1% (Table 3-2). The coulombic efficiency with propionate and butyrate was not reported here due to the extreme low consumption of in the propionate-fed tests and the butyrate-fed tests. Moreover, since the measurement of the consumption of hydrogen was difficult because hydrogen injection flow was unknown in this study, the coulombic efficiency with hydrogen was not reported either.

Substrate	Maximum current production (mA)	Coulombic efficiency (%)
Formate	2.4±0.7	26.9±2.1
Acetate	3.9±0.3	75.2±6.4
Ethanol	0.8±0.2	55.9±21.5
Propionate	0.4±0.0	N/M
Hydrogen	1.3±0.2	N/M
Butyrate	0.6±0.1	N/M

N/M: Not measured

Table 3-2 Summary of electrogenic performance in glucose-fed BES with individual GDIPs feed.

The major electrogenic pathways in the glucose-fed BESs

The major electrogenic pathway in the glucose-fed BESs was investigated here. In particular, no production of other organic GDIPs or hydrogen was observed in either closed circuit tests or open circuit tests in the formate-fed tests in the glucose-fed BESs (Table 3-3). The consumption of fomrate in the open circuit tests (1.20±0.09Cmeq/L) was 70% lower than the closed circuit tests (3.53±0.25Cmeq/L) (Table 3-3). Therefore, formate was possibly direct electrogenic in the glucose-fed BESs. In the acetate-fed tests in the glucose-fed BESs, the consumption of acetate in the close circuit tests was 1.51±0.39Cmeq/L while minor acetate was consumed in the open circuit tests (Table 3-3). Moreover, trace amount of propionate was detected in both of the closed circuit tests and the open circuit tests (Table 3-3). However, propionate was non-electrogenic because little current was produced in propionate tests (Table 3-2). Therefore, acetate was an direct electrogenic electron donor and the acetate oxidation was an electrogenic process in the glucose-fed BESs. In the ethanol-fed tests in the glucose-fed BESs, trace amount of acetate and formate were detected in the closed circuit ethanol tests (Table 3-3). Therefore, the current production (~0.8mA) in the closed circuit ethanol-fed tests was likely driven by acetate and formate, rather than ethanol itself. In propionate-fed test in the glucose-fed BESs, negligible propionate was removed and trace amount of acetate and formate were detected in both closed circuit tests and the open circuit tests (Table 3-3). This indicates that propionate was unable to largely participate in either electrogenic process or non-electrogenic process in the glucose-fed BESs. In addition, negligible GDIPs was detected in hydrogen test in the glucose-fed BESs.

GDIPs	Production in 9 hours in closed circuit (Cmeq/L)				Production in 9 hours in open circuit (Cmeq/L)			
	Acetate tests	**Ethanol tests**	**Propionate tests**	**Formate tests**	**Acetate tests**	**Ethanol tests**	**Propionate tests**	**Formate tests**
Acetate accumulation	18.4	0.42	<0.1	n/a	20	0.28	<0.1	n/a
Ethanol accumulation	n/a	19.8	n/a	n/a	n/a	19.6	n/a	n/a
Propionate accumulation	0.22	n/a	20	n/a	<0.1	n/a	20	n/a
Formate accumulation	n/a	0.11	<0.1	16.4	n/a	0.02	<0.1	18.8
Hydrogen accumulation	n/a	n/a	n/a	n/a	n/a	n/a	n/a	n/a
	Carbon removal in 9 hours in closed circuit (Cmeq/L)				**Carbon removal in 9 hours in open circuit (Cmeq/L)**			
	Acetate tests	**Ethanol tests**	**Propionate tests**	**Formate tests**	**Acetate tests**	**Ethanol tests**	**Propionate tests**	**Formate tests**
	1.51±0.39	0.21±0.05	<0.1	3.53±0.25	<0.01	0.41±0.12	<0.1	1.20±0.09

n/a: No applicable as the production< 0.001Cmeq/L or not detected

Table 3-3 Summary of by-products accumulation and the total carbon removal in 9 hours glucose degradation intermediates and products (GDIPs)-fed cycles in both closed and open circuit in glucose-fed BESs

The current production of the pyruvate-fed tests in the glucose-fed BESs reached as high as ~3.6mA, which was much higher than the current production with glucose (Table 3-4). Likewise, the acetate accumulation in the pyruvate-fed tests reached 8.39Cmeq/L, which was much higher than the glucose-fed tests (Figure 3-3). Moreover, the propionate accumulation in the pyruvate-fed tests and the in the glucose-fed tests was similar (Figure 3-3). Besides, formate accumulation in the pyruvate-fed tests was half of that observed in the glucose-fed tests (Figure 3-3). Notably, 5.9Cmeq/L of ethanol was accumulated in the glucose-fed tests, whereas no ethanol accumulation was observed in the pyruvate-fed tests.

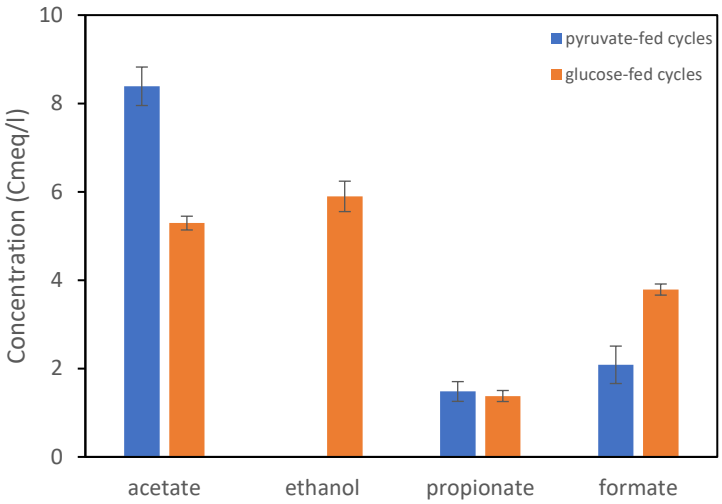

Figure 3-3 Comparison of GDIPs accumulation at 9 hours in the pyruvate-fed tests and the glucose-fed tests

9 hours pyruvate removal was similar in both of the close circuit pyruvate-fed tests and open circuit pyruvate-fed tests. Besides, the coulombic efficiency of the pyruvate-fed tests was 19.7± 6.3%, which was similar to the glucose-fed tests at 9th hours (14.8±2.1%).

Mode	Maximum current production (mA)	Coulombic efficiency (%)	Total pyruvate removal (Cmeq/L)
Closed circuit	3.6±0.3	19.7± 6.3	17.2±0.8
Open circuit	n/a	n/a	17.0±2.7

n/a: not applicable

Table 3-4 Summary of the pyruvate-fed tests in glucose-fed BESs.

In summary, in all the glucose-fed BESs in this study, acetate and formate was firstly produced from glucose via pyruvate in a rapid rate. Ethanol could continue to produce acetate and formate after glucose was depleted, but the production was very slow. The brief glucose degradation pathway and the approximate conversion rate of glucose and GDIPs in the glucose-fed BESs were shown in Figure 3-5. The calculation of the conversion rate in this figure was shown in Appendix A.

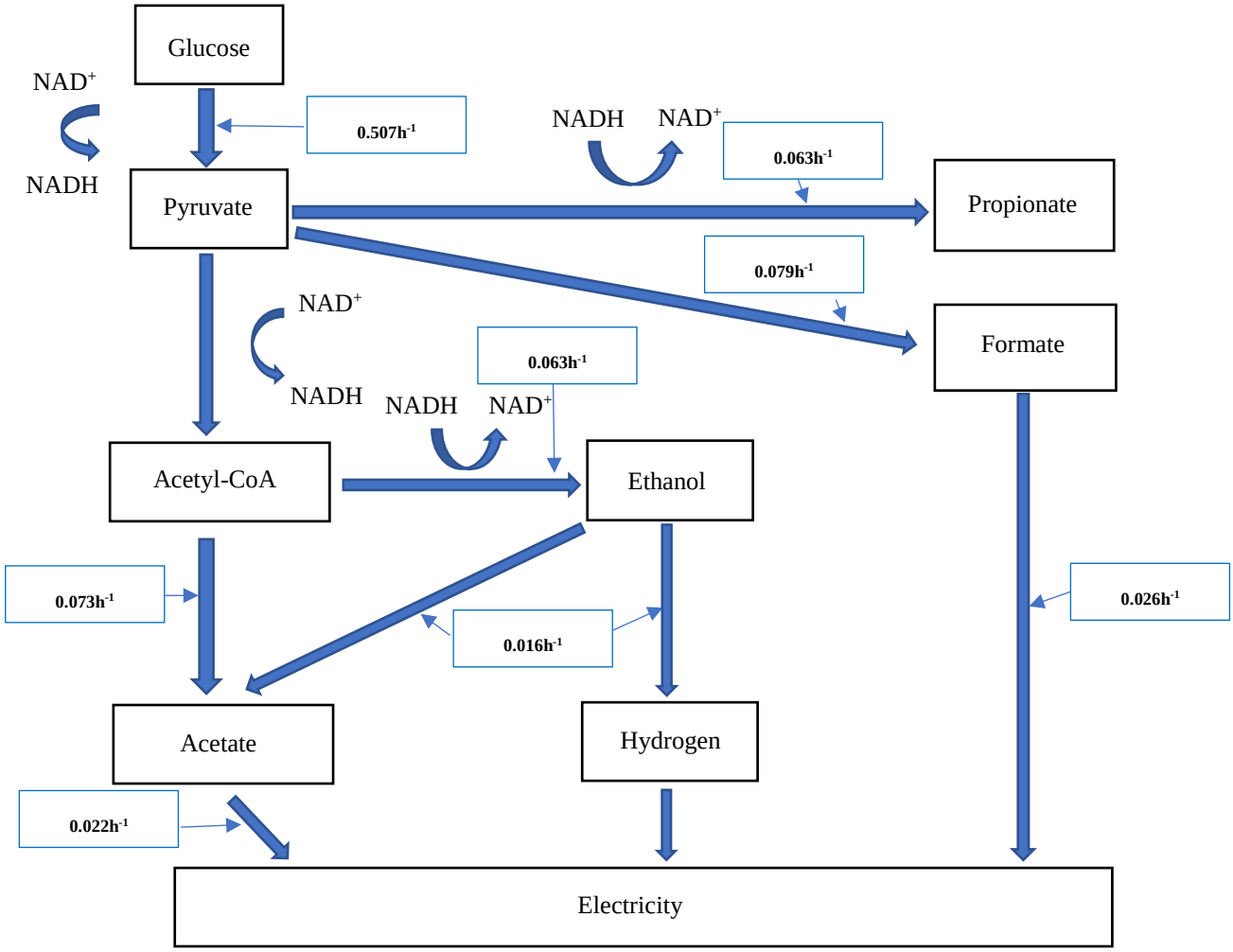

Figure 3-4 Schematic description of the possible pathway of glucose and GDIPs in the 102 hours glucose-fed cycle in the glucose-fed BESs.

3.3.3. To identify the electrogenic constraints in the glucose-fed BESs

The decrease of the coulombic efficiency in the degradation pathways of glucose and GDIPs in the glucose-fed BESs

Based on the analysis of Figure 3-1, the electron loss in the glucose-fed BESs was due to the degradation of glucose in first 9 hours and the degradation of GDIPs after 9th hour until 102nd hour. Figure 3-2 showed the electron balance of the effluent at 9th hour and 102nd hour in the glucose-fed cycle in a selected glucose-fed BES based on the data in Figure 3-1 and Table 3-1. In particular, glucose was almost depleted at 9th hour while the accumulation of GDIPs at 9th hour were acetate, propionate, formate and ethanol, which respectively accounted for 23.5%, 9.0%, 12.6% and 21.2% of the initial glucose feed in terms of the electron balance. Based on the coulombic efficiency of glucose-fed BESs in Table 3-1, Only 2.2% of the electron from the initial glucose feed was used for current production in the first 9 hours, and therefore 12.6% of the electrons from initial glucose feed was consumed by non-electrogenic activities in this period (Figure 3-6). After glucose was depleted from 9th hour to 102nd hour, acetate, formate and ethanol was continued to be consumed (Figure 3-1). The accumulation of ethanol at 102nd hour was decreased to 4.1% of the electrons from the initial glucose feed while acetate and formate was depleted. In contrast, the accumulation of propionate at 102nd hour increased to 10.0% of the electrons from the initial glucose feed. Additionally, the final encapsulated electron in hydrogen and methane at 102nd hour accounted for only <1% of the total consumed electrons. The electron from the initial glucose feed for current production, however, increased to 25.4% at 102nd hour. The electron from the initial glucose feed consumed by non-electrogenic activities at 102nd hour also increased and reached 39.3%, and therefore the non-electrogenic electron loss between 9th hour and 102nd hour were ~26.7% as 12.6% of the electrons from initial glucose feed was consumed by non-electrogenic activities in first 9 hours (Figure 3-6). when assuming that:

1. The electron loss of the degradation pathways of acetate, ethanol and formate in the glucose-fed tests was similar to their individual-fed tests in the glucose-fed BESs;

2. There was no major production of either acetate, ethanol and formate between 9th hour and 102nd hour in this test.

Therefore the difference of the availabilities of acetate/formate/ethanol between 9th hours and 102nd hour were used to calculate the total consumed electron. In which case, the non-electrogenic loss of the degradation of acetate, formate or ethanol between 9th hour and 102nd hour in this test were ~6.6%, ~9.5 or ~11.7% respectively. The detailed calculation of these three electron losses was shown in Appendix B.

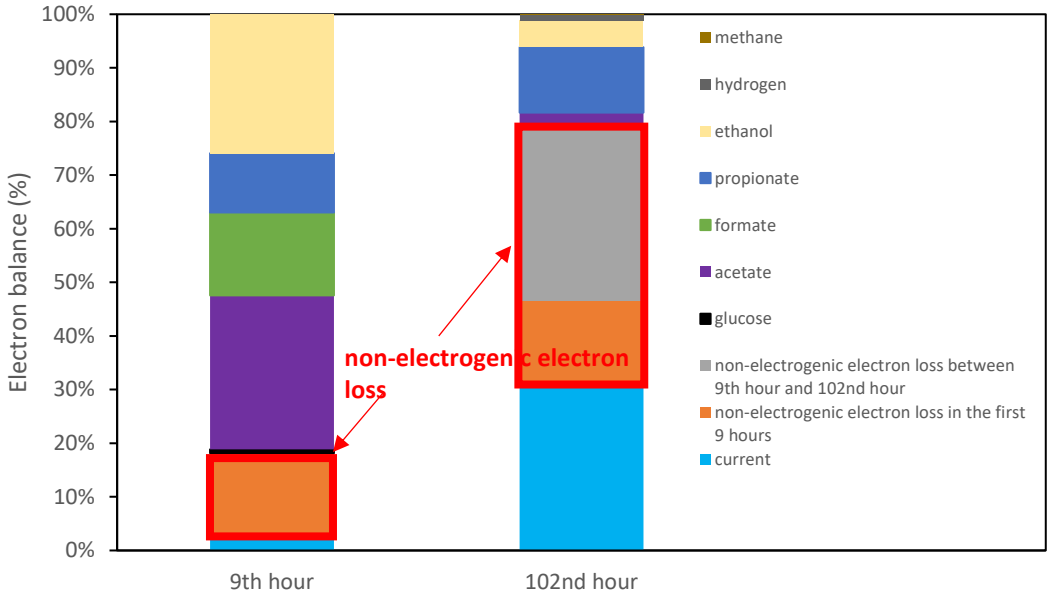

Figure 3-5 The electron distribution of effluent of the glucose-fed cycle in a selected glucose-fed BES at 9th hour and 102nd hour.

The minimum availabilities of acetate and formate for saturated current production in the glucose-fed BESs.

We inferred that acetate and formate were the major electrogenic GDIPs in the glucose-fed BESs. In which case, the minimum availabilities of either acetate or formate for the saturated current production in the glucose-fed BESs was evaluated. In particular, the relationship between the availabilities of acetate and the current production in the glucose-fed BESs was fitted with nonlinear regression (Figure 3-6A). The predicted maximum current production in the glucose-fed BESs with acetate was ~5.8mA. On the other hand, the *Ks* value of the such current production was 6.24Cmeql/L, and therefore the minimum availabilities of acetate for the saturated current production in the glucose-fed BESs was 12.48Cmeq/L (6.24mM). With the same nonlinear regression, the predicted maximum current production in the glucose-fed BESs with formate was ~1.53mA (Figure 3-6C). The *Ks* value of the such current production was 3.80Cmeql/L, and therefore the minimum availabilities of formate for the saturated current production in the glucose-fed BESs was 7.60Cmeq/L (7.60mM).

However, the maximum accumulation of acetate and formate were only 5.9Cmeq/L and 3.2Cmeq/L respectively in the 102 hours glucose-fed cycle in the glucose-fed BESs (Figure 3-1). In particular, the individual acetate test shared a similar fit curve with the variation of acetate availability in the 102 hours glucose-fed cycles in Figure 3-1 (Figure 3-6B). On the other hand, the variation of formate in the 102 hours glucose-fed cycle in Figure 3-1 was independent of the current production in the glucose-fed BESs (Figure 3-6D). Therefore, acetate was the major electrogenic molecule and the shortage of acetate was a major electrogenic constraint in the glucose-fed BESs.

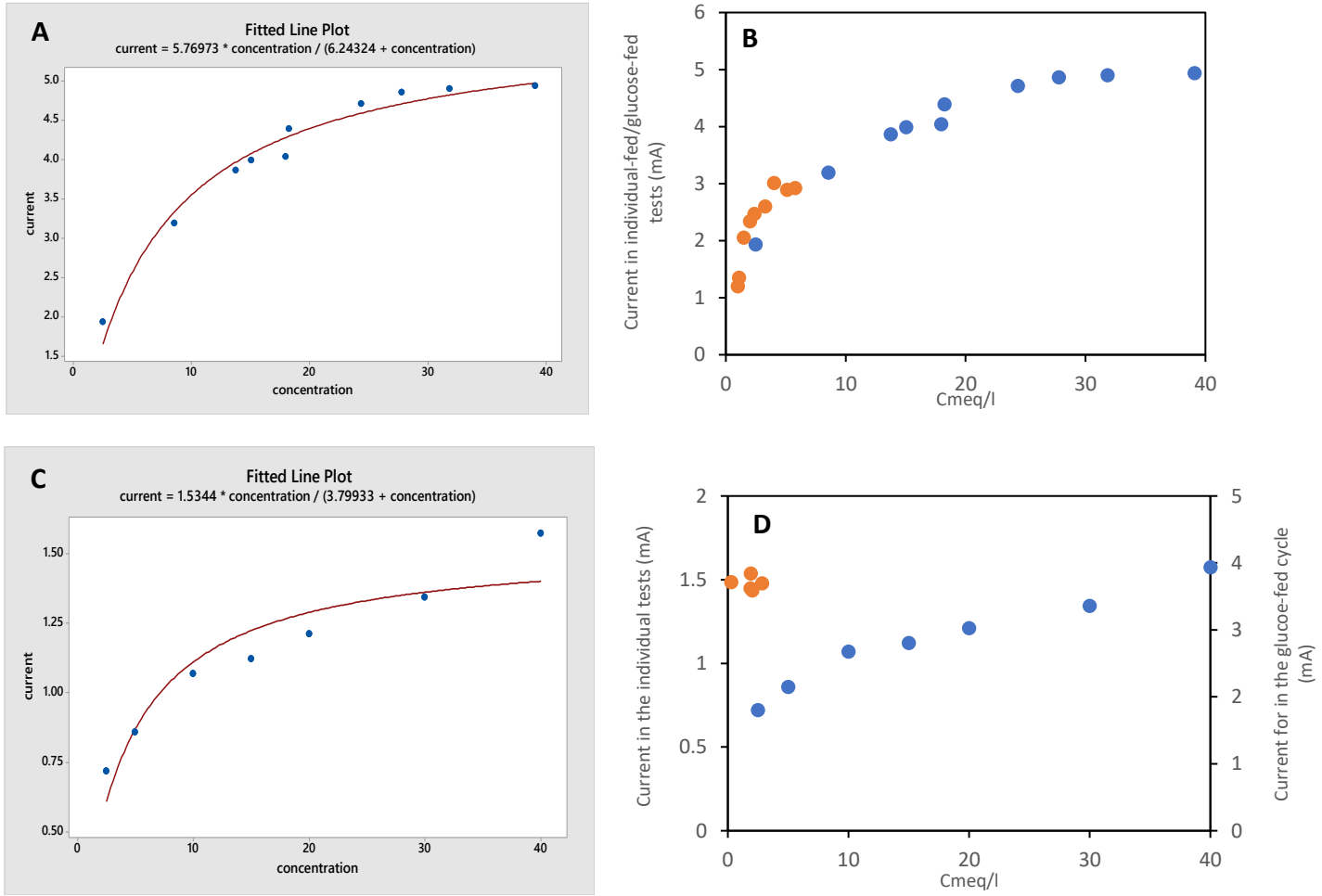

Figure 3-6 The relation of the availability of acetate(A-B), formate (C-D) and the current production in the glucose-fed BESs: (orange circles) glucose-fed cycles; (blue circles) acetate/formate-individual tests.

The effect of the pathway of ethanol and propionate on the availability of acetate in the glucose-fed BESs.

The effect of the presence of ethanol and propionate on the electrogenic performance of the glucose-fed BESs was investigated here. Figure 3-7 showed that the current production from the acetate+formate+ethanol+propionate tests was similar to the current production from the acetate+formate tests in the glucose-fed BESs. This demonstrates that the presence of ethanol and propionate did not suppress the current production in the glucose-fed BESs when acetate and formate were sufficient.

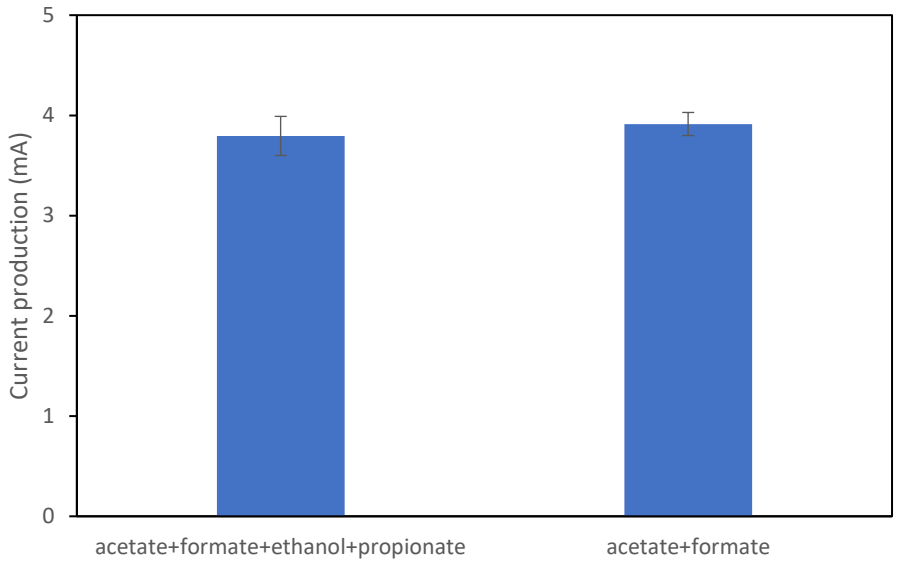

Figure 3-7 The current production in the saturated acetate+formate tests and the saturated acetate+formate+ethanol+propionate tests in the glucose-fed BESs

In order to investigate whether hydrogen accumulation caused the accumulation of ethanol and propionate in the 102 hours glucose-fed cycle in the glucose-fed BESs, the threshold concentration of hydrogen and acetate for ethanol-based acetogenesis and propionate-based acetogenesis in the glucose-fed BESs was determined. Moreover, in order to investigate the thermodynamic feasibility of hydrogenotrophic methanogenesis and homoacetogenesis for hydrogen scavenging in the glucose-fed BESs, the threshold concentration of hydrogen and acetate for these two reactions were also determined. The detailed calculation was demonstrated in Appendix C. The hydrogen concentration in glucose-fed BESs at both 24th hour and the 102nd hour were below the ethanol-based acetogenesis slopes (Figure 3-8). Therefore, the hydrogen accumulation in glucose-fed

BESs was thermodynamically favoured to ethanol-based acetogenesis. In contrast, the hydrogen concentration in the glucose-fed BESs at both the 24th hour and the 102nd hour were above the propionate-based acetogenesis slopes (Figure 3-8). Therefore, the hydrogen accumulation in glucose-fed BESs was not thermodynamically favoured to propionate-based acetogenesis. Since the saturated acetate concentration for current production in the glucose-fed BESs was ~12.48Cmeq/L (log acetate = -2.20), hydrogen $<4.5\times10^{-4}$atm was needed to trigger propionate-based acetogenesis in the glucose-fed BESs (Figure 3-8). In addition, the hydrogen concentration in the glucose-fed BESs at both the 24th hour and the 102nd hour were above both hydrogenotrophic methanogenesis and homoacetogenesis (Figure 3-8). Therefore, both hydrogenotrophic methanogenesis and homoacetogenesis was thermodynamically favoured at both 24th hours and 102nd hours in the 102 hours glucose-fed cycle. The blue square represents the optimal conditions for hydrogen and acetate promoting acetogenesis whilst repressing methanogenesis and thus both high current production and high coulombic efficiency in the glucose-fed BESs were achieved in such conditions (Figure 3-8).

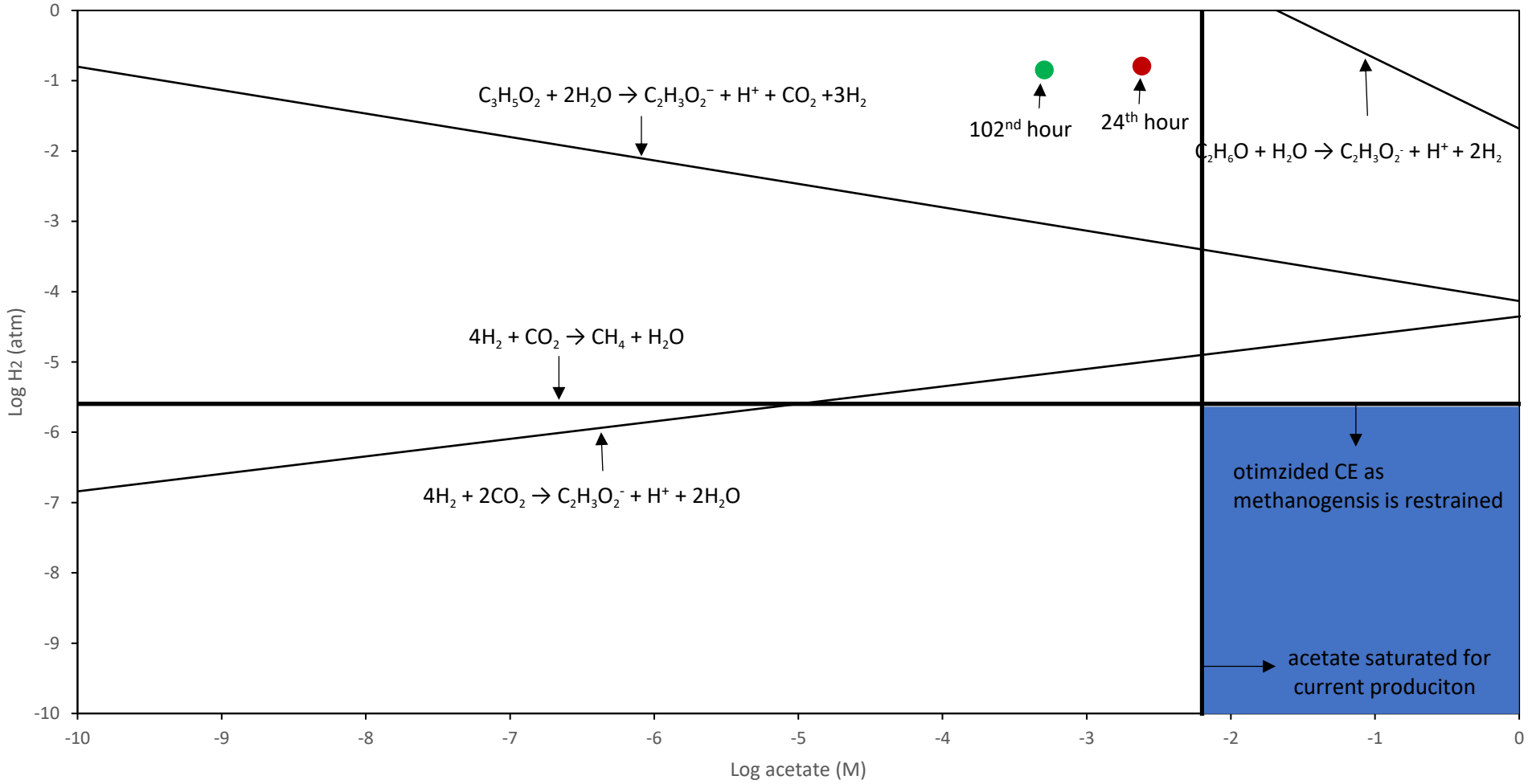

Figure 3-8 Thermodynamic feasibility of the acetate production related-reactions in glucose-fed BESs.

In order to investigate whether anode potential prevent the current production from ethanol and propionate in the glucose-fed BESs, the threshold anode potential and the threshold concentration of propionate/ethanol for current production was evaluated. Figure 3-9 shows that the potential (-150mV) in this study was higher than threshold value of the anode potentials for both propionate and ethanol-based current production when the concentration of these two GDIPs reached the peak value in the glucose-fed cycle in the glucose-fed BESs. Therefore, neither propionate-based current production nor ethanol-based current production was constrained by anode potential.

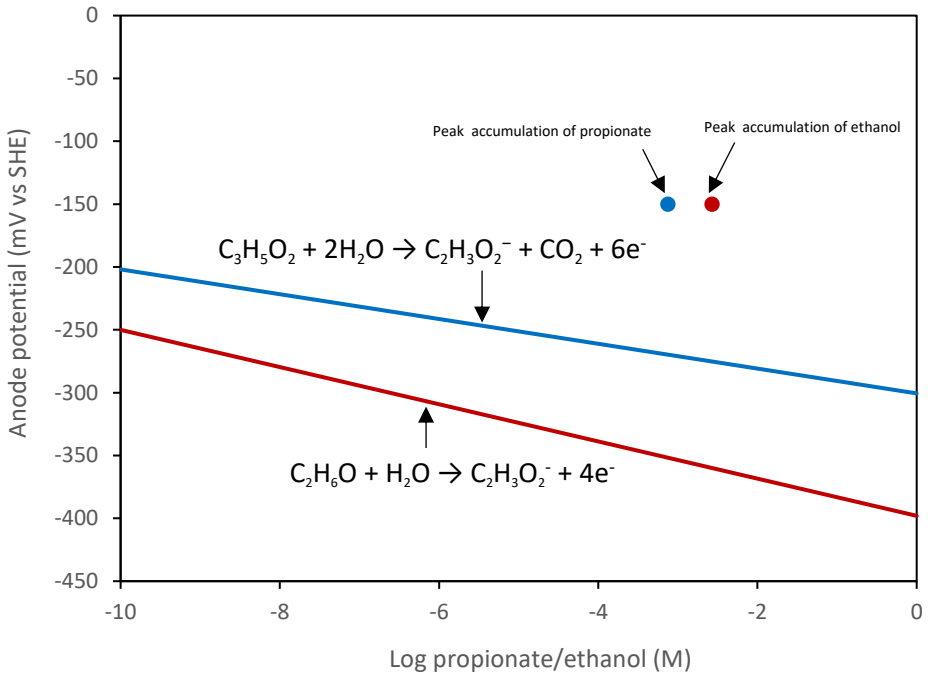

Figure 3-9 The relationship between anode potential and the propionate/ethanol-based current production in the glucose-fed BESs.

The comparison of the electrogenic performance between the glucose-fed BESs with optimized feed and the acetate-fed controls

In order to identify the electrogenic constraints in the glucose-fed BESs other than the low availabilities of acetate and formate from glucose degradation, the electrogenic performance of the glucose-fed BESs applied with optimized feeds was investigated. In particular, the coulombic efficiency in the acetate+formate-fed tests in the glucose-fed BESs was ~18.9%, which was similar to both of the glucose-fed cycle (~14.8%) and the formate-fed cycle (~26.9%) in the glucose-fed BESs (Table 3-5). In contrast, the coulombic efficiency in the acetate-fed tests in the glucose-fed BESs (~75.2%) reached a similar level to the acetate-fed controls (~78.4%) (Table 3-5). On the other hand, the maximum current production from both of the acetate+formate-fed tests and the acetate-fed tests in glucose-fed BESs reached ~3.9mA, which was higher than the maximum current production in the glucose-fed cycles in the glucose-fed BESs (Table 3-5). However, the current of neither cases reached the similar level of the current production in the acetate-fed controls (Table 3-5). Therefore, there were electrogenic constraints other than the low availabilities of acetate and formate to cause the inferior current production of the glucose-fed BESs, compared with the acetate-fed controls.

Reactor	Feed	Maximum current production (mA)	Coulombic efficiency (%)
Glucose-fed BESs	Glucose	2.3±0.2	14.8±2.1
Glucose-fed BESs	Formate	2.4±0.7	26.9±2.1
Glucose-fed BESs	Acetate+formate	3.9±0.1	18.9±3.8
Glucose-fed BESs	Acetate	3.8±0.1	75.2±6.4
Acetate-fed controls	Acetate	6.5±0.2	78.4±1.1

Table 3-5 The electrogenic performance of the BESs with different feed.

A relationship between the coulombic efficiency and the current production in these BESs with different feeds was built (Figure 3-10). In particular, glucose feed leaded to the lowest coulombic efficiency and current production. In contrast, acetate feed caused the highest current production and coulombic efficiency. Formate feed, however, decreased the coulombic efficiency in regardless of the presence of acetate feed. In which case, acetate feed was in responsibility to high current production in the glucose-fed BESs whereas glucose and formate feed caused non-electrogenic electron loss and low coulombic efficiency in the glucose-fed BESs.

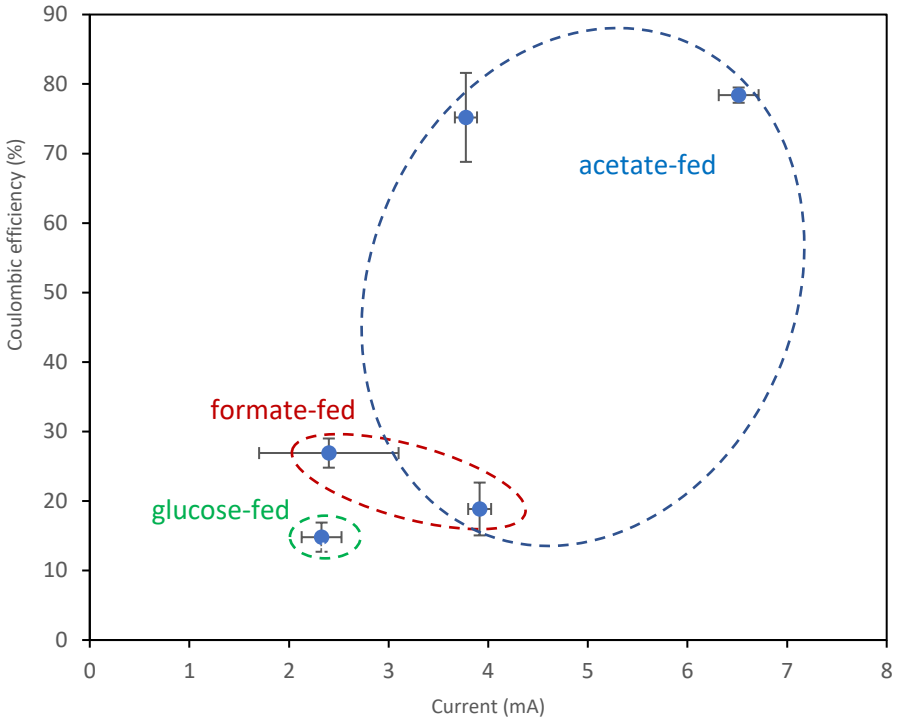

Figure 3-10 The current production and coulombic efficiency in the glucose-fed BESs with acetate/formate/acetate+formate/glucose and the acetate-fed controls with acetate.

3.3.4. The electrogenic microorganisms in the glucose-fed BESs.

Geobacteraceae was predominant on the anodic microbial communities of the acetate-fed controls as they occupied 91% of (Figure 3-11). *Geobacteraceae* was also a major group in the anodic microbial communities of the glucose-fed BESs, but the proportion decreased to 31%. *Aeromonadaceae* and *Acidaminococcaceae* were the second biggest groups in the anodic microbial communities of the glucose-fed BESs as they accounted for 20.4% and 20.7% of the anodic microbial communities respectively. *Bacteroidaceae* and *Enterobacteriaceae* were also found in the anodic microbial communities of the glucose-fed BESs as their proportions were 7.9% and 6.8% respectively (Figure 3-11).

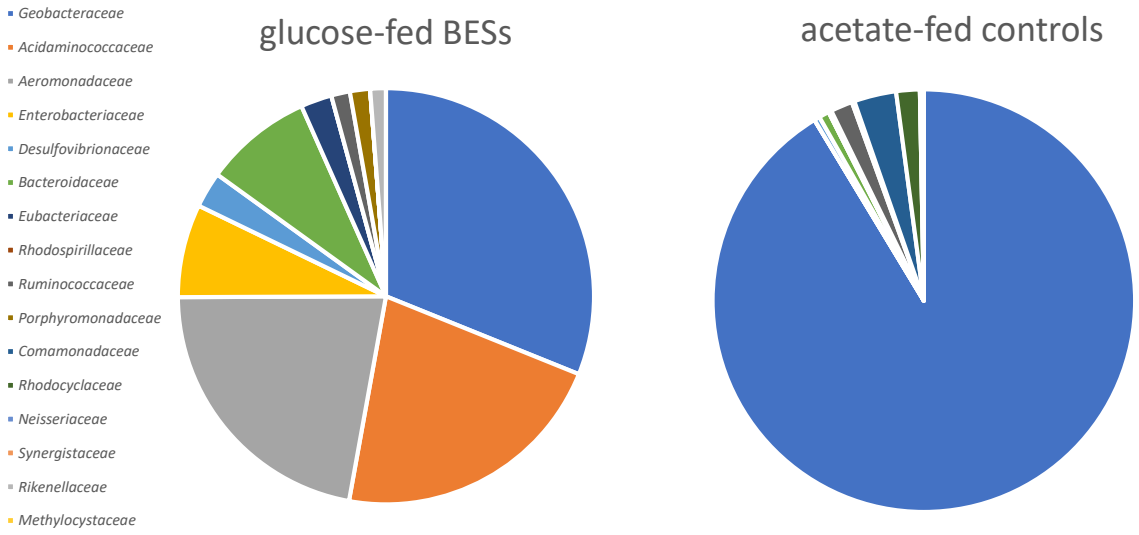

Figure 3-11 Summary of selected taxonomy of anodic microbial communities in the glucose-fed BESs and the acetate-fed controls at family level.

3.4. Discussion

This study used glucose as a model of complex substrate to identify the electrogenic role of glucose and GDIPs. Moreover, the effect of the degradation pathway of glucose on the current production and non-electrogenic electron loss in glucose-fed BESs was investigated.

The major electrogenic role of acetate and the constraints of acetogenesis in the pathways of glucose and GDIPs in the glucose-fed BESs

Acetate was identified as, by far, the most effective electrogenic GDIP in the glucose-fed BESs as the highest current production and coulombic efficiency was achieved in the individual acetate-fed cycle in the glucose-fed BESs. The importance of acetate for high current production in glucose-fed BESs was emphasized in earlier work (Freguia et al., 2008). This study further pointed out that 12.48Cmeq/L (6.24mM) acetate was needed for saturated current production in the glucose-fed BESs, which was similar to the acetate saturation point in fermentation products mixture-acclimated BESs (Torres et al., 2007). In contrast, lower saturation point of 6Cmeq/L in a *Geobacter*-cultured BESs and higher saturated point at 20Cmeq/L in wastewater-acclimated BESs (where normally the proportion of *Geobacter* in anodic microbial communities was low) was observed (Marsili et al., 2008; Sleutels et al., 2011). Therefore, acetate saturation point probably depends on the anodic microbial communities in BESs. Moreover, it seems that the proportional abundance of the *Geobacter* in the anodic microbial communities positively related to the acetate saturated point. Only degradation pathways of glucose and ethanol produced detectable acetate in the glucose-fed BESs in this study. Therefore, the glucose-fed cycle in the glucose-fed BESs (Figure 1-1) relied on the glucose degradation in the first 9 hours and the ethanol degradation between 9^{th} hour to 102^{nd} hour, when glucose was depleted, to produce acetate, and consequently to produce current. However, neither of these pathways permitted acetate accumulation >12.48Cmeq/L.

In particular, the acetate production from glucose degradation in Figure 1-1 could only accounted for up to 32% of the total glucose in this study (assuming acetate was the only electrogenic substance during that period). However, the acetate production in conventional glucose fermentation system could achieve up to 2/3 carbon equivalent of the total glucose. This indicates that a maximum of ~13.4Cmeq/L acetate production from

20Cmeq/L glucose could be achieved in this study. This was sufficient to support the high acetate availability for the current production in the glucose-fed BESs. Notably, the ethanol accumulation was avoided and the saturated acetate accumulation was reached in the individual pyruvate-fed tests in the glucose-fed BESs in this study (Figure 3-3). According to the proposed pathways in the glucose-fed BESs (Figure 3-4), ethanol production from Acetyl-CoA requires NADH, which was partially produced by anaerobic glycolysis during glucose degradation. Therefore, this inhibition of ethanol production in the pyruvate-fed tests in the glucose-fed BESs was possibly due to the lack of NADH from glycolysis. It inferred that the acetogenesis in the glucose-acclimated system could be enhanced by regulating the $NADH/NAD^+$ pool in glycolysis, and to produce sufficient acetate for the current production in the glucose-fed BESs. It was surprisingly that the increase of initial applied glucose did not result in a higher current production in the glucose-fed BESs at 9^{th} hour and 15^{th} hour in this study (Figure 3-2). In theory, since glucose degradation was faster than acetate consumption in the glucose-fed cycle, more acetate should accumulate in the glucose-fed BESs when initial glucose was increased. However, anodic microorganism could switch to biomass synthesis when the surface area of anode ($38cm^2$) was limited to high glucose concentration in glucose-fed BESs (Velasquez-Orta et al., 2011). The anode surface in this study ($40cm^2$) was similar to their study while the glucose concentration was even higher in this study. In which case, the function of anodic microorganisms could also be limited by the surface area of anode in the glucose-fed BESs with higher glucose feed in this study. Consequently, acetate production and current production was barely changed in such condition.

Ethanol-based acetate production was unable to achieve this 12.48Cmeq/L of acetate in the glucose-fed BESs between 9^{th} hour and 102nd hour in the glucose-fed cycle either. The ethanol consumption rate was only $\sim 0.016 h^{-1}$ in the glucose-fed BESs, which was very similar to those ethanol-acclimated BESs (Kim et al., 2007; Parameswaran et al., 2009). However, this rate was far behind the maximum electrogenic acetate consumption rate and glucose degradation rate in the glucose-fed BESs in this study. In which case, the major acetate production in the glucose-fed BESs was possibly attributed to glucose degradation rather than ethanol degradation.

The accumulation of propionate in the glucose-fed BESs was also considered as a reason of the low acetate availability. The analysis shown in Figure 3-8, propionate-based acetate

production in the glucose-fed BESs was inhibited by hydrogen accumulation. Previous study suggests that hydrogen accumulation in BESs could be removed by methanogens, homoacetogens and electrogenic microorganisms (Parameswaran et al., 2009). Electrogenic microorganism acted as hydrogen scavenger in the glucose-fed BESs in this study as current production was produced from the individual hydrogen-fed tests. However, this electrogenic hydrogen removal failed to meet the requirement of the low hydrogen ($<4.5\times10^{-4}$atm) for propionate-based acetate production in this study. The hydrogen removal effort from both methanogenesis and homoacetogenesis was minor in the glucose-fed BESs in this study. In particular, methane and methanogens were negligible in the headspace of the glucose-fed BESs and the anodic microbial communities respectively. Notably, it reported that methanogens primarily presented in suspended cells in BESs (Parameswaran et al., 2010). However, the glucose-fed BESs was run in batch-fed mode in this study, and thus any suspended methanogens cells were presumably constantly washed out. In which case, methanogens was not enriched in the glucose-fed BESs and this possibly explains the minor effort of hydrogen removal by methanogenesis in the glucose-fed BESs. On the other hand, hydrogen removal by homoacetogenesis was also minor in the glucose-fed BESs in this study because acetate accumulation was negligible in the hydrogen tests in the glucose-fed BESs. However, the presence of homoacetogenesis in the glucose-fed BESs could not be ruled out in this study as the duration of the individual hydrogen-fed tests was short (~2 hours) for the accumulation of acetate. Interestingly, *Geobacter*, the major electrogenic microorganism in the glucose-fed BESs in this study, could stimulate the propionate degradation via a DIET (direct interspecies electron transfer) between *Geobacter* and methanogens regardless of the presence of hydrogen constraints in an anaerobic system (Zhao et al., 2016). The pili for the connection of DIET were also the ones that connected *Geobacter* and the electrode in BESs (Richter et al., 2009). This suggests that the possibility of electrogenic syntrophic propionate degradation can occur in BESs. (Ishii et al., 2014) showed complete slow propionate degradation (~0.06Cmeq/L·h^{-1}) in 168 hours in a glucose-fed BESs. ~65% of the peak current production was still maintained and propionate was the remaining organic after the depletion of acetate in their glucose-fed BESs. Therefore, electrogenic propionate degradation possibly presented in their study. This study further suggests that the electrogenic propionate degradation was theoretically triggered when anode potential is > -200mV and propionate is <1M. However the

electrogenic propionate degradation was not present in the glucose-fed BESs in this study although these two conditions were satisfied. In which case, the feasibility of the electrogenic propionate degradation in BESs needs to be further studied.

The electrogenic role of formate in the glucose-fed BESs

Formate was also an electrogenic GDI in the glucose-fed BESs in this study. This was because major current was produced while no other GDIPs accumulation was detected in the 9 hours in the formate-fed tests (Table 3-2 and Table 3-3). Moreover, even if acetate was produced from formate and rapidly consumed by electrogenic processes, it was not the only electrogenic pathway in the formate-fed tests because current was produced at -350mV in the glucose-fed BESs, where electrogenic acetate oxidation (-280mV, at 25°C, pH=7.0) was thermodynamically suspended while electrogenic formate oxidation was still feasible (-410mV, at 25°C, pH=7.0). However, since the redox potential of hydrogen oxidation (-414mV, at 25°C, pH=7.0) was close to the redox potential of formate oxidation, it could not rule out the electrogenic hydrogen oxidation in the formate-fed tests in the glucose-fed BESs at this anode potential. Nevertheless, the current production with hydrogen was much lower than formate in the individual tests in glucose-fed BESs (Table 3-2). This indicates that any putative electrogenic hydrogen oxidation was unable to fully support the current production with formate in the glucose-fed BESs. Therefore, direct electrogenic formate degradation was present in the glucose-fed BESs in this study. However, due to the relatively low current production and significant electron loss in the formate-fed test in the glucose-fed BESs, electrogenic formate oxidation was not a priority for electrogenic processes in the glucose-fed BESs. Notably, similar current production from formate and acetate in *Geobacter sulfurreducens*-cultured BESs with same biomass abundance was reported (Speers and Reguera, 2012). Because the species level of the anodic microbial communities in the glucose-fed BESs in this study was not determined, whether *Geobacter sulfurreducens* was the only species in *Geobacteraceae* in this study was unknown. It shown that acetate could also be used by *Geobacter* microorganisms other than *Geobacter sulfurreducens* (Rotaru et al., 2015). This indicates that acetate was possibly also used by other *Geobacter* microorganisms in the glucose-fed BESs whereas formate was not able to do so in this study. This therefore caused the lower current production from the formate-fed tests than the acetate-fed tests.

The role of glucose in the glucose-fed BESs

This study showed that glucose oxidation was not a major direct electrogenic processes in the glucose-fed BESs, which was consistent with previous studies (Freguia et al., 2008; de los Ángeles Fernandez et al., 2016). This was because that the current production in the glucose-fed BESs was barely affected by the absence of glucose when GDIPs were present. In particular, *Aeromonadaceae* was the second largest group (~23.7%) in the anodic microbial communities of the glucose-fed BESs. As an *Aeromonadaceae* specie, *Aeromonas ISO2*-3, could directly use glucose to produce current and generate acetate in BESs (Chung and Okabe, 2009), which explains the current production at the beginning step of the glucose-fed cycle in the glucose-fed BESs when the concentration of GDIPs were low. However, the current production from glucose was relatively low (~0.03A/m^2 at 100Ω) in (Chung and Okabe, 2009), compared to the current production in the glucose-fed BESs in this study (~0.63A/m^2). Therefore, the direct electrogenic contribution of glucose oxidation by *Aeromonadaceae* in glucose-fed BESs was possibly low. Moreover, *Enterobacteriaceae* accounted for ~5.6% of the anodic microbial communities in the glucose-fed BESs. In particular, *Klebsiella pneumoniae*, a species from *Enterobacteriaceae*, was able to directly use glucose for current production. Relatively high current production (~1.2A/m^2 at 150Ω) from glucose in *Klebsiella pneumoniae* cultured MFCs was reported (Zhang et al., 2008). However, the cyclic voltammetry of the *Klebsiella pneumoniae*-biofilm in their study suggests that the current production was negligible at the -150mV, which was the applied anode potential in the glucose-fed BESs in this study. Moreover, *Enterobacteriaceae* only occupied a small portion on the anodic microbial communities of the glucose-fed BESs in this study. It inferred that the direct electrogenic contribution from glucose oxidation by *Enterobacteriaceae* was also low in this study.

In which case, the glucose-fed BESs did not achieve the theoretical maximum current production and energy recovery from glucose oxidation in this study. In fact, glucose contains more energy than acetate (glucose = 1438kJ/mol;stoichiometric equivalent of acetate = 1125kJ/3mol at pH=7.0, 25°C) (Freguia et al., 2008). However, because glucose was not primarily electrogenic, a more positive anode potential will be set in such BESs when artificial anode potential control is absent (~-220mV of acetate compared to ~-

400mV of glucose (Gildemyn et al., 2017)). This resulted lower cell voltage in BESs and lower current production as well as lower energy recovery in such glucose-fed BESs.

The kinetic advantage of non-electrogenic glucose degraders was considered as the reason of this minor direct electrogenic contribution from glucose in this study. For instance, non-electrogenic glucose degradation process was 2.2Cmeq/L·h^{-1} in this study. This was much faster than *Geobacter*-driven acetate oxidation (0.17Cmeq/L·h^{-1}) in this study, which although was considered as one of the most rapid electrogenic processes in BESs by far. The electrogenic processes of *Aeromonas ISO2-3* was even slower than *Geobacter* because *Aeromonas ISO2-3* conducted a voltammetry with smaller peak than *Geobacter* (Chung and Okabe, 2009). Therefore, it is difficult to avoid the non-electrogenic glucose degraders in glucose-fed BESs in real applications. In which case, anodic mixed culture of glucose degraders and electrogenic intermediates user are more adaptive in glucose-fed BESs applications even though some energy from glucose are inevitable lost.

The attribution of electron loss in the glucose-fed BESs.

The coulombic efficiency in glucose-fed BESs was 45.8%, which was much lower than the 78.5% in the acetate-fed controls. In particular, the first 9 hours glucose degradation period caused significant electron loss (~12.6%), which accounted for ~32% of the total electron loss in the 102 hours glucose-fed cycle. Moreover, based on the analysis in Figure 3-6, the non-electrogenic electron loss between 9^{th} hour and 102^{nd} hour (~26.7%) was very similar to the sum of electron loss (~22.6%) in the degradation pathway of acetate (~5.6%), ethanol (~7.7%) and formate (~9.3%). Therefore, it suggests that the pathway of glucose, formate and ethanol caused the major electron loss in the glucose-fed BESs. The largest electrons loss (~26%) was caused by biomass terminal electron balance in a mixed cultured glucose-acclimated BES (Lee et al., 2008). Therefore, the biomass synthesis was possibly the major non-electrogenic electron sinks in this study although the change of biomass in glucose-fed cycle in the glucose-fed BESs was not measured due to the concern of anodic microbial communities damaging. It reported that *Aeromonadaceae,* as one of the putative major glucose users in this study, could only deliver ~5% of the electron to electrogenic process in BESs while ~29% was restored in biomass (Chung and Okabe, 2009) and the rest was restored in acetate. In contrast, high coulombic efficiency (~80%) was achieved in the glucose-fed BESs with direct

electrogenic glucose user *Rhodoferax ferrireducens*, even the current production was low (~0.07A/m^2) (Chaudhuri and Lovley, 2003). Therefore, the high electron loss in the glucose-fed BESs in this study was possibly because of that massive energy between the anode potential (-150mV) and standard redox potential of glucose (-400mV) was left for the biomass synthesis of non-electrogenic glucose users (Gildemyn et al., 2017). In which case, to develop the efficient direct electrogenic glucose oxidizer was important to minimize the energy for the synthesis of non-electrogenic biomass, and hence improve the coulombic efficiency in glucose-fed BESs.

The formate degradation pathway also caused major electron loss in glucose-fed BESs. In particular, non-electrogenic formate degradation was the major reason of this electron loss as the formate consumption in the open circuit formate-fed tests reached nearly half of the formate consumption in the close circuit formate-fed tests in the glucose-fed BESs (Table 3-3). Low coulombic efficiency (~5.3%) was also observed in a formate-acclimated BESs (Ha et al., 2008). Although the microaerobic consumption was the reason of low coulombic efficiency in their study, which was not likely to be case in this study since no significant aerobic microorganisms was detected in the anodic microbial communities of the glucose-fed BESs. Nearly half of the electron (~44.1%) in ethanol pathway were lost in non-electrogenic sinks in the glucose-fed BESs, which was similar to previous ethanol-fed BESs (49% to 60%) (Parameswaran et al., 2009; Torres et al., 2007). Although methane accounted for the major electron loss in their ethanol-fed BESs whereas the electron loss caused by methane production from ethanol degradation pathway was negligible in this study (Parameswaran et al., 2009; Torres et al., 2007). Notably, the standard error of coulombic efficiency in the individual ethanol tests in this study was large (±21.5%) due to the low consumption of ethanol in such tests (<1Cmeq/L). The consumption of biomass and organic residues from previous cycles also possibly caused errors in the assessment of coulombic efficiency in this case. However, because of the concern of the impact of ethanol on the glucose-acclimated microbial communities, long terms individual ethanol-fed test in the glucose-fed BESs was not carried out in this study. The propionate consumption was negligible in both of the 102 hours glucose-fed cycle and the individual propionate-fed tests in the glucose-fed BESs. Therefore, the electron loss in the propionate degradation pathway in the glucose-fed BESs was insignificant in this study. However, the coulombic efficiency of propionate-

acclimated BESs could reach as low as ~50% where biomass synthesis (~15.25% to 27.03%) and methane (~22.9% to 41.1%) was recognized as the major non-electrogenic electron sinks (Hari et al., 2016). This indicates that propionate degradation pathway could cause non-electrogenic electron loss in the glucose-fed BESs in this study when propionate degradation occurred.

Anodic microbial communities

The current production in the glucose-fed BESs with sufficient acetate and formate failed to level the current production with the acetate-fed controls (Figure 3-7). Both of acetate and formate were able to be directly used by *Geobacter*-like microorganisms (Speers and Reguera, 2012). Therefore, *Geobacteraceae* might engage in the major electrogenic processes in the glucose-fed BESs in this study. However, the abundance of *Geobacteraceae* in the glucose-fed BESs (~31%) was lower than the acetate-fed controls (~91%). This was considered as the major reason to cause the lower current production in the glucose-fed BESs even sufficient acetate was applied. Because the peak acetate accumulation in the glucose-fed BESs was lower than the peak supplied acetate in the acetate-fed controls, this lower abundance of *Geobacteraceae* in the glucose-fed BESs was possibly caused by the shortage of acetate at the acclimation stage of glucose-fed BESs. Therefore, the availabilities of electrogenic preferred substrates such as acetate need to be maintained at acclimation stage in order to obtain abundant electrogenic microorganisms in BESs.

Implications

This study demonstrated that acetate was the only suitable electrogenic GDI in the glucose-fed BESs. High acetate availability lead to high current production and high coulombic efficiency in glucose-fed BESs with an initial feed of 20Cmeq/L of glucose. In particular, 12.48Cmeq/L acetate availability, which is equal to ~399.4mgCOD/L, needs to be achieved for high current production in glucose-fed BESs. This indicates that acetate production from glucose degradation is particularly important to the BESs-based secondary wastewater treatment with low COD strength as the total available carbon source in the influent of such wastewater was normally similar to this minimum acetate requirement. However, acetate production caused low coulombic efficiency in the glucose-fed BESs since electron was significantly lost in fermentative biomass synthesis

for acetate production in glucose-fed BESs. Therefore, complex-fed BESs possibly have high current production and low coulombic efficiency when acetate was the major electrogenic molecules. Although low coulombic efficiency is one of major barriers for optimizing volumetric efficiency (e.g. electron recovered/kgCOD·m^{3-1}) in practical scale-up BESs.

3.5. Conclusion

This study identified the major electrogenic pathways and the electrogenic constraints in the glucose-fed BESs. In particular, the current in the glucose-fed BESs was produced through the glucose degradation intermediates and products such as acetate and formate, rather than glucose. Moreover, *Geobacteraceae* was the major anodic electrogenic microorganism for such current production. The major electrogenic constraint of low current production in the glucose-fed BESs was the low production of acetate and formate from glucose degradation, because the peak accumulations of acetate and formate in the glucose-fed BESs was unable to reach the minimum availabilities requirement to produce saturated current. Moreover, low relative abundance of *Geobacteraceae* in the glucose-fed BESs was also the major electrogenic constraint to cause this low current production. On the other hand, the low coulombic efficiency in the glucose-fed BESs was mainly due to the electrons loss in the degradation of glucose, formate and ethanol, and these degradation pathways respectively leaded ~12.6%, ~9.3% and 7.7% of the decrease of the total coulombic efficiency in the glucose-fed BESs. These results illustrated the relationship between the major electrogenic pathways and the electrogenic performance in the glucose-fed BESs, and this can be used to understand the effect of the engineered parameters such as anode potentials on the electrogenic performance of glucose-fed BESs.

Chapter 4 The effect of anode potentials on the degradation pathway of glucose and the development of anodic microbial communities in glucose-fed BESs

4.1. Introduction

Glucose is an appropriate model of complex organic to study the characteristics of complex-fed bioelectrochemical systems (BESs). This is because the degradation of glucose contains multiple pathways such as glycolysis and acetogenesis. Moreover, the characteristics of these pathways in conventional glucose fermentation system were well studied (Lee and Rittmann, 2009; Temudo et al., 2007). In addition, the electrogenic role and the degradation pathways of glucose and glucose degradation intermediates (GDIPs) in glucose-fed BESs were identified in chapter 3. In particular, acetate and formate were the major electrogenic GDIPs in the glucose-fed BESs at anode potential of -150mV (vs SHE). Moreover, acetate was the most effective electrogenic GDI in the glucose-fed BESs for high current production and high coulombic efficiency. Besides, *Geobacteraceae* was identified as the major electrogenic microorganism in the glucose-fed BESs.

However, the electrogenic constraints was presented in the glucose-fed BESs since both of the current production and coulombic efficiency in such BESs were much lower than the acetate-fed controls. In particular, the peak acetate availability in glucose-fed BESs was only ~2.95mM in such BESs, which was lower than the saturated acetate availability (~6.24mM) for current production. This was because of the low acetate production from glucose and the GDIPs such as ethanol and propionate. The proposed reasons of this low acetate production was firstly because of the excess-production of the reducing equivalents such as ethanol and propionate from glucose rather than acetate, which decreased the acetate production from glucose. Moreover, because of the presence of the thermodynamic constraints of hydrogen accumulation, the acetate production from propionate in the glucose-fed BESs was minor. Besides, the maximum current production from the glucose-fed BESs with sufficient acetate was lower than the acetate-fed controls with sufficient acetate. Because the anodic microbial communities of the acetate-fed controls was predominated by *Geobacteraceae* (~91%) while *Geobacteraceae* in the anodic microbial communities of the glucose-fed BESs was much lower (~31%), lack of

Geobacteraceae in the anodic microbial communities in glucose-fed BESs was also recognised as a major constraint for the current productions. In which case, in order to optimize the electrogenic performance in glucose-fed BESs, encouraging the acetate production from both glucose and GDIPs is needed. Moreover, the abundance of *Geobacteraceae* in the anodic microbial communities in glucose-fed BESs needs to be increased.

Notably, the degradation pathway of glucose in glucose fermentation system can be regulated by the intracellular NADH/NAD^+ pool. (Hoelzle et al., 2014b; Temudo et al., 2007). The results in chapter 3 indicates that the degradation pathway of glucose in BESs could also be regulated via intracellular NADH/NAD^+ pool because the peak acetate accumulation in the glucose-fed BESs was significantly increased when pyruvate was fed, where the NADH produced from glycolysis was absent. In particular, electrogenic microorganisms can regulate the intracellular NADH/NAD^+ pool to adapt specific redox potentials (Logan, 2008). Moreover, anode potential (E_{anode}) is considered as the terminal redox potential of the electrogenic processes. Therefore, to alter anode potential could potentially regulate intracellular NADH/NAD^+ pool of electrogenic fermenters when they are present, and thus it can alter the degradation pathway of glucose to produce more acetate. In addition, hydrogen was possibly electrogenic in BESs (Bond and Lovley, 2003). Therefore, to alter anode potential can also improve hydrogen scavenging, and consequently eliminate the thermodynamic constraints of hydrogen accumulation in the acetate production from GDIPs. In which case, anode potential in glucose-fed BESs is potentially decisive to the availabilities of the electrogenic preferred substrates such as acetate.

On the other hand, the available energy for the growth of electrogenic microorganism in BESs is described by

$$\Delta G = -knF(E_{substrate}^{0'} - E_{anode}) \quad (6)$$

Where ΔG is the possible available energy at standard condition (J) (T = 25°C, pH = 7.0), k is the moles of the substrates that involved in electrogenic processes, n is the numbers of the electron transferred in the reaction, F is the Faraday constant (96.48 J/mV), $E_{substrate}^{0'}$ is the standard redox potential of the electrogenic substrates. E_{anode} is the anode potential of BESs (mV) (Wei et al., 2010). In acetate-fed controls, the value of kn and $E_{substrate}^{0}$ is easy to be defined because acetate was normally the only electrogenic

substrate. In which case, $E_{substrate}^{0'}$ equals to $E_{acetate}^{0'}$, which is ~-280mV under standard conditions (T = 25°C, pH = 7.0). Moreover, the electrogenic kinetics of acetate oxidation determines the value of *kn* since the reaction with higher rate could transfer more electrons in a certain period. When acetate is sufficient in BESs, the electrogenic kinetics of acetate oxidation reach the maximum rate. In which case, more positive anode potentials (E_{anode}) can lead to higher value of ΔG. This provides thermodynamic advantage to electrogenic microorganisms when terminal respiring acceptor is not saturated and thus results higher abundance of the electrogenic microorganisms in the anodic microbial communities of acetate-fed controls (Wei et al., 2010). On the other hand, in the BESs acclimated with complex organics such as glucose, the value of $E_{substrate}^{0'}$ was normally higher than $E_{glucose}^{0'}$ (-430mV when T = 25°C, pH = 7.0) because the direct electrogenic effort of glucose oxidisers is minor. In which case, glucose is degraded by fermentative microorganisms to produce electrogenic preferred intermediates such as acetate and formate. This increased the $E_{substrate}^{0'}$ to more positive value and consequently decreased the available energy (ΔG) for glucose-fed BESs. Therefore, the value of $E_{substrate}^{0}$ in the BESs acclimated glucose is determined by the degradation pathway of glucose and the type of electrogenic molecules. Moreover, the relationship between electrogenic kinetics of electrogenic molecules and the availabilities of electrogenic molecules is subjected to Michaelis–Menten kinetics, and therefore this electrogenic kinetics of electrogenic molecules was also determined by the degradation pathway of glucose. Since anode potential can potentially determine the degradation pathway of glucose and the availabilities of the electrogenic molecules, the value of $E_{substrate}^{0'}$ and *kn* in glucose-fed BESs can be potentially determined by anode potential. Therefore, altering anode potential of glucose-fed BESs can improve the ΔG and increase the abundance of electrogenic microorganisms.

Previous studies frequently reported that different anode potentials could influence the anodic microbial communities and change the electrogenic performance in BESs (Dennis et al., 2016; Ishii et al., 2014; Torres et al., 2009; Wagner et al., 2010). However, there was still lack of agreement about the optimal anode potential for the electrogenic performance of BESs (Wagner et al., 2010; Zhu et al., 2014). In particular, there was still large unknown about the effect of anode potential on the availabilities of electrogenic molecules and the abundance of electrogenic microorganisms in the BESs. Consequently,

this study continued to use glucose as a model of complex organic to investigate the effect of anode potential on the degradation pathway of glucose and the availabilities of electrogenic molecules such as acetate in these glucose-fed BESs. Moreover, the effect of anode potentials on the abundance of electrogenic microorganisms in glucose-fed BESs was also investigated. In particular, the configuration of the reactors, the type of inocula and operation modes are also common variables in BESs (Logan, 2008). Therefore, in order to extensively understand the effect of anode potential on the anodic microbial communities the BESs, the effect of anode potential was compared with the effect of other variables such as configurations, inocula, operation modes on the anodic microbial communities in glucose-fed BESs. Therefore, this study is aiming:

1. To investigate the effect of anode potential on the glucose degradation profile and the peak availabilities of electrogenic molecules in glucose-fed BESs.

2. To investigate the effect of anode potential on the anodic microbial communities and the abundance of electrogenic microorganisms in BESs.

4.2. Method

4.2.1. Reactor start up

H-type reactors start up

The H-type reactors used in this chapter were described in 2.1 and Figure 2-1. The anodic media and cathodic media used in these reactors were described in 2.2. The glucose-fed BESs and the acetate-fed controls were initially fed with either 80e^-mmol/L glucose (0.61g/L) or 80e^-mmol/L acetate (0.88g/L) respectively. The conversion between the carbon equivalent of substrates and the real concentration of substrates was shown in 2.6. All the reactors were inoculated with the settled sewage from Tudhoe mill domestic wastewater treatment plant (Durham, UK). The treatment of media and inoculum was described in 2.2. All the reactors were operated in microbial electrolysis cells (MECs) mode and the anode potentials of them were stabilized at three different values: -150mV, 0mV and +200mV vs standard hydrogen electrode (SHE) through all the tests. The details of operation were described in 2.3.

Tubular reactors start up

Tubular reactors used in this chapter were described in 2.1 and Figure 2-1. The anodic media and cathodic media used in these reactors were described in 2.2. The glucose-fed BESs and the acetate-fed controls were initially fed with either 80e^-mmol/L glucose (0.61g/L) or 80e^-mmol/L acetate (0.88g/L) respectively. The glucose-fed reactors with controlled anode potentials were inoculated with the Tudhoe settled sewage. On the other hand, the glucose-fed reactors without controlled anode potentials was inoculated with Tudhoe settled sewage, Howden settled sewage, Howden activated sludge or arctic resource respectively. The information of the inocula was provided in 2.2. Moreover, the treatment of media and inoculum was described in 2.2. All the reactors were operated in microbial electrolysis cells (MECs) mode. Both potentiostat and power unit was used as the power source of MECs. The details of operation were described in 2.3.

4.2.2. Experiment design

The glucose degradation profile of the glucose-fed BESs at different anode potentials

Once acclimatized and reproducible current was obtained in the H-type reactors, these reactors were run at six individual 9 hours cycles with six anode potentials: open circuit, -

250mV, -150mV, 0, +200mV vs SHE using an initial concentration of 80e^-mmol/L glucose. The end products in the effluent of these reactors at the end of the tests was measured based on the method in 2.4. The current production in these 9 hours tests was monitored per min.

To investigate the fate of GDIPs (glucose degradation intermediates and products) in the glucose-fed BESs, all the glucose-fed BESs were individually fed with 20mM of carbon equivalent of acetate or formate or ethanol or propionate respectively. All the tests were operated for 9 hours. Both closed circuit condition and open circuit condition of these reactors with different feeds were tested separately. The current production in these 9 hours tests was monitored per min. The GDIPs in the effluent of each test was measured based on the method in 2.4.

The effect of anode potentials on the electrogenic function of the anodic biofilm in the glucose-fed BESs

To investigate whether acclimation at different anode potentials can result in the enrichment of different microbial groups, the anodic microbial communities controls at three anode potentials (-150mV, 0mV, +200mV) of both of the glucose-fed BESs and acetate-fed controls were investigated. The sequencing of the anodic microbial communities was described in 2.5. Moreover, abundance of the *Geobacteraceae* in all the reactors was evaluated based on the method in 2.5. Principle component analysis (PCA) was used to conclude the effect of anode potential, reactor configuration, inocula, operation mode on the anodic microbial communities of glucose-fed BESs. The details of PCA was mentioned in 2.6.

4.3. Results

4.3.1. The effect of anode potential on the electrogenic substrate availability of glucose-fed BESs.

The effect of the anode potential on the glucose degradation pattern.

Glucose were depleted in 9 hours in all the glucose-fed BESs (Figure 4-1). Acetate, formate, ethanol and propionate were produced as the glucose degradation intermediates in all the polarization conditions in these glucose-fed BESs. In the aspect of acclimation anode potential, there was no statistically difference of the accumulation of acetate and formate between these glucose-fed BESs acclimated at -150mV, 0mV or +200mV (ANOVA, $p>0.05$). In contrast, the accumulation of ethanol and propionate between these glucose-acclimated BESs demonstrates significant difference (ANOVA, $p<0.05$). In particular, the accumulation of ethanol and propionate in the 0mV and 200mV-acclimated BESs were about 11.6% and 12.4% higher respectively than the -150mV-acclimated BESs. On the other hand, refer to the 9 hours applied anode potentials, the accumulation of acetate and formate in the 0mV and +200mV-acclimated BESs was decreased with the increase of anode potential in 9 hours cycles (ANOVA, $p<0.05$). However, the 9 hours anode potential alteration on the accumulation of acetate and formate in the -150mV-acclimated BESs was minor (ANOVA, $p>0.05$). Moreover, the accumulation of ethanol and propionate was barely affected by the 9 hours anode potential alteration in all the glucose-fed BESs (ANOVA, $p>0.05$).

There was significant difference between close circuit and open circuit in both of the acetate-fed tests and the formate-fed tests (ANOVA, $p<0.05$) (Table 4-1). Therefore, the consumption of acetate and formate was significantly affected by the activities at anode. This indicates that the lower accumulation of acetate and formate in 0mV-acclimated BESs and +200mV-acclimated BESs was partially because of the higher consumption of these two molecules at higher anode potential. In contrast, no significant difference of the consumption of either ethanol or propionate between the close circuit tests and the open circuit tests in these glucose-fed BESs was observed (ANOVA, $p>0.05$) (Table 4-1). Therefore, the consumption of ethanol and propionate in these glucose-fed BESs was unaffected by anodic activities. This indicates that the higher accumulation of ethanol and propionate in the glucose-fed BESs acclimated at 0mV and 200mV was mainly because of the higher production of these two GDIPs from glucose degradation.

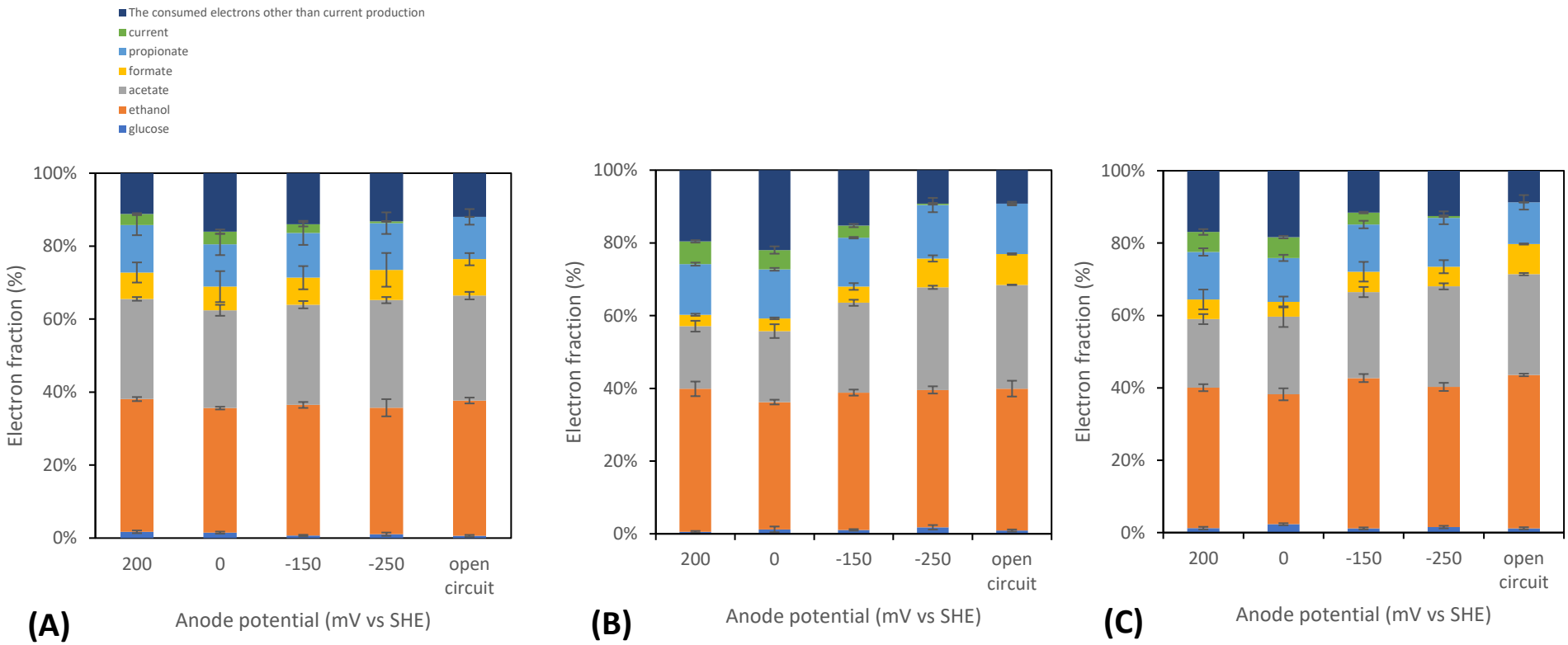

Figure 4-1 The 9 hours accumulation of the glucose degradation intermediates and current in glucose-fed BESs with altered applied anode potential in the -150mV-acclimated BESs (A); the 0mV-acclimated BESs (B); the +200mV-acclimated BESs (C).

	+200mV acclimated BESs		0mV acclimated BESs		-150mV acclimated BESs	
	Closed circuit	**Open circuit**	**Closed circuit**	**Open circuit**	**Closed circuit**	**Open circuit**
Glucose cycle	75.96±4.86	72.00±0.09	78.84±1.35	71.28±0.36	79.56±5.31	79.92±0.18
Acetate cycle	9.92±2.52	<0.01	9.00±3.72	<0.01	4.24±1.56	<0.01
Formate cycle	14.04±1.00	3.76±2.28	14.0±2.24	3.16±1.08	13.24±3.00	3.80±1.00
Ethanol cycle	0.88±0.56	1.36±0.24	0.92±0.60	0.88±0.24	1.12±0.20	1.40±0.48
Propionate cycle	<0.01	<0.01	<0.01	<0.01	<0.01	<0.01

Table 4-1 The consumption of glucose, acetate, formate, ethanol and propionate in individual 80e^-mmol/L-fed tests in glucose-fed BESs (e^-mmol/L).

In order to investigate the effect of anode potential on the amount of electrogenic electrons (*kn*) in the glucose-fed BESs, the amount of electrogenic electrons in 9 hours between the glucose-fed BESs and acetate-fed controls was compared at applied anode potential of -150mV, 0mV and 250mV. Both acclimation anode potential and 9 hours applied anode potential at -150mV caused lower amount of electrogenic electrons in 9 hours in the glucose-fed BESs (ANOVA, $p<0.05$) (Table 4-2). In contrast, similar amount of electrogenic electrons was achieved in the 0mV and +200mV glucose-fed BESs at 9 hour applied anode potential of 0mV and +200mV (ANOVA, $p>0.05$) (Table 4-2). On the other hand, the amount of electrogenic electrons in 9 hours in all the acetate-fed controls were generally higher than the glucose-fed BESs. However, the amount of electrogenic electrons between the acetate-fed controls was very similar despite of the difference in the short-term anode potentials alteration and the initial acclimated anode potentials (ANOVA, $p>0.05$) (Table 4-2).

	Acetate-fed controls			**Glucose-fed BESs**		
Initial acclimated anode potentials (mV vs SHE) / **9 hours applied anode potential (mV vs SHE)**	**+200**	**0**	**-150**	**+200**	**0**	-150
+200	7.2±0.2	6.9±0.2	6.9±0.1	4.9±0.7	5.6±0.3	2.6±0.2
0	7.0±0.3	6.8±0.2	6.9±0.2	5.1±0.7	4.7±0.9	3.0±0.5
-150	6.7±0.1	6.9±0.1	7.0±0.2	2.9±0.2	3.0±0.4	2.0±0.5

Table 4-2 Comparison of the amount of electrogenic electrons between the glucose-fed BESs and the acetate-fed controls at anode potential of -150mV, 0mV, +200mV (e^-mmol/L)

The types of the major electrogenic GDIPs in the glucose-fed BESs at different anode potentials

Major current production was observed in both of the formate-fed tests and the acetate-fed tests in close circuit although the current production from acetate was much higher than formate (Figure 4-2). In contrast, the current production in both ethanol and propionate tests were relatively low (Figure 4-2). This indicates that acetate was the major electrogenic molecule in all the glucose-fed BESs.

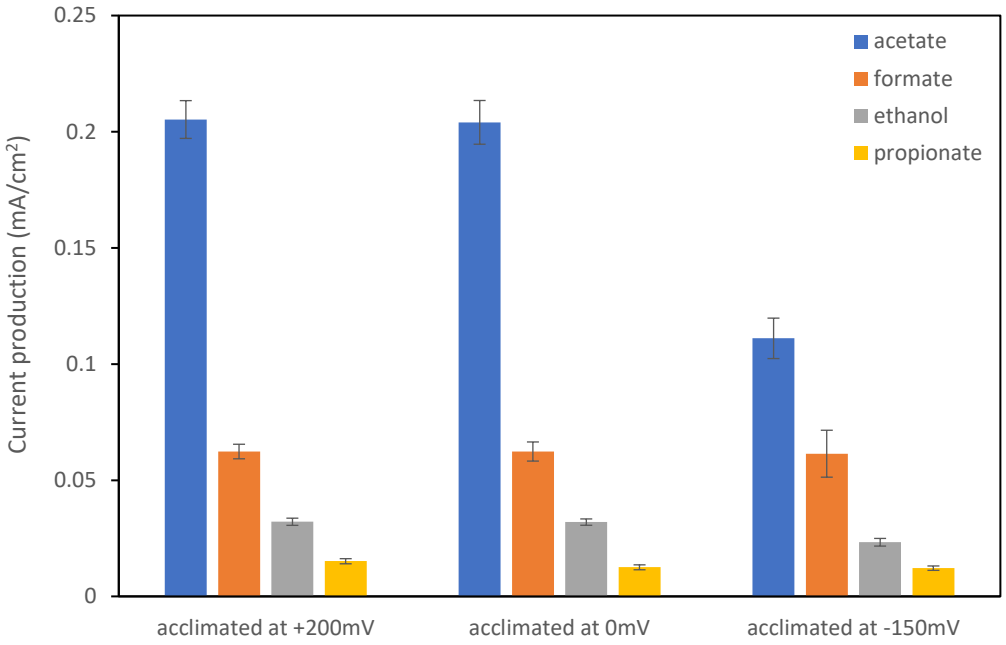

Figure 4-2 The current production from major GDIPs in the glucose-fed BESs acclimated at anode potentials of +200mV, 0mV and -150mV.

4.3.2. The effect of anode potential and the acetate availability on the Geobacteraceae abundance in BESs

Anode potential could influence the abundance of *Geobacteraceae* in the glucose-fed BESs (ANOVA, $P<0.05$). In particular, the abundance of *Geobacteraceae* in -150mV-glucose-fed BESs was as low as 4.0×10^5 cells/cm^2. However, the abundance of *Geobacteraceae* in the +200mV and the 0mV-glucose-fed BESs increased to 7.9×10^5 cells/cm^2 and 8.1×10^5 cells/cm^2 respectively (Figure 4-3A). In contrast, anode potential had little effect on the abundance of *Geobacteraceae* in the acetate-fed controls since the abundance of *Geobacteraceae* in these acetate-fed controls was similar and they ranged from 1.4×10^6 cells/cm^2 to 1.7×10^6 cells/cm^2 (ANOVA, $P>0.05$) (Figure 4-3A).

The current production in acetate-fed controls ranged around 0.20mA/cm^2 at acclimation anode potential at -150mV, 0mV and +200mV, which was similar to the variation of the abundance of *Geobacteraceae* in acetate-fed controls at these three anode potentials. In contrast, 0.07mA/cm^2 of current was produced in the -150mV glucose-fed BESs and it increased to 0.12mA/cm^2 to 0.13mA/cm^2 in the 0mV and the +200mV glucose-fed BESs in the glucose-fed cycle ,which was linear to the variation of the abundance of *Geobacteraceae* (Linear regression, $P>0.05$) (Figure 4-3B). When switching the feed from glucose to acetate+ formate in such BESs, the current production in the -150mV-glucose-fed BESs increased to 0.11mA/cm^2 although it was ~50% lower than the current production in the -150mV-acetate-fed controls. However, the current production with acetate+formate in both of the 0mV and +200mV acclimated glucose-fed BESs increased to ~0.20mA/cm^2, which was similar to the current production in the 0mV and the +200mV-acclimated acetate-fed controls (Figure 4-3B). The detailed information of the polarization curves and the abundance of *Geobacteraceae* of these BESs is in Figure 8-2 and Figure 8-3.

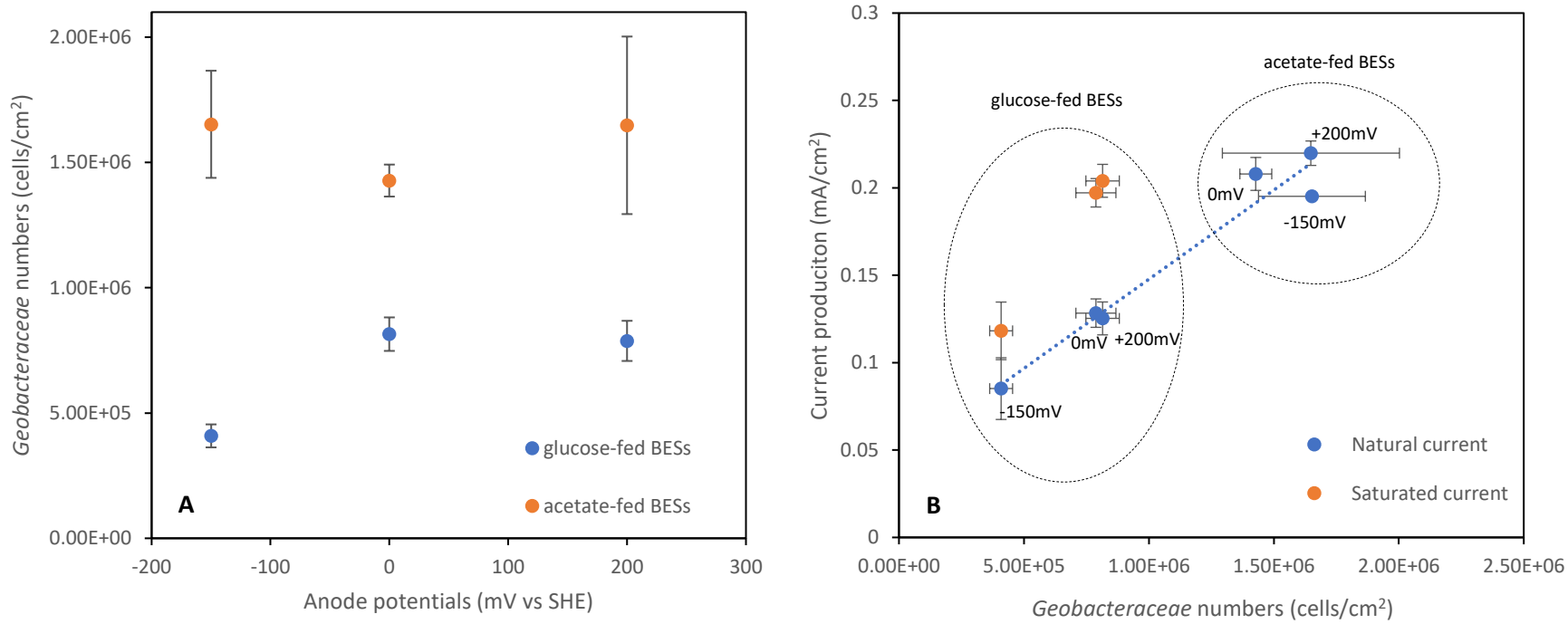

Figure 4-3 The summary of (A) the relationship between the initial acclimated anode potentials and the abundance of *Geobacteraceae*; (B) The relationship between the current production and the abundance of *Geobacteraceae* in BESs.

4.3.3. Comparison of the effect of anode potential and the effect of configuration, operation mode and inocula on the glucose-fed BESs.

Does configuration influence the current production and the anodic microbial communities in the BESs?

According to the analysis in Figure 4-3B, the saturated current production from the glucose-fed BESs and the acetate-fed controls at +200mV and 0mV were statistically indistinguishable (T-test, $p>0.05$). Despite the fact that the abundance of *Geobacteraceae* was statistically different (T-test, $p<0.05$). The effect of variables other than anode potential were therefore studied to determine if this discrepancy was caused by these variables. In particular, alternative tubular perspex two-chambers BESs with more electrogenic favoured factor (smaller electrode space) were used in this section (Liu et al., 2005). The key parameters of the tubular reactors were listed in Table 4-3. Since porosities anode material in tubular reactors allowed bacteria to grow underneath the surface of anode, units such as cells/cm^2 and mA/cm^2 were not suitable to describe the abundance of *Geobacteraceae* and the current production in these tubular BESs. Therefore, the total cells of *Geobacteraceae* and the total current production in tubular BESs were reported here.

	H-type reactors	**Tubular reactors**
Working volume (mL)	250	78.5
Membrane size (cm^2)	19.6	19.6
Anode size (cm^2)	40	22.5
Anode material	Graphite plate	Carbon felt
Electrodes distances (cm)	7	1

Table 4-3 The major parameters of the H-type reactors and the tubular reactors.

The current production of glucose-fed cycle in the glucose-fed tubular BESs was 1.6mA, which was much lower than the acetate-fed cycle in the acetate-fed controls. To switch from glucose to acetate increased the current production to 2.5mA in the glucose-fed BESs (Figure 4-4). However, this saturated current production was much lower than the

acetate-fed controls. On the other hand, the abundance of *Geobacteraceae* in the acetate-fed controls was also much higher than the glucose-fed BESs.

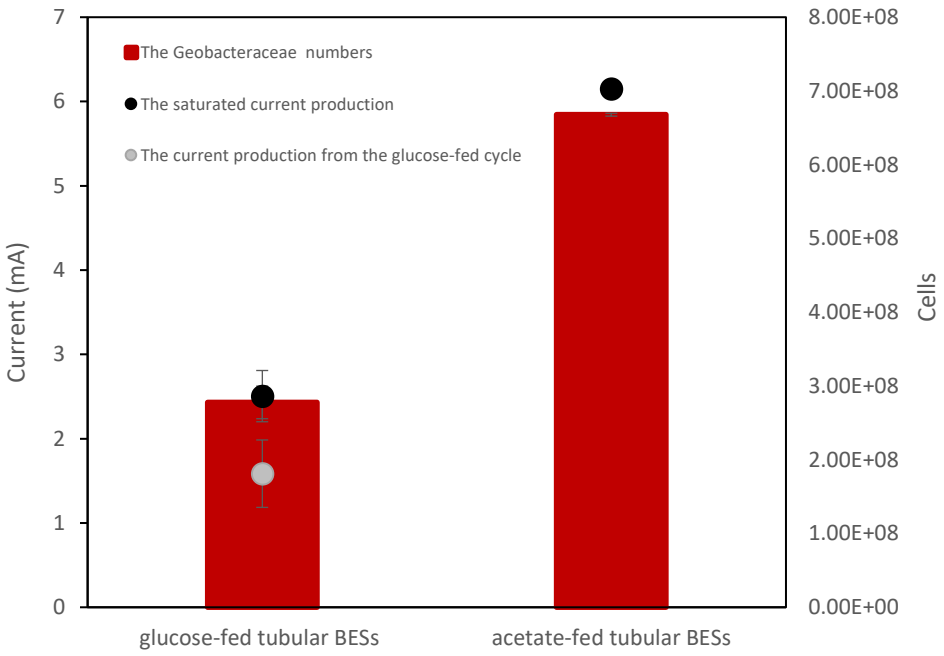

Figure 4-4 Summary of the current production and the abundance of *Geobacteraceae* in the tubular BESs.

4.3.4. The effect of the anode potentials, operation mode, configuration and inocula on the anodic microbial communities.

The principal component analysis (PCA) analysis of the anodic communities of the H-type BESs showed that the acclimation anode potentials at -150mV, 0mV and +200mV had limited effect on the anodic microbial communities in both of the glucose-fed BESs and the acetate-fed controls (Figure 4-6). In particular, in those glucose-fed BESs, *Geobacteraceae* occupied 27% in the -150mV-glucose-fed BESs and it slightly increased to 34% and 39% in the +200mV and the 0mV-glucos-fed BESs respectively (Figure 4-5). *Acidaminococcaceae* and *Aeromonadaceae,* were the second biggest function group in glucose-fed BESs as they occupied about 17% to 20% of the anodic microbial communities under in the glucose-fed BESs (Figure 4-5). On the other hand, *Geobacteraceae* was also the major functional group and occupied 87% to 92% in all the acetate-fed controls (Figure 4-5). Moreover, there was no specific major electrogenic microorganisms derived at specific anode potentials in both types of BESs.

Anode potential had limited effect on the anodic microbial communities in H-type BESs. It inferred that there were other variables other than anode potential to affect the anodic microbial communities in BESs. In which case, the effect of other variables such as operation mode, inocula and configuration were investigated here. The description of these variables were in (Table 4-4).

Variables	Types
Substrates	Acetate; Glucose
Configurations	H-type reactor; Tubular reactor
Operation modes	Fixed anode potential at 150mV, 0mV, +200mV; Additional voltage supply with 800mV
Inocula	Tudhoe sewage; Tudhoe sludge; Howdon sludge; Arctic resource

Table 4-4 The description of the variables in the BESs.

Figure 4-6 shows that the configuration of the tubular reactors had small selection pressure on the anodic microbial communities in both of the glucose-fed BESs and the acetate-fed controls when anode potential was fixed at 0mV. However, the operation mode of additional voltage supply of 800mV significantly changed anodic microbial communities in the tubular reactors. In particular, *Sporomusaceae* appeared as new function groups in BESs with additional voltage supply. Moreover, major fermentative function groups in BES with fixed anode potentials such as *Acidaminococcaceae* and *Aeromonadacea* were lower than the BESs with additional voltage supply. Notably, *Geobacteraceae* was generally higher in all the glucose-fed BESs with additional voltage supply than the glucose-fed BESs with anode potential fixation (Figure 4-5). However, neither current production nor peak acetate accumulation in the glucose-fed BESs with additional voltage supply was higher than the glucose-fed BESs with anode potential fixation (Figure 4-5). On the other hand, selection pressure of inocula on the anodic microbial communities in glucose-fed BESs was lower than the operation mode. In particular, *Brucellaceae* appeared as new microbial group and occupied for 7.6% in the anodic microbial communities in the BESs inoculated with arctic resource. Moreover, the proportion of *Enterobacteriaceae* in the anodic microbial communities in the BESs inoculated with Howdon activated sludge was 14.8%. (Figure 4-5).

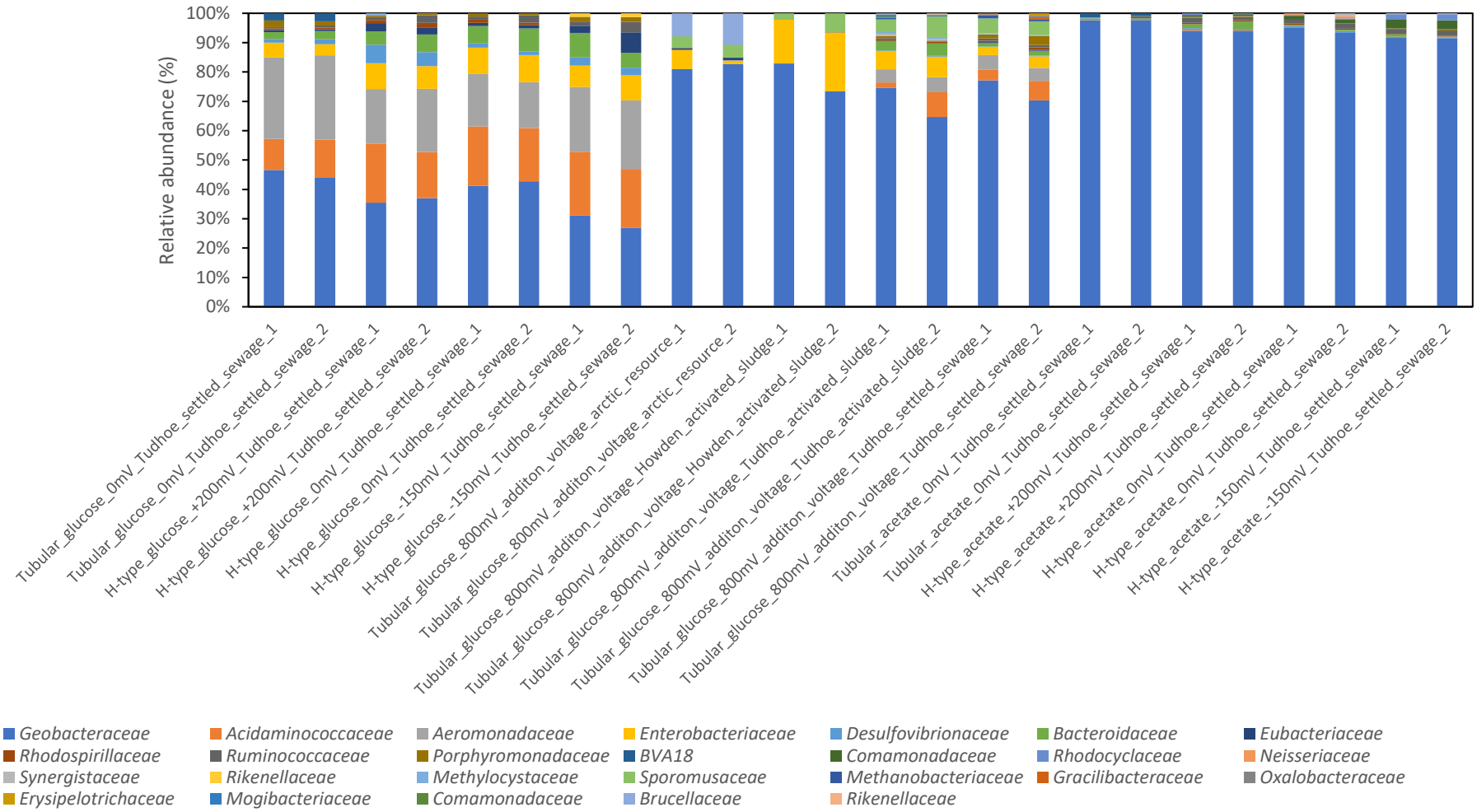

Figure 4-5 Summary of taxonomy of the anodic microbial communities in the glucose-fed BESs and the acetate-fed controls at family level.

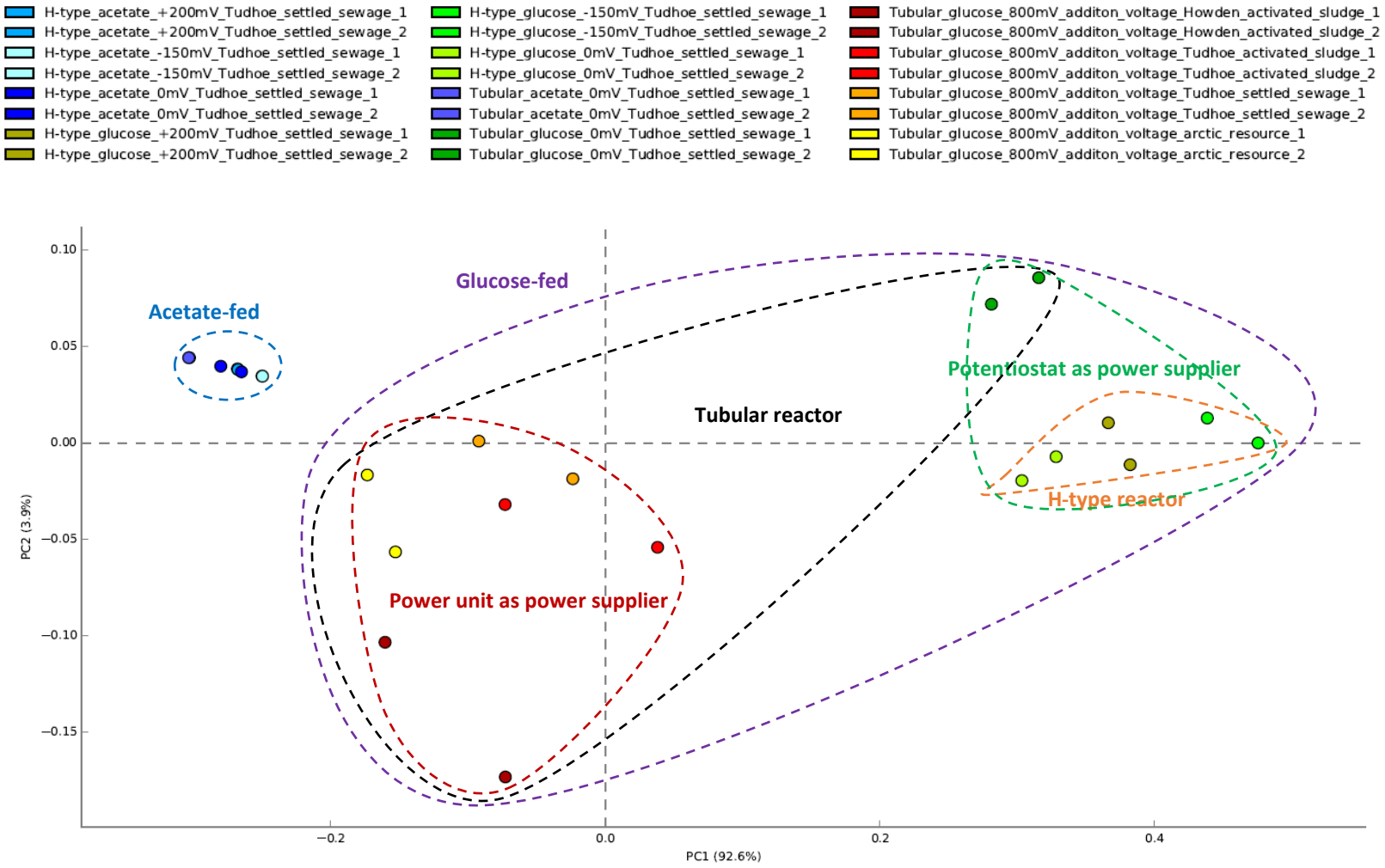

Figure 4-6 principal component analysis (PCA) of the effect of anode potential, configuration, operation mode and inocula on the anodic microbial communities in BESs.

4.4. Discussion

This study illustrates the effect of anode potential on the glucose degradation pathway and the electrogenic substrates availabilities as well as the abundance of the corresponding electrogenic microorganisms in glucose-fed BESs.

The effect of anode potential on the glucose degradation pathway and the availabilities of electrogenic substrates.

To alter acclimation anode potentials in the glucose-fed BESs regulated the degradation pathway of glucose as the accumulation of ethanol and propionate was changed. This regulation did not change the electrogenic role of acetate. Moreover, the acetate concentration was still below minimum requirement of 4.4mM for saturated current production in glucose-fed BESs. In particular, higher ethanol and propionate accumulation at high anode potential (0mV, +200mV) was observed in these glucose-fed BESs. Moreover, the consumption of ethanol and propionate was not stimulated by anode. This indicate that high acclimated anode potential induced higher production of ethanol and propionate in the glucose-fed BESs. On the other hand, both lower acetate accumulation and higher individual acetate consumption at higher anode potential in the glucose-fed BESs acclimated with higher anode potentials (0mV, +200mV) was observed. Therefore, higher anode potential acclimation also possibly encouraged higher acetate production although this was still not sufficient to satisfy the saturated current production.

A small increase of the amount of electrons recovered as current (*kn*) in 9 hours was observed in all the glucose-fed BESs at the high anode potentials. Acetate accumulation at higher anode potential was possibly unable to increase the electrogenic kinetic and *kn* in 9 hours . Moreover, acetate consumption in the individual acetate tests in the glucose-fed BESs was obviously increased when switching from closed circuit to open circuit where anode played role (Table 4-1), Therefore, this small increase of *kn* in all the glucose-fed BESs at the high anode potentials was possibly because of the higher acetate consumption rate at higher anode potential rather than the proposed change of degradation pathway and the availability of acetate.

The effect of anode potential on microbial communities.

The anodic microbial communities were similar in all the glucose-fed BESs irrespective of the initial acclimated anode potentials. This was consistent with the similar degradation pathway of glucose in these glucose-fed BESs in Figure 4-1. In particular, since acetate was the major electrogenic substrate in all the glucose-fed BESs, the syntrophic electrogenic pathways were present in such reactors. In which case, glucose fermenters such as *Acidaminococcaceae* and *Aeromonadacea*, and the electrogenic acetate user *Geobacteraceae* appeared in all the anodic microbial communities. Therefore, the occurrence of similar degradation pathways of glucose under different anode potentials was possibly the reason to result the similar anodic microbial communities in these glucose-fed BESs. Similar *Geobacteraceae*-based anodic microbial communities at three different anode potentials (-250mV, 0mV, +250mV) were also observed in propionate-acclimated BESs (Hari *et al.*, 2016), where acetate was also the putative major electrogenic substrate. In particular, only the taxonomic relative abundances of the anodic microbial communities were varied under different anode potentials while no specific major species was introduced under specific anode potential in their study. Notably, it suggested that the anode potential was effective to the selection of *Geobacteraceae* group at species level in MFCs (Commault et al., 2013). However, the *Geobacter* species have distinguished electrogenic abilities between each other (Rotaru et al., 2015). In which case, the similar current production from the acetate-fed controls with similar abundance of *Geobacteraceae* under different anode potentials in this study suggests that anode potential selection effort to the *Geobacteraceae* group at species level was possibly minor. In contrast, anode potential significantly influenced anodic microbial communities in both of the mixture of volatile fatty acids-fed BESs and the sucrose-fed BESs where the degradation pathways were complex (Dennis et al., 2016; Ishii et al., 2014). Moreover, significant effect of anode potential on anodic microbial communities in acetate-fed controls was also observed, and the degradation pathways in these reactors were relatively simple (Torres et al., 2009). In which case, there were factors other than the complexity of the degradation pathways of substrates in BESs to cause this controversy of anode potential selection effort on anodic microbial communities in BESs.

This study therefore also examined the effect of the configuration and the operation modes and inocula on the anodic microbial communities. Changing the configuration of

reactors with smaller electrodes distance had small effect on the anodic microbial communities of the glucose-fed BESs when anode potential was fixed. Therefore, the discrepancy of the effect of the fixed anode potential on anodic microbial communities was possibly not attributed to the difference of configurations. The experiment to investigate the effect of inocula was only conducted in the BESs with additional voltage supply. Moreover, the changing of operation mode of BESs from fixed anode potential to addition voltage supply had stronger selection effort to deviate the anodic microbial communities. However, these results did not directly demonstrate that the anodic microbial communities in the glucose-fed BESs with fixed anode potential affected by the type of inocula. Although the variation of the anodic microbial communities in the glucose-fed BESs with additional voltage supply was small when switching inocula from sewage to either sludge or arctic resource except one replicate of Howdon sludge. In which case, more evidences are needed to explain this discrepancy.

Notably, continuous-fed mode was applied in the BESs where anodic microbial communities were selected by anode potentials (Torres *et al.*, 2009; Dennis *et al.*, 2016). In contrast, batch fed mode was applied in the BESs where anodic microbial communities were independent to anode potentials (Zhu *et al.*, 2014; Hari *et al.*, 2016). Since batch fed mode was used in the BESs in this study, the tolerance of the anode microbial communities of the BESs to the initial acclimation anode potential was possibly attributed to the batch fed mode. This was possibly because the complex pathway of substrates and the suspended cells could influence on anodic microbial communities in much longer period when continuous-fed mode was applied. Therefore, more diverse anode potential-selectable anodic communities were introduced in BESs. In contrast, suspended cells and substrates were periodically washed out in batch fed mode BESs. In which case, the anodic microbial communities in batch fed mode BESs became more anodic electrogenic functional and convergent than continuous-fed mode BESs.

The effect of anode potential and electrogenic substrate availability on the abundance of electrogenic microorganisms in BESs.

This study investigated the effect of anode potential and the acetate availability on the abundance of major electrogenic microorganisms *Geobacteraceae* in BESs. Interestingly, the abundance of *Geobacteraceae* was linear correlated ($p<0.05$) with the current production from initial substrate in both of the glucose-fed BESs and acetate-fed controls

at all the three anode potentials in this study. This suggests that the abundance of *Geobacteraceae* in BESs was highly related to the current production from initial substrate, which is largely determined by the degradation pathway of initial substrates and the electrogenic substrates availability. Higher abundance of *Geobacteraceae* appeared in glucose-fed BESs acclimated at higher anode potentials of +200mV and 0mV, compared to the BESs acclimated at -150mV. In contrast, the effect of the alteration of the anode potentials on the abundance of *Geobacteraceae* on the anode of the acetate-fed controls was minor. In particular, the electrogenic substrates availability was insufficient to produce high current in glucose-fed BESs whereas the electrogenic substrates availability was enough to the high current production in acetate-fed controls. This indicates that when the degradation pathway was not favoured for high production of electrogenic substrates, the growth of *Geobacteraceae* was able to be improved at high anode potential at anode potential ranging from -150mV to +200mV in BESs. In contrast, when the degradation pathway was favour for the high production of electrogenic substrates, the effect of the high anode potential at the same range on the growth of *Geobacteraceae* in BESs was limited.

Moreover, under the similar energy input, the abundance of *Geobacteraceae* in the acetate-fed controls was much higher than the abundance of *Geobacteraceae* in the glucose-fed BESs. This indicates that the energy utilization in the BESs with high electrogenic substrate availability was more efficient. Notably, this 9 hours electrogenic energy was obtained by rough estimation since acetate was assumed as the only electrogenic substrate in the glucose-fed BESs. This was because the proportion of the formate electrogenic contribution was unknown while the formate electrogenic contribution was much lower than acetate in the glucose-fed BESs since both current production and coulombic efficiency in the individual formate-fed tests in the glucose-fed BESs was low. Moreover, the value of *kn* was not recorded throughout the experiments in this study. Therefore, the mathematic function of the exact value of available energy (ΔG) for the growth of electrogenic microorganism and the abundance of electrogenic microorganism was not built in this study. Therefore, in order to better understand the relationship between the abundance of electrogenic microorganism and the available energy for glucose-fed BESs, more precise evaluation of the total energy is needed.

The constraints on the saturated current production in H-type BESs

Notably, for those H-type reactors used in the anode potential-related experiments in this study, similar saturated current production in acetate-fed controls and glucose-fed BESs at 0mV and +200mV was achieved. However, the abundance of *Geobacteraceae* on the anode of the acetate-fed controls was significant higher the glucose-fed BESs. In contrast, both of the saturated current production and the abundance of *Geobacteraceae* in the glucose-fed BESs was much lower than acetate-fed controls in those tubular reactors. In which case, the difference of the saturated current production and the abundance of *Geobacteraceae* in the acetate-fed controls in H-type reactors were possibly restrained by configurational factors. In particular, those tubular reactors had smaller electrodes distance and thus had lower internal resistance. Therefore, internal resistance was possible a more decisive factor than fixed anode potential to determine the current production in BESs. In which case, the difference of the saturated current production between the glucose-fed BESs and the acetate-fed controls in the H-type reactors was possibly underrated. However, the microorganisms in those tubular reactors could grow to the inside of the anode while the microorganisms in the H-type reactors was unable to do so because carbon felts were used as anode in tubular reactors while graphite plates were used as anode in H-type reactors. Therefore, the comparison of abundance of *Geobacteraceae* between H-type reactors and tubular reactors was not paralleled in this study. As such, a more systematic comparison of the relationship between the saturated current production and the abundance of the corresponding electrogenic microorganisms between the reactors with different internal resistance are needed. Moreover, DNA-based quantitative-PCR was used for the quantification of the abundance of *Geobacteraceae* in this study. However, both live and dead cells were possibly counted in DNA-based quantitative-PCR, and therefore the relationship between the abundance of *Geobacteraceae* and the current production in these reactors could not be explained by only DNA-based quantitative-PCR. It inferred that the current production in BESs was controlled by the gene expression of electrogenic function of the electrogenic microorganisms in real time. Therefore, the relationship between the saturated current production and a real-time gene expression quantification for both glucose-fed BESs and acetate-fed controls is needed.

Implications

This study demonstrates that the effect of anode potential on the availability of acetate was minor. In fact, in the real BESs application cases where artificial anode potential fixation is absent, anode potential is an integrated variable of anodic downstream factors such as the characteristics of cathode and the configuration of reactor and anodic upstream factors such as the electrogenic substrates availability in BESs. Therefore, it inferred that the adjustment of anode potential by downstream factors is possibly unable to improve the acetate availability in the glucose-fed BESs in real cases. Moreover, this study demonstrates that higher artificial anode potential fixation increased the abundance of anodic electrogenic microorganism in the glucose-fed BESs, but barely influenced the abundance of electrogenic microorganisms in the acetate-fed controls. Therefore, it inferred that in the BESs where degradation pathway was favoured for acetate production such as fermentation effluent-fed BESs, to improve the abundance of electrogenic microorganisms by adjusting anode potential is not a priority. In contrast, when the degradation pathway was not favoured for high production of electrogenic preferred substrates in the BESs such as glucose-rich BESs, to adjust anode potential is important for obtaining high abundance of electrogenic microorganisms in BESs.

4.5. Conclusion

This study was the first one to explain the effect of anode potentials (+200mV, 0mV and -150mV) on the electrogenic performance of glucose-fed BESs in terms of the variation of the availabilities of major electrogenic molecules and the abundance of major electrogenic microorganisms. In particular, acetate and formate were the major electrogenic molecules and *Geobacteraceae* was the major group of electrogenic microorganism in all the glucose-fed BESs in despite of the initial anode potentials. However, the availabilities of acetate and formate from glucose degradation in all the glucose-fed BESs were little changed by different initial anode potentials whereas the abundance of *Geobacteraceae* in the glucose-fed BESs initially set at +200mV and 0mV was similar, but higher than the glucose-fed BESs initially set at -150mV. This higher abundance of *Geobacteraceae* caused the higher current production in the glucose-fed BESs initially set at +200mV and 0mV. However, the initial anode potentials had little effect on the abundance of *Geobacteraceae* and the current production in the acetate-fed controls, and which was much higher than the abundance of *Geobacteraceae* and the current production in the glucose-fed BESs. In which case, this study suggests that high anode potentials increased the current production of glucose-fed BESs by increasing the abundance of *Geobacteraceae* rather than increasing the availabilities of acetate and formate. Moreover, to increase the availabilities of the electrogenic molecules such as acetate was more effective to robust the growth of the major electrogenic microorganism such as *Geobacteraceae* than to increase anode potentials.

Chapter 5 The effect of sulphate in the organic-based BES (Bioelectrochemical System)

5.1. Introduction

Bioelectrochemical systems (BESs) are viewed as promising low cost wastewater treatment technologies because they can, in principle, both remove waste and produce energy or valuable chemicals (Li et al., 2013). The basic mechanism of BESs is to use biocatalysts on electrode to transfer the electrons from the electrogenic substrates in influent to external circuit to form current and achieve energy recovery or to produce desired products at the other end of circuit (Logan et al., 2006; Rabaey and Rozendal, 2010b). Sulphate is one of the most abundant anions in environment and is ubiquitous in wastewater. It is well-known that sulphate can act as electron acceptor as sulphate reducing bacteria (SRB) compete with other anaerobic microbial processes, such as methanogenesis, for the electrons from organic electron donors in anaerobic wastewater treatment systems (Dar et al., 2008; Omil et al., 1998). Likewise, SRB could, potentially, compete with the anode for the electrons from substrates in organic-driven BESs in presence of sulphate. This competition is detrimental to the anodic electrogenic processes in BESs once those electrons are permanently trapped by sulphate. Other terminal electron sinks as nitrogen or methane are, once formed, not thought to interact with the functioning of BESs. However, the reduced forms of sulphate (e.g. sulphide or sulphur) can participate in various downstream processes in electrochemical systems (Sukkasem *et al*., 2008; Parameswaran *et al*., 2009). Therefore, to understand the effect of sulphate and its derivative reactions on the electrogenic performance of organic-based BESs is of great interest for gaining comprehensive insight on the effect of the alternative electron terminal sinks on BESs.

The major possible electron transfer pathways in BESs in presence of sulphate were described in Table 5-1 (acetate was the organic electron donor here). In particular, sulphate is typically reduced to sulphide by capturing the electrons from organic substrates by various SRBs such as *Desulfatirhabdium* and *Desulfovibrio* (reaction 2) (Zheng et al., 2014). Then sulphide can be spontaneously removed by anode via either abiotic pathway or biotic pathway by sulphur oxidizers such as *Thiomonas* (reaction 3) (Dutta et al., 2008; Rabaey et al., 2006; Zheng et al., 2014). The major product of

sulphide oxidation, elemental sulphur, can be further oxidized to sulphate via biotic electrogenic pathways by microorganisms such as *Desulfobulbus* (reaction 4) (Holmes et al., 2004). Sulphur can be reduced to sulphide and sulphate using organic such as acetate as electron donor via sulphur reducing bacteria such as *Desulfuromonas* in non-electrogenic disproportionation (reaction 5) (Dutta et al., 2009).

These reactions make the fate of sulphate in BESs rather variable, and this makes the effect of sulphate reduction on BESs more complicated than the other electron terminal sinks. In stoichiometry, although electrons from organics were potentially intercepted by sulphate in the BESs in presence of sulphate, those electron lost in sulphate reduction can be completely recovered as electricity at the anode when reaction 3 and 4 proceed rapidly. Moreover, reaction 5 can also release the electron from elemental sulphur, the product of reaction 3, to sulphide and recover more electrogenic electrons via reaction 3. In which case, the decline of the electrogenic performance of the organic-fed BESs in the presence of sulphate can be avoided. In contrast, ineffective sulphate-related electrogenic reactions could cause the decline of the electrogenic performance of the organic-fed BESs in the presence of sulphate once substantial electrons from organic substrates are trapped by sulphate. Although each of these sulphate derivative reaction in BESs was individually studied, there was lack of an integral investigation of that whether these sulphate derivative reactions can synergetically contribute to the electrogenic processes in the organic-based BESs in presence of sulphate. Notably, the availabilities of both organics and sulphate determined the extent of sulphate reduction and its derivative reactions in anaerobic wastewater treatment systems (Omil et al., 1998). Therefore, it inferred that these availabilities are also decisive to the competition between electrogenic microorganism and sulphate reducing bacteria in the BESs in presence of sulphate and therefore influence the electrogenic performance of such BESs.

Consequently, the effect of the initial feed availabilities of organics and sulphate on the electrogenic performance of BESs needs to be investigated. Moreover, it proposed that reaction 3 and reaction 4 are the key electrogenic processes to recover the electrons from sulphate reduction. Therefore, the electrogenic effectiveness of these two reactions was compared with reaction 1 to investigate whether they caused the such electrogenic constraints.

Reaction		ΔG^0 (kJ/mol)	Type	Reference
(1) Direct electrogenic acetate oxidation	$CH_3COO^- + 4H_2O \rightarrow 2HCO_3^- + 9H^+ + 8e^-$	-223.0 ± 13.6	Biotic	(Bond and Lovley, 2003)
(2) Sulphate reduction	$CH_3COO^- + SO_4^{2-} \rightarrow HS^- + 2HCO_3^-$	-64.6 ± 13.9	Biotic	(Zheng et al., 2014)
(3) Electrogenic sulphide oxidation	$H_2S(aq) / HS^- \rightarrow S(s) + 2e^- + 2H^+ / H^+$	-34.4 ± 8.2	Biotic and abiotic	(Dutta et al., 2008; Zheng et al., 2014)
(4) Electrogenic elemental sulphur oxidation	$S(s) + 4H_2O \rightarrow SO_4^{2-} + 6e^- + 8H^+$	-134.4 ± 9.2	Biotic and abiotic	(Holmes et al., 2004)
(5) Sulphur reduction	$CH_3COO^- + 4S(s) + 4H_2O \rightarrow 4HS^- + 2HCO_3^- + 5H^+$	-95.8 ± 35.5	Biotic	(Dutta et al., 2009)

ΔG^0 is at standard condition: reactant= 1M, pH=7.0, T=25°C , anode potential = 0mV vs SHE,

Table 5-1 The proposed sulphate pathways in BESs.

Once these sulphate derivative reactions give negative effect on the electrogenic performance of BESs, sulphate reduction needs to be avoided in order to improve the electrogenic performance of such BESs. It is believed that anode potential can regulate the amount of the energy that anodic electrogenic microorganisms utilize in BESs (Wagner et al., 2010). Theoretically, the microbial reaction with the most energy will be able to outcompete other reactions in an engineered microbial system (Rittmann and McCarty, 2012). Therefore, in principle, altering anode potential could thermodynamically provide more energy for electrogenic processes. This allows the electrogenic microorganisms to outcompete SRB in the BESs in presence of sulphate and thus attenuate the negative impact of sulphate reduction. However, it reported that the extent of denitrification in BESs in the presence of nitrite was determined by the availability of nitrite rather than the anode potential (Kashima and Regan, 2015). Moreover, (Chou et al., 2013, 2014) reported that negative potential (-300mV) had greater effect on the electrogenic performance of BESs in the presence of sulphate than positive potential (+300mV). Nevertheless, only two anode potentials were tested and there was no illustration of the fate of sulphate in their studies. Therefore, it was still unknown of the reason of why low anode potential had positive effect on the BESs in their studies. Consequently we sought to determine if altering the potential in BESs is an effective way to restrain sulphate reduction by obtaining detailed description of the fate of sulphate at a wider range of anode potentials.

Notably, the oxygen from either water electrolysis or oxygen diffusion triggered non-electrogenic sulphur oxidation (van den Brand et al., 2015; Pikaar et al., 2011). In which case, the electrons in elemental sulphur were cycled into water rather than recovered by electrode and this process transferred the electrons from organics into non-electrogenic terminal electron sinks. Therefore, these analyses were conducted in microbial electrolysis cells (MECs) mode with fixed anode potential (0mV vs Standard hydrogen electrode (SHE)) to avoid the sulphur oxidation by oxygen incursion and water electrolysis. Moreover, acetate-fed controls were used to study the effect of sulphate on the electrogenic performance and the effect of anode potential on sulphate reduction because acetate is non fermentable, which simplify the analysis of electron transfer pathway in BESs.

However, the organics in real wastewater resource are normally more complex than acetate and therefore more diverse electron transfer pathways occurred in complex organics-fed BESs. In which case, it is more complicated to understand the effect of sulphate on the electrogenic performance of complex organics-fed BESs. In particular, organic-fed BESs are most electrogenically efficient when the electrogenic microorganisms favour to use simple organic substrates such as acetate (Torres et al., 2007). Sulphate reducing bacteria (SRB), on the other hand, can efficiently utilize a wide range of organics (Muyzer and Stams, 2008). It is possible that SRBs enjoy a competitive advantage over electrogenic microorganisms in BESs fed complex wastes because complex organics are degraded into a wide range of organic products, that are perhaps more likely to be taken up by SRBs than by electrogenic microorganisms. In which case, sulphate reduction can be more detrimental to the electrogenic processes in complex-fed BESs as electrons are more to be trapped in the sulphur cycle. In contrast, the electrogenic performance of BESs fed with complex is usually inferior than the BESs fed with simple organics. This was presumably due to the low production of electrogenic preferred substrates products such as acetate from fermentation and hydrolysis in complex-fed BESs (Chapter3; Velasquez-Orta *et al.*, 2011). In which case, higher affinity of SRB for those less electrogenic organics can potentially improve the electrogenic performance of complex-fed BESs since some of those less electrogenic organics can participate in the electrogenic processes via sulphate reduction and sulphide oxidation routes (reaction 2+3) when sulphate is present in such BESs. Therefore, although detailed information of sulphate derivative reactions in acetate-fed BESs was studied, it is necessary to investigate the effect of sulphate on the electrogenic performance of BESs with a wider range of organics feeds. Consequently, the effect of sulphate on the electrogenic performance of the BESs acclimated with different organics was investigated in this study.

Therefore, this study was aiming:

1. To investigate the effect of sulphate on the electrogenic performance in acetate+sulphate-fed BESs with different availabilities of sulphate and acetate.

2. To identify the presence of reaction 2, 3, 4 and 5 in acetate+sulphate-fed BESs in the presence of sulphate.

3. To investigate the electrogenic effectiveness of electrogenic sulphide oxidation (reaction 3) and electrogenic elemental sulphur oxidation (reaction 4) in acetate+sulphate-fed BESs.

4. To investigate whether high anode potentials restrain the sulphate reduction in the acetate+sulphate -fed BESs in presence of sulphate.

5. To compare the effect of sulphate on the electrogenic performance in the BESs individually acclimated with four different organics (acetate, glucose, sucrose, starch).

5.2. Method

5.2.1. Tubular reactors start up

Tubular reactors used in this chapter were described in 2.1 and Figure 2-1. The anodic media and cathodic media used in these reactors were described in 2.2. The anodic chambers of reactors was fed with 80e^-mmol/L of sodium acetate (0.88g/L) or glucose (0.61g/L) or sucrose (0.6g/L) or starch (0.6g/L) respectively as well as 40e^-mmol/L of sodium sulphate (0.72g/L). The conversion between the carbon equivalent of substrates and the real concentration of substrates was shown in 2.6. All the reactors were inoculated with the Tudhoe settled sewage. Moreover, the BESs fed with 20Cmeq/L of sodium acetate (0.88g/L), glucose (0.61g/L), sucrose (0.6g/L) and starch (0.6g/L) respectively but without sulphate was built as positive controls. The information of applied chemicals and the inocula was provided in 2.2. Moreover, the treatment of media and inoculum was described in 2.2. All the reactors were operated in microbial electrolysis cells (MECs) mode and potentiostat was used to stabilize the anode potentials of all the reactors at 0mV vs standard hydrogen electrode (SHE) through all the tests. The details of operation were described in 2.3.

5.2.2. Experiment design

The presence of the sulfur pathway in the acetate+sulphate-fed BESs

When reproducible current was obtained in all the reactors, four tests were carried out to investigate presence of the individual sulphur pathway in the BESs in presence of sulphate. **Test 1:** In order to examine the presence of sulphate reduction (reaction 2), a mixture 40e^-mmol/L (0.72g/L) of sulphate and 80e^-mmol/L (0.88g/L) of acetate was fed in the BESs fed with acetate+sulphate. The concentration of sulphate in the influent and effluent was tested. The test was carried out until the current production was < 0.1mA. **Test 2:** In order to examine the presence of electrogenic sulphide oxidation (reaction 3), 40e^-mmol/L of sulphide was fed in the BESs acclimated with acetate+sulphate. This test was carried out for only 2 hours due to the concern of the high toxicity of sulphide and the potential excessive accumulation of anodic sulphur deposit. Moreover, scanning electron microscope (SEM) and energy-dispersive X-ray spectroscopy (EDX) (details were described in 2.4) were used to investigate the surface of the anode in the acetate+sulphate-fed BESs at the end of the entire experiment. **Test 3:** In order to

examine the presence of electrogenic elemental sulphur oxidation (reaction 4), blank media was fed into the BESs acclimated with acetate+sulphate where the putative anodic elemental sulphur deposit was the only potential electrogenic electron donor for current production. **Test 4:** In order to examine the presence of sulphur reduction (reaction 5), 80^{-}emmol/L (0.88g/L) acetate was fed into the BESs acclimated with acetate+sulphate. The concentration of sulphide was tested at the end of the test since sulphide was possibly produced from the reduction of anodic elemental sulphur. The concentration of sulphide, sulphate and acetate in the influent and effluent of these cycles was measured as described in 2.4.

The electrogenic constraints in the acetate+sulphate-fed BESs

In order to the investigate whether electrogenic constraints were present in the BESs in the presence of sulphate, the effect of either high sulphate availability or low acetate availability on the electrogenic performance of sulphate-acclimated BESs was evaluated.. All the tests were conducted after stable and reproducible current was produced from all the reactors. Firstly, the initial applied sulphate in the acetate+sulphate-fed BESs stepwise was increased from 0e^{-}mmol/L, 40 e^{-}mmol/L, 80e^{-}mmol/L, 120e^{-}mmol/L, 160e^{-}mmol/L and 240 e^{-}mmol/L while maintaining initial applied acetate at 80e^{-}mmol/L in six different 24 hours cycles. The applied sodium chlorine with same conductivity to the sulphate was also increased in the acetate-fed controls in six cycles. Then, the initial applied acetate in the acetate+sulphate-fed BESs stepwise was decreased from 80e^{-}mmol/L, 40e^{-}mmol/L, 20e^{-}mmol/L, 10e^{-}mmol/L, 0e^{-}mmol/L while maintaining initial applied sulphate at 40e^{-} mmol/L in five different 24 hours cycles. The applied acetate was also deceased from 80e^{-}mmol/L, 40e^{-}mmol/L, 20e^{-}mmol/L, 10e^{-}mmol/L, 0e^{-}mmol/L in the acetate-fed controls in five cycles. The concentration of sulphide, sulphate and acetate in the influent and effluent of these cycles was measured as described in 2.4.

The electrogenic performance of the acetate+sulphate-fed BESs at different anode potentials

To investigate the effect of anode potentials on the electrogenic performance of sulphide oxidation, polarization curve was obtained by fed 40e^{-}mmol/L of sulphide in the acetate+sulphate-fed BESs with stepwise increased anode potentials from -250mV to +700mV once the current production reached plateau. The polarization curves of the

control of acetate oxidation or negative control was obtained by fed acetate or blank media in the acetate+sulphate-fed BESs with stepwise increased anode potentials in the same range. To investigate the effect of anode potentials on the overall electrogenic performance of BESs in presence of sulphate, 80e^-mmol/L of acetate+40e^-mmol/L of sulphate was fed into the acetate+sulphate-fed BESs in six individual 24 hours cycles with anode potentials of -250mV, -150mV, 0mV, +200mV, +500mV and +700mV individually.

The co-effect of the degradation of organics and sulphate cycles on the electrogenic performance of BESs

All the tests were conducted after these BESs were cultured until stable and reproducible current was obtained. The conditions of the tests were described as below:

Reactors	Test A (e^-mmol/L)	Test B (e^-mmol/L)	Test C (e^-mmol/L)
Acetate-fed BESs	80 acetate	80 acetate	80 acetate
Acetate+sulphate-fed BESs	80 acetate + 40 sulphate	80 acetate	80 acetate + 40 sulphate
Glucose-fed BESs	80 glucose	80 glucose	80 acetate
Glucose+sulphate-fed BESs	80 glucose + 40 sulphate	80 glucose	80 acetate + 40 sulphate
Sucrose-fed BESs	80 sucrose	80 sucrose	80 acetate
Sucrose+sulphate-fed BESs	80 sucrose + 40 sulphate	80 sucrose	80 acetate + 40 sulphate
Starch-fed BESs	80 starch	80 starch	80 acetate
Starch+sulphate-fed BESs	80 starch + 40 sulphate	80 starch	80 acetate + 40 sulphate

Table 5-2 The feed in three different tests in the BESs in the presence of sulphate.

The test for each condition was processed until current production dropped <0.1mA. The current production was monitored and the coulombic efficiency in all the reactors in each test was evaluated based on the method in 2.6. Moreover, The concentration of sulphide, sulphate and acetate in the influent and effluent of these cycles was measured as described in 2.4. In addition, the calculation method of the current loss was shown in Table 5-3. Moreover, the current production of each tests and the detailed calculations of current loss was shown in Appendix J.

Illustration: "**The effect on the electrogenic process**" was based on the current production differences in different cycles in the same BESs, which were caused by the limiting steps in either fermentation/hydrolysis or sulphur cycle. On the other hand, "**The effect on the anodic biofilm**" was based on the current production differences between different BESs, which were caused by differences in the electrogenic abilities of bioanodes due to the acclimation in the presence of fermentable/hydrolysable organics or sulphate.

*In particular, the "acetate-fed cycle" was recognized as the optimal condition for current production since no fermentation/hydrolysis constraint was applied in such cycle. "acetate+sulphate cycle" was regarded as the approximate optimal condition since the differences in current production between acetate-fed tests and acetate+sulphate-fed tests were negligible (Figure 5-1B). As such, any other differences in current production under either of these two tests was caused by the difference in anodic biofilm, which was indicated as "**The effect on the anodic biofilm**".

Reason of current loss	Color	Calculation method
The effect of sulphate reduction on the electrogenic process		The differences in current production between the tests fed with or without sulphate in those BESs initially acclimated with sulphate
The effect of sulphate reduction on the anodic biofilm		The differences in current production between the BESs initially acclimated with sulphate and the BESs initially acclimated without sulphate when switching organic feed into acetate
The effect of fermentation/hydrolysis on the electrogenic process		The differences in current production between the acetate/acetate+sulphate-fed tests and the initial substrate/ initial substrate+sulphate-fed cycles in all the BESs.
The effect of fermentation/hydrolysis on the anodic biofilm		The difference of current production between the acetate/acetate+sulphate-fed tests in the BESs acclimated with either glucose, sucrose or starch and the acetate-fed tests in the acetate-fed controls.

Table 5-3 The illustration of the calculation of the current loss.

5.3. Results

5.3.1. The presence of the electrogenic constraints in the acetate+sulphate-fed BESs with high sulphate availabilities or low acetate availabilities.

The presence of the electrogenic constraints in the acetate+sulphate-fed BESs with high sulphate availabilities.

The coulombic efficiency in the acetate+sulphate-fed BESs decreased (76.2% to 65.3%) with the increase of the proportion of the acetate removal for sulphate reduction (20.1% to 39.0%) (Figure 5-1A) (linear regression, $p<0.05$). In particular, the lowest coulombic efficiency (65.3%) occurred with the highest sulphate reduction proportion (39.0%). On the other hand, the coulombic efficiency in the acetate-fed controls was little changed and ranged between 77.5% to 80.3% when changing the initial concentration of NaCl (linear regression, $p>0.05$). Moreover, higher proportion of sulphate reduction in total electron balance did not result the high proportion of sulphide accumulation as they only ranged from 0.1% to 1.7% in total electron balance (Figure 5-1A).

Moreover, both of the proportion of sulphate reduction and the proportion of sulphide accumulation in total electron balance had limited effect on the current production in the acetate+sulphate-fed BESs (linear regression, $p>0.05$) (Figure 5-1B). On the other hand, the changing of NaCl had limited effect on the current production in the acetate-fed controls either (linear regression, $p>0.05$) (Figure 5-1B). Detailed information of current production, sulphate reduction, sulphide accumulation and carbon oxidation is shown in (Appendix Figure 8-4).

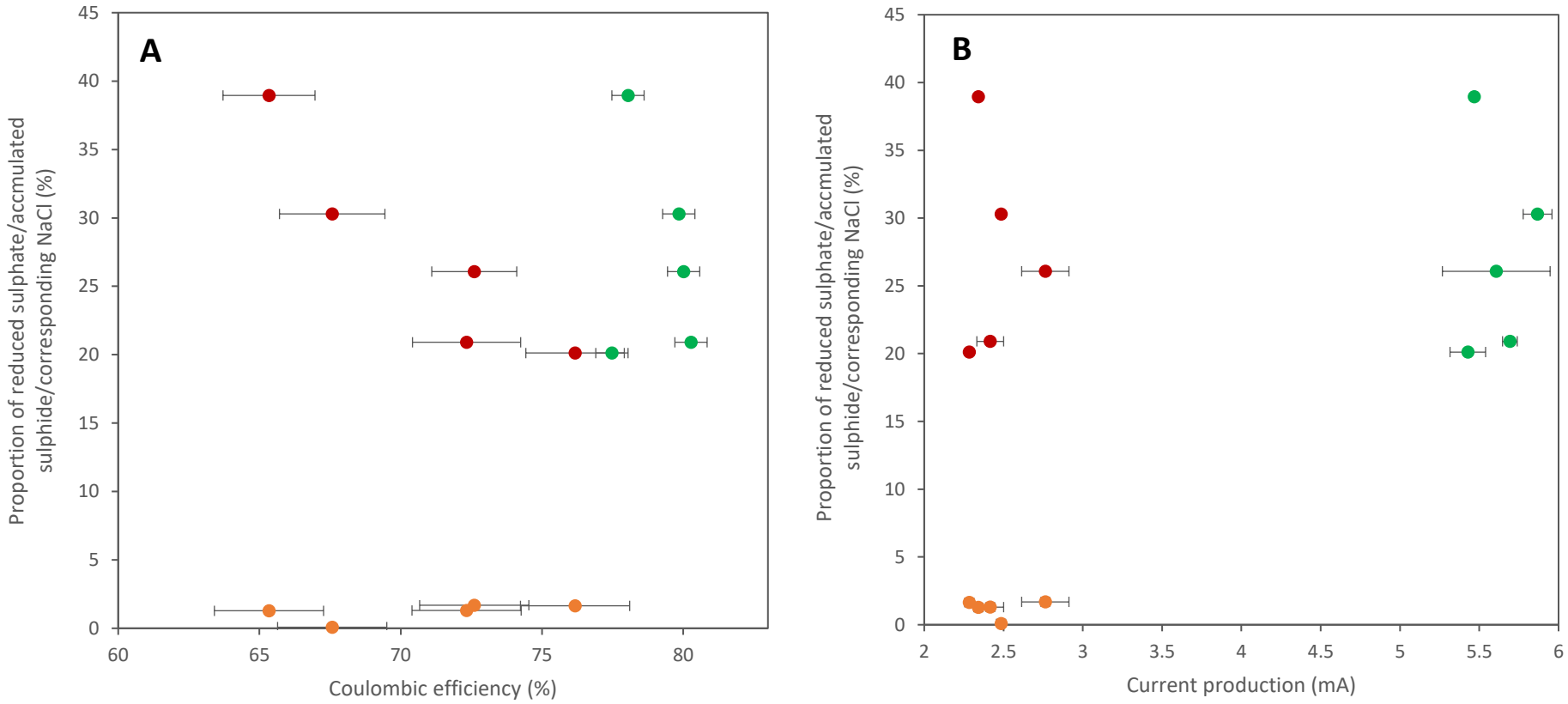

Figure 5-1 Coulombic efficiency (A) and current production (B) in the acetate+sulphate-fed BESs responds to: red: reduced sulphate; orange: accumulated sulphide; green: corresponding in the acetate-acclimated controls with equivalent conductivity of NaCl.

The presence of the electrogenic constraints in the acetate+sulphate-fed BESs with low acetate availabilities.

Though acetate+sulphate-fed reactors produced good current in regardless of the presence of sulphate, we speculated that this was because there was sufficient acetate for both of the electrogenic processes and the sulphate reduction.

Figure 5-2 shows that both current production and coulombic efficiency in the acetate+sulphate-fed BESs and the acetate-fed controls was decreased when applied acetate decreased from 40e^-mmol/L to 0e^-mmol/L (linear regression, $p<0.05$). However, the proportion of sulphate reduction in the total electron balance was slightly changed with the decreased of initial acetate feed at the same range. Therefore, sulphate reduction had limited contribution on the change of current production and coulombic efficiency in the acetate+sulphate-fed BESs with low acetate availability (linear regression, $p>0.05$). This suggests that the decrease of the current production and the coulombic efficiency in the acetate+sulphate-fed BESs with low acetate availability was likely due to the low acetate concentration rather than the competition between sulphate and anode. Moreover, both current production and coulombic efficiency in the acetate+sulphate-fed BESs and the acetate-fed controls were barely changed when increasing initial concentration of acetate from 40e^-mmol/L to 80e^-mmol/L. The detailed information of current production, coulombic efficiency, sulphate reduction, carbon oxidation and sulphide accumulation is shown in (Appendix Figure 8-5).

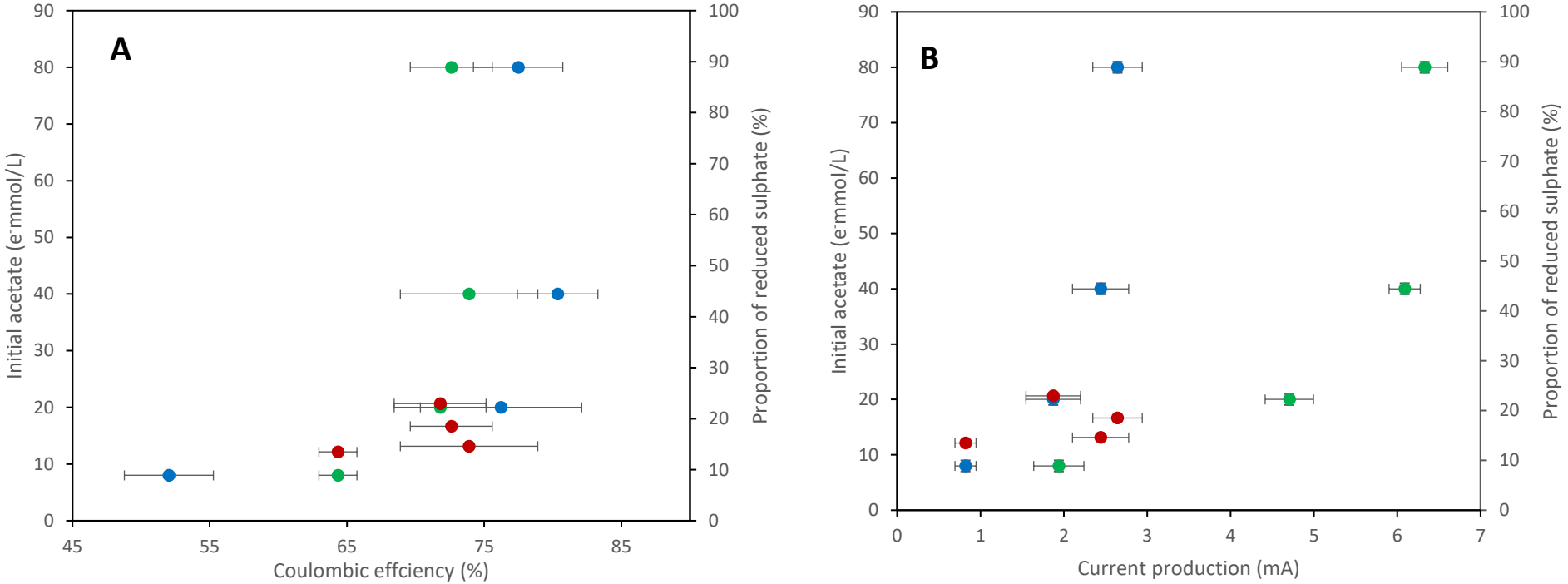

Figure 5-2 Coulombic efficiency (A) and current production (B) in the acetate+sulphate-fed BESs responds to: blue: initial acetate; red: reduced sulphate; green: corresponding in the acetate-fed controls with the same initial acetate.

5.3.2. The fate of sulphate in the acetate+sulphate-fed BESs.

To investigate the presence of the proposed sulphur pathways in the acetate+sulphate-fed BESs in Table 5-1, a series of tests described in 5.2 were conducted.

Test 1. The presence of sulphate reduction (Reaction 2)

In test 1, 9.14e^-mmol/L of sulphate in the acetate+sulphate-fed BESs was consumed in 48 hours (Table 5-4). Moreover, only 0.59e^-mmol/L of sulphide was detected in the effluent of these BESs at the end of the tests. Therefore, sulphate reduction was present in the acetate+sulphate-fed BESs.

Test 2. The presence of electrogenic sulphide oxidation (Reaction 3)

In test 2, 0.83mA of current was detected in the acetate+sulphate-fed BESs with 40$^-$ mmol/L of sulphide (Table 5-4). Therefore, sulphide was able to provide electrons for the electrogenic processes in acetate+sulphate-fed BESs alone. On the other hand, crystal particles structure covered the anode of the acetate+sulphate-fed anode while only smooth surface or foaming structure covered on the anode of the blank reactors or the acetate-acclimated controls respectively. Moreover, a large amount of sulphur was discovered on the surface of the anode of the acetate+sulphate-fed reactors (Figure 5-4) In contrast, only carbon source or a combination of carbon and oxygen were discovered on the anode of the abiotic blank reactors or acetate-fed controls respectively (Figure 5-4). These suggest that sulphur was deposited on the anode of the acetate+sulphate-fed BESs. Therefore, electrogenic sulphide was oxidized to elemental sulphur in the acetate+sulphate-fed BESs (reaction 3).

Moreover, Figure 5-3 shows that the acetate+sulphate-fed reactors with sulphide produced current at anode potentials from -250mV to +800mV. Although this current production decreased quickly after reaching plateau. Current was also produced from the abiotic reactors with sulphide although the current production only started at the anode potentials higher than -150mV. The current production from the blank BESs was negligible at high anode potentials. In which case, sulphide was electrogenic in the acetate+sulphate-fed BESs and therefore electrogenic sulphide oxidation was present in the acetate+sulphate-fed BESs.

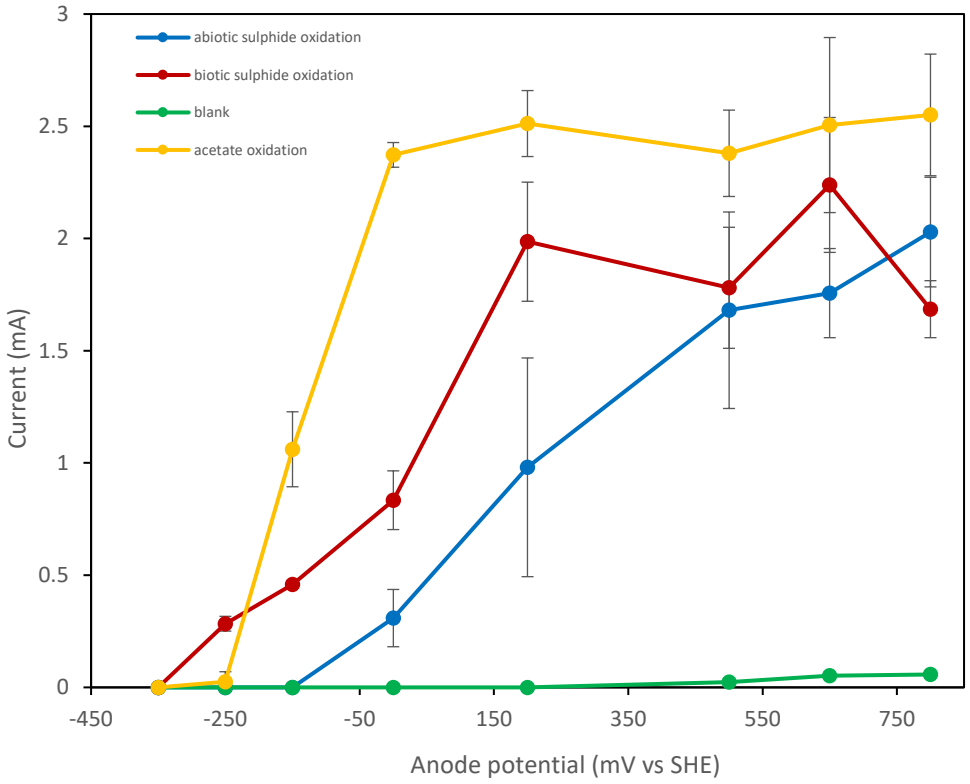

Figure 5-3 Polarization curve of sulphide oxidation in the acetate+sulphate-fed BESs.

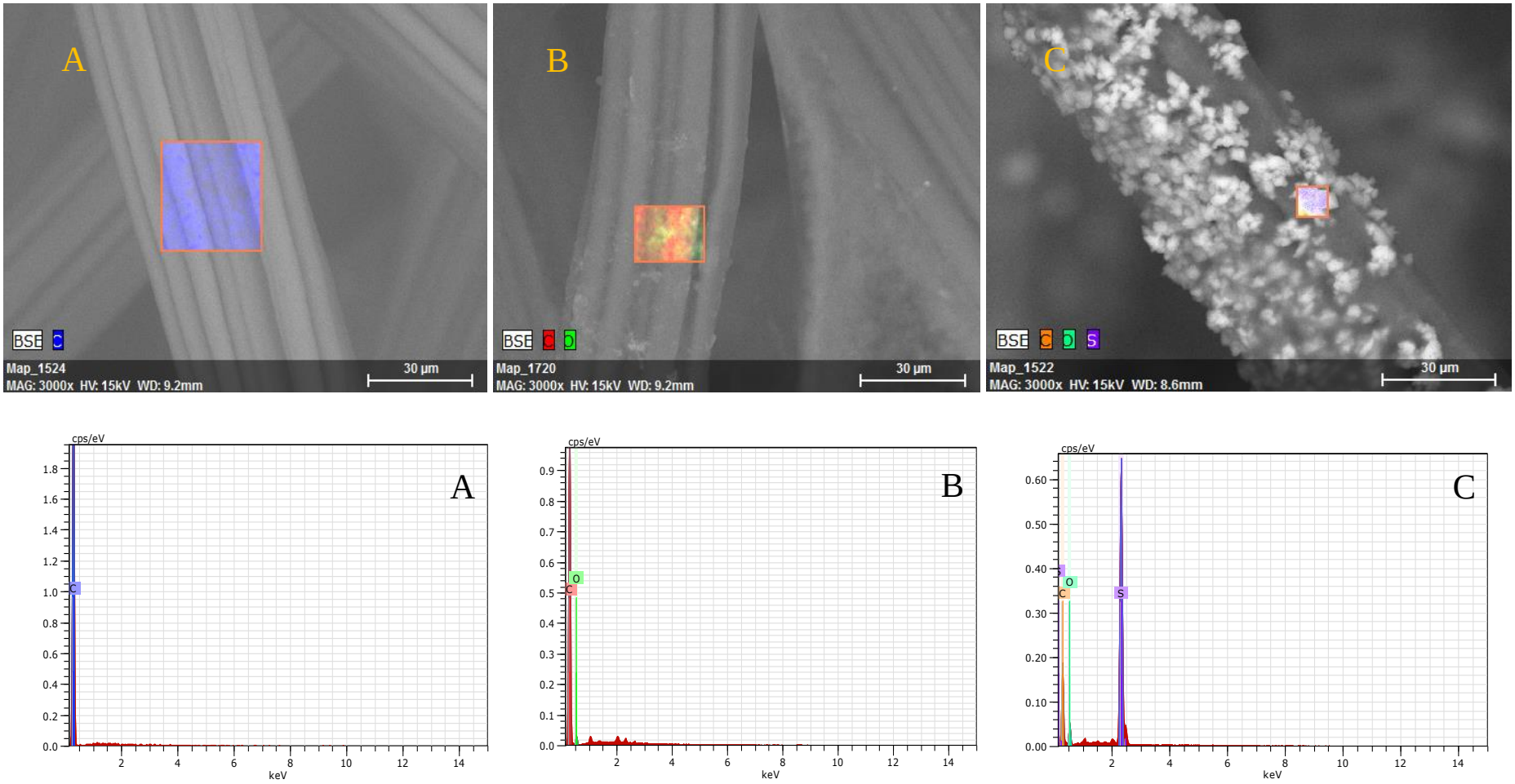

Figure 5-4 SEM images (1000x) and Energy-dispersive X-ray spectroscopy (EDX) of blank anode (A); The anode of the acetate-fed controls (B); The anode of the acetate+sulphate-fed BESs (C).

Test 3. The presence of electrogenic elemental sulphur oxidation (reaction 4)

Although anodic sulphur deposit accumulation was detected in the acetate+sulphate-fed BESs (Figure 5-4), negligible current production was observed in these BESs in the absence of acetate in test 3 (Table 5-4). It indicates that acetate was acting as the sole electron donor in the acetate+sulphate-fed BESs. In which case, electrogenic elemental sulphur oxidation was absent in the acetate+sulphate-fed BESs.

Test 4. The presence of elemental sulphur reduction (reaction 5)

Sulphide was detected in the effluent of the acetate+sulphate-fed BESs in the absence of sulphate in test 4 (Table 5-4). In which case, sulphide was produced by sulphur reduction (reaction 5) rather than sulphate reduction. Therefore, sulphur reduction was present in the acetate+sulphate-fed BESs.

	Maximum current (mA)	Δsulphate (e^-mmol/L)	Δsulphide (e^-mmol/L)	Δacetate (e^-mmol/L)
Test 1 (Reaction 2)	2.5	-9.14	+0.59	-35.07
Test 2 (Reaction 3)	0.83	N	N	N
Test 3 (Reaction 4)	N	N	N	N
Test 4 (Reaction 5)	2.6	N	0.63	-32.05

N: negligible.

Δ represents the value difference between the influent and the effluent of a test.

Table 5-4 The summary of the evidences to verify the presence of the individual major sulphur pathways in the BESs in the presence of sulphate.

5.3.3. The effect of anode potential on sulphate reduction in the acetate+sulphate-fed BESs.

Current production in both of the acetate+sulphate-fed BESs and the acetate-fed controls was increased with the increase of anode potentials from -250mV to 0mV although the current production in the acetate+sulphate-fed BESs was generally lower than the acetate-fed controls (linear regression, $p<0.05$) (Figure 5-5A). In contrast, the coulombic efficiency in the acetate+sulphate-fed BESs was increased with the increase of anode potential at the same range (linear regression, $p<0.05$) while the coulombic efficiency in the acetate-fed controls was slightly changed in such conditions (linear regression, $p>0.05$) (Figure 5-5A). Moreover, neither coulombic efficiency nor current production in the acetate+sulphate-fed BESs and the acetate-fed controls was increased with the increase of anode potential from +200mV to +700mV (linear regression, $p>0.05$).

In particular, the increase of the anode potential from -250mV to +700mV in the acetate+sulphate-fed BESs increased the extent of acetate oxidation from 6.2e^-mmol/L to 44.4e^-mmol/L (linear regression, $p<0.05$). However, this increase of anode potential barely changed sulphate reduction (3.3e^-mmol/L to 8.7 e^-mmol/L) (linear regression, $p>0.05$) (Figure 5-5B). Moreover, sulphide accumulation in the acetate+sulphate-fed BESs was very low (0.3e^-mmol/L to 0.7e^-mmol/L) at the same range of anode potential (Figure 5-5B).

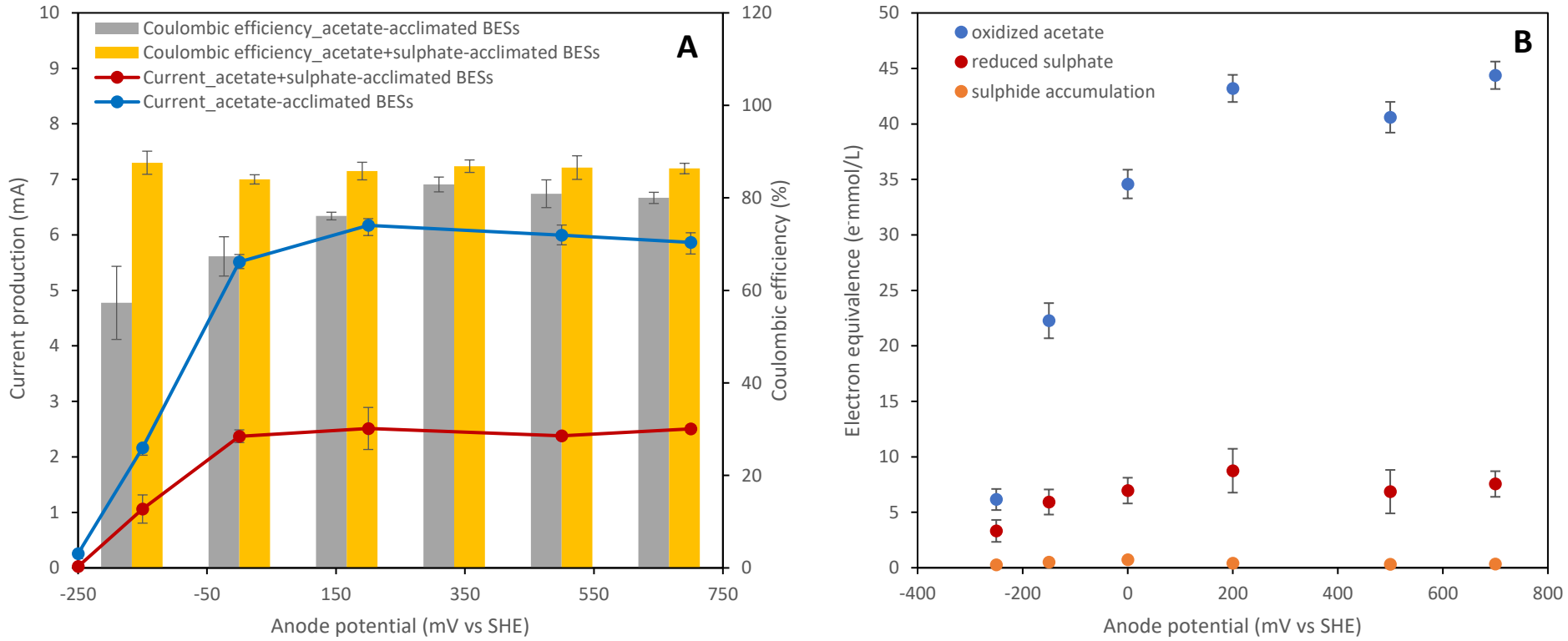

Figure 5-5 The electrogenic performance in the acetate+sulphate-fed BESs and controls with altered anode potentials (A). The relationship between oxidized carbon, reduced sulphate, sulphide accumulation and anode potentials in the acetate+sulphate-fed BESs (B).

5.3.4. The comparison of the effect of sulphate on the BESs fed with either acetate, glucose, sucrose or starch.

The electron loss in the BESs fed with different organics in the presence of sulphate

The electron loss caused by sulphate reduction in BESs was evaluated. The coulombic efficiency in acetate-fed pairs were similar as both of them reached at 76.2% to 77.4%. In contrast, the coulombic efficiency in the BESs fed with sulphate was lower than the BESs fed without sulphate when glucose, sucrose or starch were used as initial substrates (Figure 5-6). The largest difference in coulombic efficiency appeared in starch pairs where the starch-fed BESs reached 38.3% while the starch+sulphate-fed BESs reached only 24.1%. The coulombic efficiency in the sucrose-fed BESs was 73.3%, which was 11.2% higher than the sucrose+sulphate-fed BESs. The coulombic efficiency in glucose-fed BESs was 74.2%, which was 12% higher than the glucose+sulphate-fed BESs. The proportion of sulphate reduction/sulphide accumulation in the total electron balance in the glucose+sulphate-fed BESs and the sucrose+sulphate-fed BESs were 28.4%/2.5% and 31.6%/2.3% respectively (Figure5-7A), which were higher than the acetate+sulphate-fed BESs (17.9%/1.4%) and the starch+sulphate-fed BESs (17.2%/1.5%) (Figure5-7A).

Withdrawing sulphate from those BESs initially acclimated with sulphate slightly increased the coulombic efficiency (Figure 5-6). In particular, the starch+sulphate-fed BESs had the lowest coulombic efficiency of 27.4%. The coulombic efficiency in both of the glucose+sulphate-fed BESs and the sucrose+sulphate-fed BESs reached at 73.9% and 65.0% respectively (Figure 5-6). The highest coulombic efficiency was 78.7% in the acetate+sulphate-fed BESs, which was similar to its coulombic efficiency when sulphate was applied. Low sulphide accumulation was detected in these BESs in absence of sulphate and they ranged from 2.4% to 4.2% (Figure5-7B).

When acetate was used as a substrate in these BESs, the coulombic efficiency was increased significantly in the glucose-fed pairs, the sucrose-fed pairs and the starch-fed BESs pairs (Figure 5-6). In particular, the coulombic efficiency in those BESs fed without sulphate were 89.4%, 86.5% and 86.9% respectively while the coulombic efficiency in those BESs fed with sulphate were 73.9%, 72.2% and 77.7% respectively. The portion of total reduced sulphate and sulphide accumulation in the total electron balance of the glucose+sulphate-fed BESs stayed at 22.7% and 2.6% respectively when substrates were

switched to acetate (Figure5-7C). However, the portion of total reduced sulphate in the total electron balance in the surcose+sulphate-fed BESs and the starch+sulphate-fed BESs increased to 33.5% and 29.1% respectively when substrates were switched to acetate (Figure5-7C). Moreover, the portion of sulphide accumulation in these two BESs were also increased to 4.3% and 5.0% respectively (Figure5-7C).

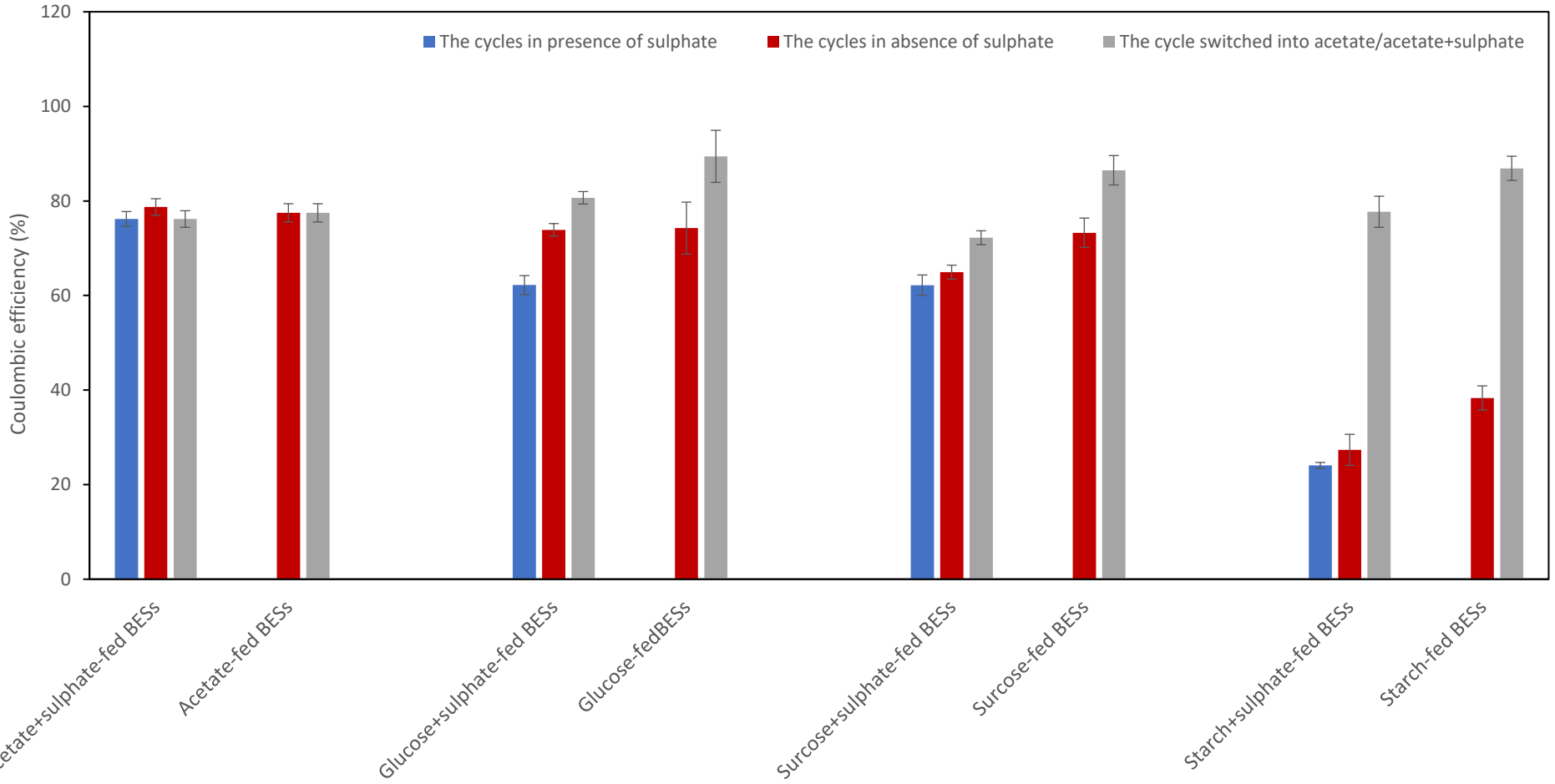

Figure 5-6 The coulombic efficiency in the BESs fed in presence of sulphate and the BESs fed in absence of sulphate.

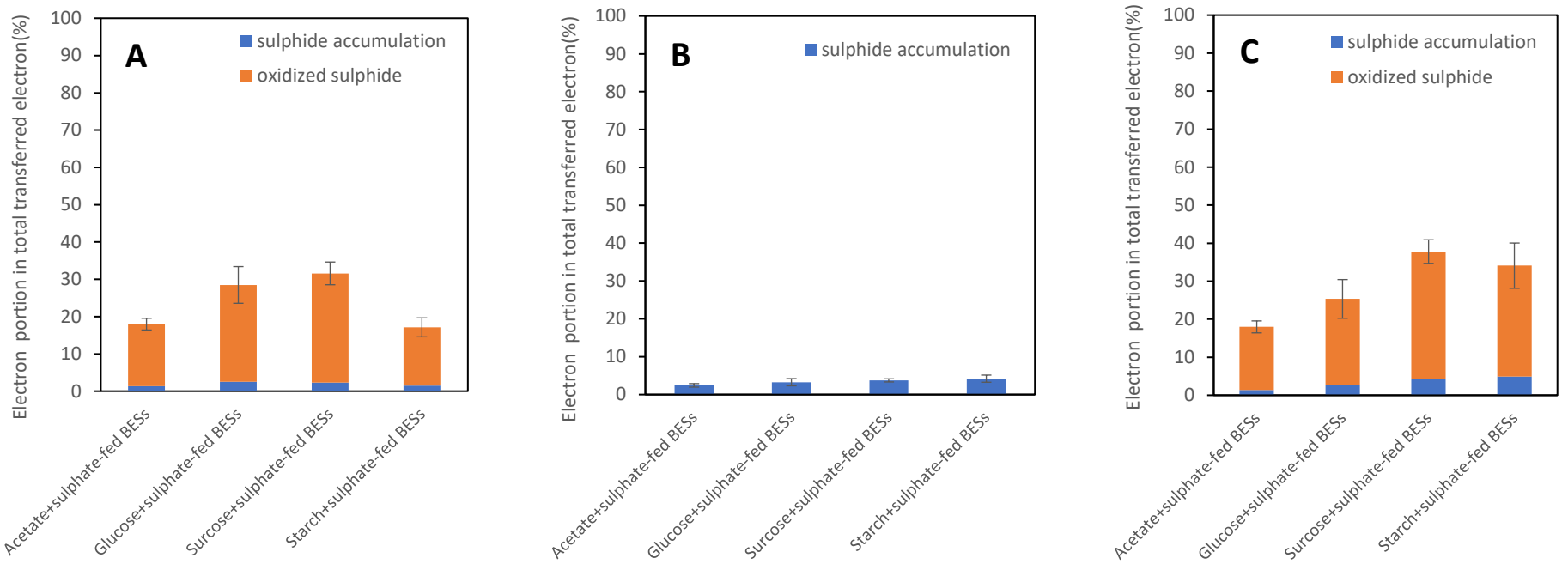

Figure 5-7 The oxidized sulphide and accumulated sulphide in the BESs in presence of (A) the cycles fed with initial substrate+sulphate; (B) the cycles fed with initial substrate only. (no sulphate); (C) the cycles fed with acetate + sulphate.

The current loss in the BESs fed with different organics in the presence of sulphate.

The cause of the current loss of these BESs was sorted here. The degradation of complex organics on the electrogenic ability of anode caused the largest loss of current as they ranged from -3.6mA to -3.8mA (Figure 5-8). The degradation of complex organics on the electrogenic process caused -0.7mA and -0.9mA reduction current in the glucose-fed BESs and the sucrose-fed BESs respectively. The current loss caused by the degradation of complex organics on the starch-fed BESs was -1.5mA. However, this loss decreased to as low as -0.21mA in the starch+sulphate-fed BESs. Sulphate reduction caused negligible current loss in all the BESs. However, the effect of sulphate on the electrogenic ability of the anode between the BESs initially acclimated with sulphate and the BESs initially acclimated without sulphate was significant. In particular, the current loss in the acetate+sulphate-fed BESs was as high as -3.1mA due to the sulphate acclimation. Moreover, -2.1mA of current loss in the starch+sulphate-fed BESs pairs was occurred because of such sulphate acclimation. However, the current loss by sulphate acclimation in the glucose+sulphate-fed BESs pairs and the sucrose+sulphate-fed BESs pairs was much lower as they were -0.4mA and -1.0mA respectively.

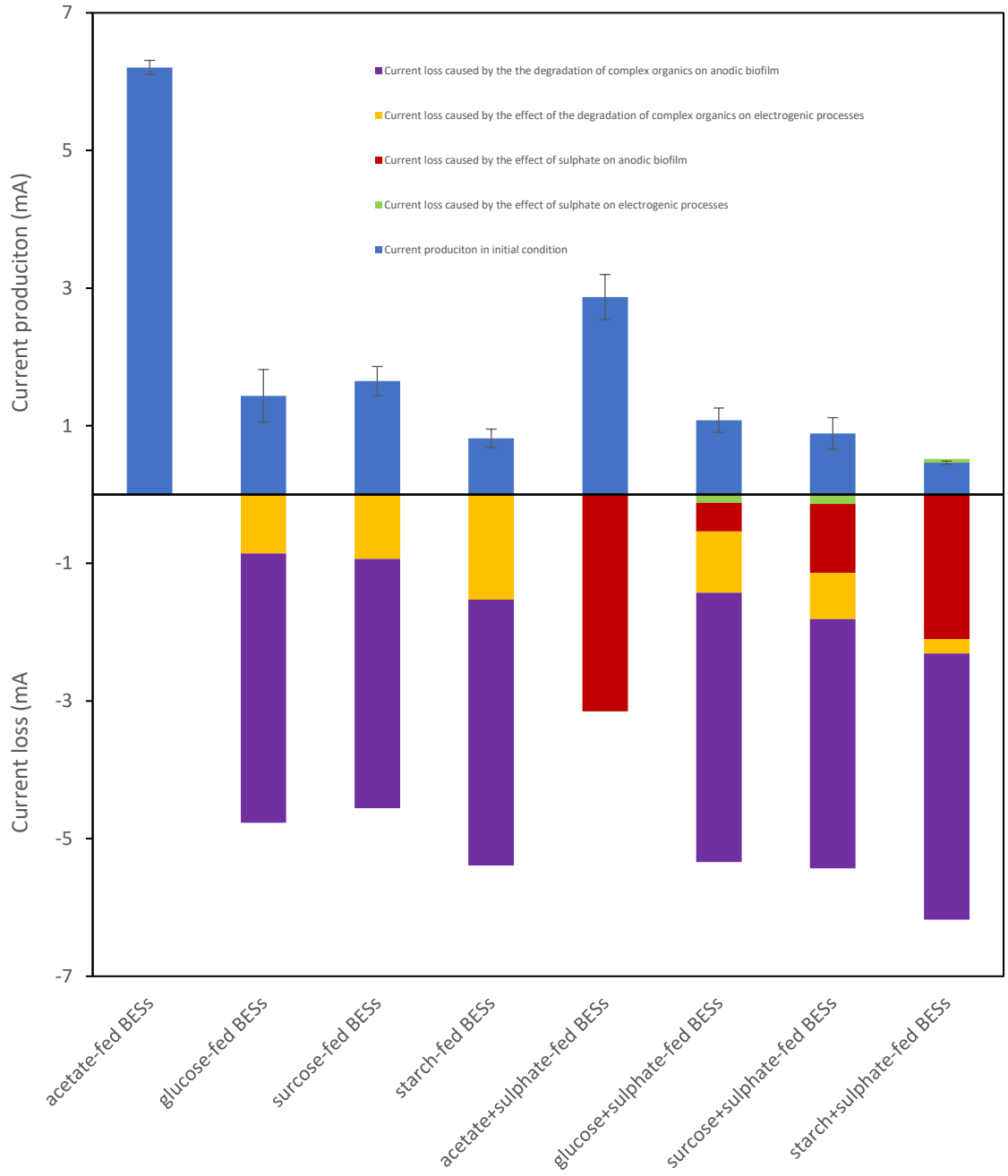

Figure 5-8 Current production in BESs in either presence or absence of sulphate and the proportion of each current loss in the BESs.

5.3.5. The effect of sulphate on anodic microbial community

In order to relate the effect of sulphate on electrogenic process with the effect of sulphate on microbial communities in these reactors, the anodic microbial communities in all the BESs were investigated at the end of the experiment.

BVA18,which belongs to the order of *Desulfuromonadales*, where contains sulphur reducing bacteria, were found in all the BESs in presence of sulphate. In particular, BVA18 comprised 42.5% and 36.3% of the anodic microbial communities in the glucose+sulphate-fed BESs and the surcose+sulphate-fed BESs respectively (Figure 5-9). Moreover, BVA18 accounted for 16.2% in the acetate+sulphate-fed BESs. However, the proportion of BVA18 in the starch+sulphate-fed BESs was only 5.3% (Figure 5-9). *Desulfovibrionaceae*, a sulphate reducing bacteria family, were also found in all the BESs in presence of sulphate. The glucose+sulphate-fed BES had the highest percentage of *Desulfovibrionaceae* (8.3%). Moreover, *Desulfovibrionaceae* constituted 4.3% of the anodic microbial communities in the surcose+sulphate-fed BESs. Additionally, both of the acetate+sulphate-fed BESs and the starch+sulphate-fed BESs had ~1.8% *Desulfovibrionaceae* (Figure 5-9).

Aeromonadaceae, a glucose degrader (Chung and Okabe, 2009), was present at high levels (21.9% to 31.9%) in all the glucose-fed BESs and sucrose-fed BESs in irrespective of the presence of sulphate. However, *Aeromonadaceae* accounted for only 10.5% in the starch+sulphate-fed BESs and none in the acetate-fed BESs (Figure 5-9). *Acidaminococcaceae* accounted for 9.1% and 5.6% in the glucose-fed BESs and the sucrose-fed BESs respectively while they were less predominate in the glucose+sulphate-fed BESs and the surcose+sulphate-fed (Figure 5-9). *Rhodocyclaceae* accounted for 22.1% in the anodic microbial communities of the starch-fed BESs but it declined to as low as 1.3% in the starch+sulphate-fed BESs. *Ruminococcaceae* was only present in the anodic microbial communities of the starch+sulphate-fed BESs, which accounted for as much as 32.7% (Figure 5-9).

Geobacteraceae, the major electrogenic family, was found in all the BESs in absence of sulphate. However, *Geobacteraceae* was extreme low in the glucose+sulphate -fed BESs, the sucrose+sulphate -fed BESs and the starch+sulphate -fed BESs. In addition, the

proportion of *Geobacteraceae* decreased from 95.7% to 76.4% in the acetate+sulphate-fed BESs in comparison with the acetate-fed controls (Figure 5-9).

Principal component analysis (PCA) was built based on the taxonomy of anodic microbial communities at family level. Detailed operational taxonomic units (OTUs) table is in Appendix Figure 8-6. Figure 5-10 shows that all the communities in the BESs initially acclimated with sulphate were separated from the communities in the BESs initially acclimated without sulphate under the same organic substrate feed. Only the starch-fed BESs pairs located at the lower part of the figure. Moreover, the first component explained 70% of the variation and this put the reactors in order of their *Geobacteraceae* abundance (Figure 5-10).

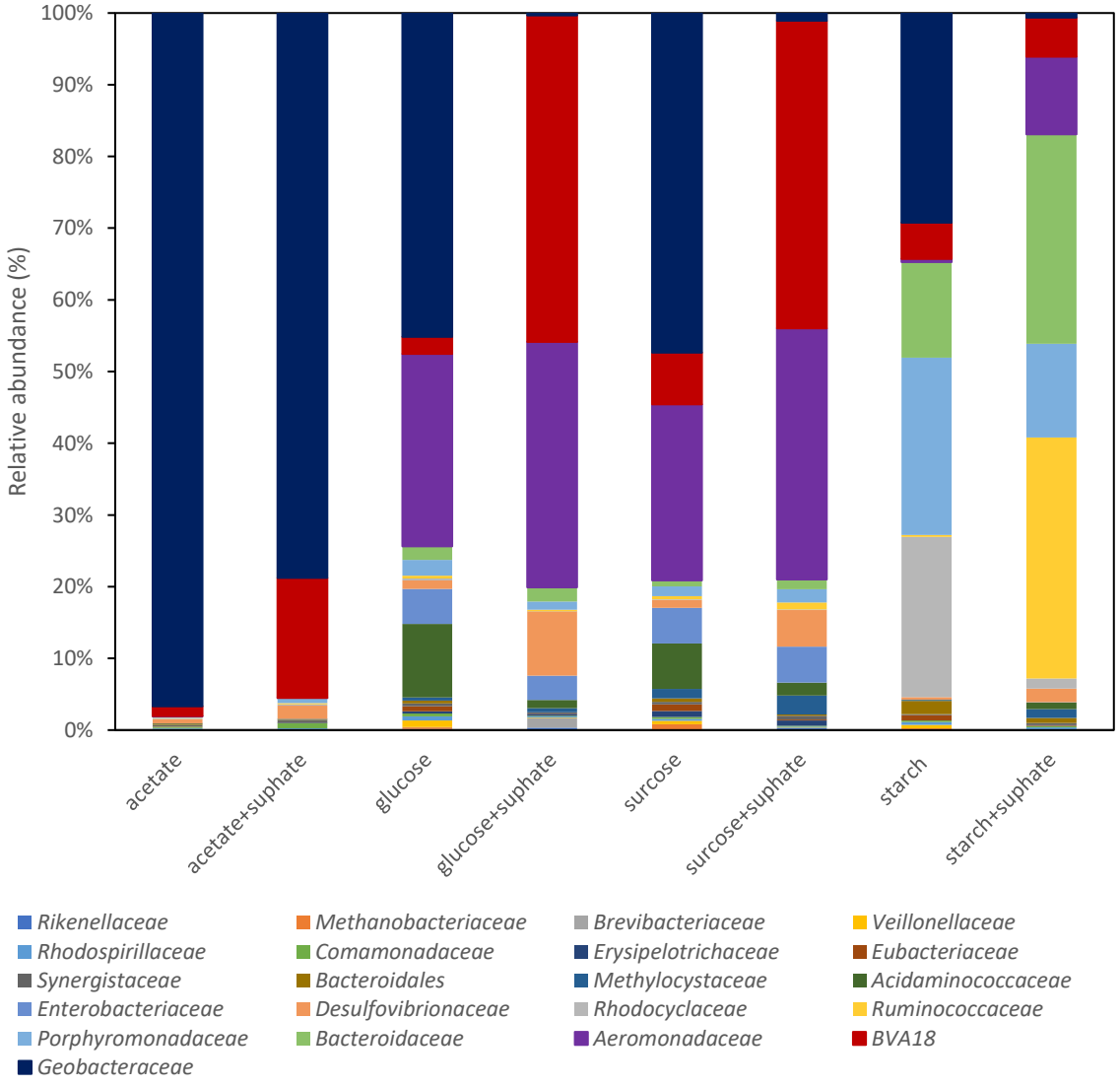

Figure 5-9 The selected relative abundance of anodic microbial communities of BESs at family level.

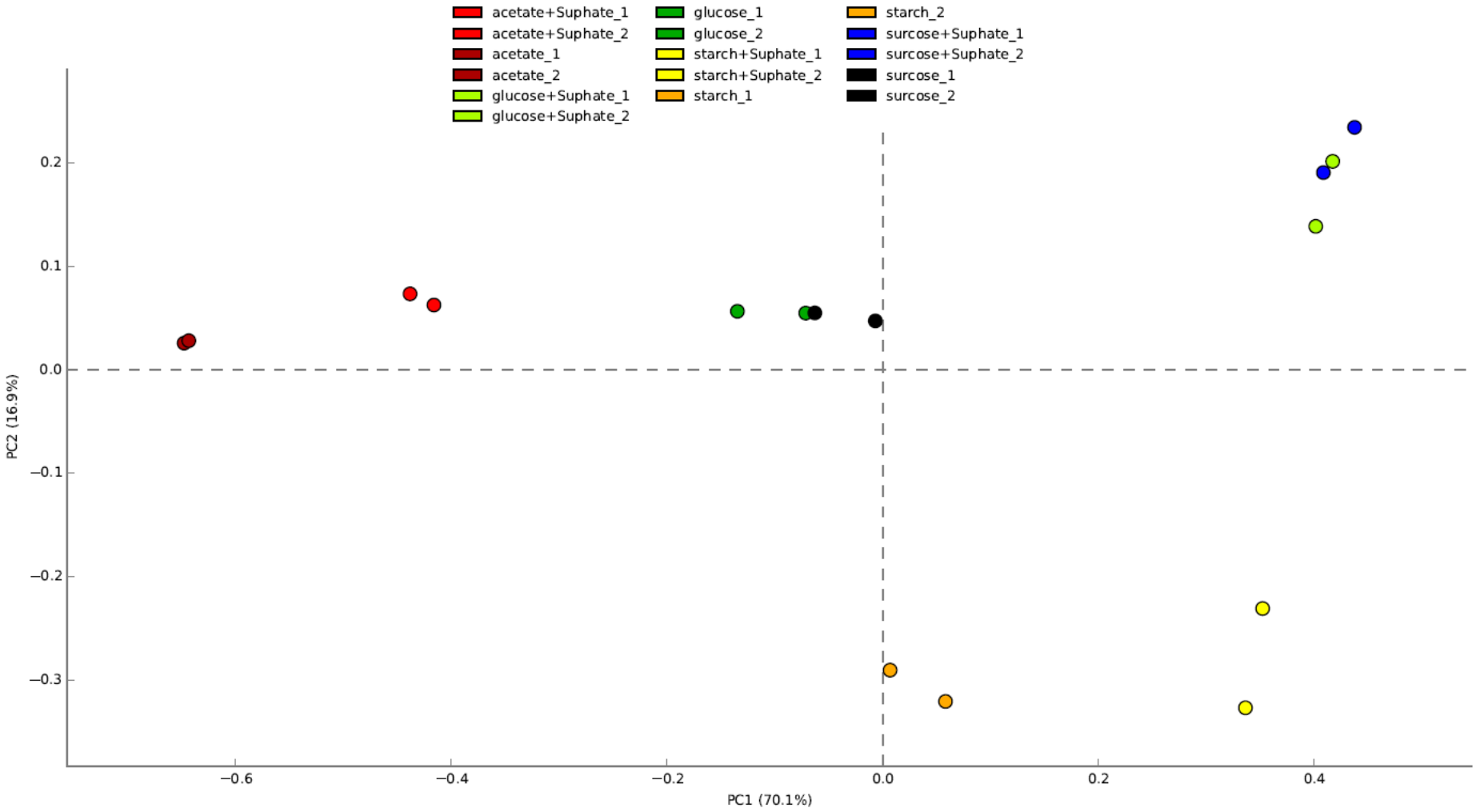

Figure 5-10 Principal component analysis of the taxa of anodic microbial communities at family level.

5.4. Discussion

In this study, the electrogenic constraints in the sulphate cycles in the acetate+sulphate-fed BESs with different availabilities of either sulphate or acetate was identified. Moreover, the effect of the anode potential on the sulphate reduction in acetate+sulphate-fed BESs was investigated. In addition, the effect of sulphate on the electrogenic function of the BESs acclimated with fermentable and hydrolysable organics was evaluated.

The electrogenic constraints in the acetate+sulphate-fed BESs with different availabilities of either sulphate or acetate.

The highest sulphate reduction in the acetate+sulphate-fed BESs occurred when 120e^- mmol/L (15mM) sulphate and 80e^-mmol/L (10mM) acetate were applied and this highest sulphate reduction induced the lowest coulombic efficiency in the acetate+sulphate-fed BESs. It suggests that this lowest coulombic efficiency was largely caused by the failure of electrogenic sulphur oxidation (reaction 4) to recover the electrons from sulphur accumulation according to the stoichiometric analysis in Table 5-1. In fact, the direct microbial electrogenic elemental sulphur oxidation has only been observed in pure culture-BESs in the absence of organic matter so far (Gong et al., 2013; Zhang et al., 2014). This suggests that the absence of biotic electrogenic elemental sulphur oxidation in the acetate+sulphate-fed BESs in this study could probably be attributed to the thermodynamic advantage of electrogenic organic oxidation (reaction 1) at anode potential of 0mV (-223kJ/mol) in the acetate+sulphate-fed BESs, compared to -134kJ/mol of electrogenic sulphur oxidation (reaction 4). No significant increase of the coulombic efficiency in the acetate+sulphate-fed BESs was observed when increasing the anode potential from 0mV to +700mV (Figure 5-5A). Therefore, the BESs at high anode potentials was unlikely to electrogenically recover electron via electrogenic sulphur oxidation (reaction 4) either. Although the current production in the acetate+sulphate-fed BESs in absence of organic feed at high anode potentials was not measured, the presence of electrogenic elemental sulphur oxidation in the acetate+sulphate-fed BESs at high anode potentials was not ruled out in this study. The presence of sulphur reduction (reaction 5) in the acetate+sulphate-fed BESs in this study could alleviate the electrons accumulation in sulphur and electrogenically recover electrons via electrogenic sulphide oxidation (reaction 3). However, new sulphur deposits were presumably also produced from electrogenic sulphide oxidation (reaction 3) while more carbon was used as electron

donor for the sulphur reduction (reaction 5). Moreover, substantial amount of sulphur was deposited on the anode of the acetate+sulphate-fed BESs at the end of the experiment. This suggests that sulphur reduction, combined with sulphide oxidation (reaction 5), was unable to completely remove the sulphur deposit in the acetate+sulphate-fed BESs in this study.

Sulphate reduction (reaction 2) did not directly cause the electron loss in the acetate+sulphate-fed BESs. Although electrogenic sulphide oxidation (reaction 3) was slower than the electrogenic acetate oxidation (reaction 1) in the acetate+sulphate-fed BESs, which was consistent with previous acetate+sulphur-fed BESs (Dutta et al., 2009). However, the sulphide oxidation was rapid enough to remove the majority of the sulphide produced from sulphate reduction in BESs as the sulphide accumulation was very low in the acetate+sulphate-fed BESs irrespective of the extent of sulphate reduction (Figure 5-1). Importantly, there was no substantial microbial sulphur oxidizer such as *Thiomonas*, which appeared in neutral-pH BESs (Zheng et al., 2014), in the anodic microbial communities of the acetate+sulphate-fed BESs in this study although the reactors were also buffered at neutral-pH. Moreover, the current production by sulphide oxidation in abiotic reactors was only slight lower than the biotic reactors. Therefore, electrogenic sulphide oxidation was possibly primary abiotic in this study.

On the other hand, current production in the acetate+sulphate-fed BESs was more affected by the acetate availability rather than the sulphate derivative reactions in these reactors. This was because the current production in the acetate+sulphate-fed BESs was only significantly decreased when acetate availability was lower than 40e^-mmol/L irrespective the sulphur accumulation in the acetate+sulphate-fed BESs. This was consistent with that the minimum acetate availability of 35.2 e^-mmol/L for the saturated current production in the glucose-fed BESs in chapter 3. Moreover, as mentioned above, electrogenic sulphide oxidation was rapid enough to recover the current loss from either sulphate reduction (reaction 2) or sulphur reduction (reaction 5) in the acetate+sulphate-fed BESs. Therefore, the effect of sulphate derivative reactions on current production in the BESs in presence of sulphate was minor.

Surprisingly, the current production in both of the acetate+sulphate-fed BESs and the acetate-fed controls was unaffected by increasing the conductivity by dosing either sulphate or sodium chlorine in this study. The rise of conductivity by high salt dosing

increased the current production in previous BESs (Cheng et al., 2006; Liu et al., 2005; Torres, Marcus and Rittmann, 2008). Notably, previous study used single-chamber BESs where the electrolyte possibly caused the major resistance between the electrodes. Hence, the optimization of the conductivity of electrolyte was more effective to the current production in such BESs. In contrast, membrane-based BESs, where the membrane presumably caused the major resistance between electrodes, were used in this study. Therefore, the optimization of the conductivity of electrolyte was presumably much less effective to the current production of BESs and hence dosing of neither sulphate nor sodium chlorine affects the current production in the BESs in this occasion in this study.

The effect of anode potential on the sulphate reduction in the acetate+sulphate-fed BESs

This study tried to minimize the extent of sulphate reduction in the acetate+sulphate-fed BESs by increasing anode potential. However, to increase the anode potential in the acetate+sulphate-fed BESs only increased the amount of acetate oxidation but barely changed the extent of sulphate reduction. In particular, increasing anode potential from -250mV to 0mV in the acetate+sulphate-fed BESs improved both current production and coulombic efficiency, which was consistent with the saturated anode potential of acetate oxidation at 0mV in *Geobacter sulfurreducens*-acclimated BESs (Wei et al., 2010). Moreover, the coulombic efficiency in the acetate+sulphate-fed BESs was also increased at the same range of anode potentials. In particular, the coulombic efficiency in the acetate+sulphate-fed BESs at these anode potentials increased with the decrease of the proportion of the acetate removal by sulphate reduction in total acetate removal. This was consistent with the low coulombic efficiency in the acetate+sulphate-fed BESs with high sulphate reduction when 150e^-mmol/L of sulphate was fed. Although, this decrease of the proportion of the acetate removal by sulphate reduction in total acetate removal was due to the increasing of acetate oxidation at these anode potentials while the variation of sulphate reduction was limited in such conditions (Figure 5-1B and Figure 5-2B). Therefore, the improvement of current production and coulombic efficiency in the acetate+sulphate-fed BESs at higher anode potentials was because the enhancement of acetate oxidation rather than the repression of sulphate reduction.

The effect of sulphate on the BESs fed with different organics.

This study demonstrates that the negative impact of sulphate was much lower than the negative impact of fermentation/hydrolysis on the electrogenic performance in complex-fed BESs. As mentioned above, the decrease of the current production in the acetate+sulphate-fed BESs was attributed to the decrease of acetate availability, while the effect of sulphate on the current production in such reactors was limited. Moreover, the current production from the glucose/sucrose/starch+sulphate-fed BESs was generally lower than the acetate+sulphate-fed BESs, but similar to their sulphate-free controls (Figure 5-8). Besides, the acetate availabilities of the glucose/sucrose/starch+sulphate-fed pairs were possibly insufficient for saturated current production according to chapter 3. This suggests that acetate availability had much higher effect on the current production of BESs than sulphate. On the other hand, although sulphide accumulation in the glucose/sucrose/starch+sulphate-fed BESs was higher than the acetate+sulphate-fed BESs, the coulombic efficiency in these BESs was only significantly increased when switching the feed of these organics to acetate in such BESs, while the coulombic efficiency in these BESs was slightly changed when withdrawing sulphate. Therefore, the election loss in the glucose/sucrose/starch-fed BESs in the presence of sulphate was largely attributed to low acetate production from fermentation/hydrolysis rather than the electron capture in sulphate reduction.

However, the negative effect of sulphate on the anodic microbial communities was much higher than the negative effect of sulphate on the electrogenic process. In particular, the presence of sulphate was lethal to the major electrogenic microorganisms *Geobacteraceae* since the abundance of *Geobacteraceae* in the BESs acclimated with sulphate was low. The toxicity of sulphide was considered as the reason of this decline of *Geobacteraceae* (Cord-Ruwisch et al., 1998). Notably, the anodic microbial communities in the acetate+sulphate-fed BESs hold 76% of *Geobacteraceae* while the abundance of *Geobacteraceae* in the glucose/sucrose/starch+sulphate-fed BESs was extreme low. This was possibly because acetate, the *Geobacteraceae* preferred substrate, was sufficient in the influent of the acetate+sulphate-fed BESs, and thus the growth of *Geobacteraceae* was favoured. It indicates that maintaining the high acetate availability is the key to achieving good electrogenic performance and high abundance of electrogenic microorganisms in the BESs in the presence of sulphate.

Caveats pertaining to the experiments.

Coulombic efficiency was used to assess the electron loss in the BESs acclimated with sulphate in this study. In particular, coulombic efficiency in BESs was defined as the proportion of the electrons participated in current in the total consumed electrons (Verstraete and Rabaey, 2006). However, in the BES with sulphur cycling, the anodic sulphur deposit could provide extra electron resource for electrogenic processes. The amount of this portion of electron is particular difficult to be evaluated because the measurement of the electron consumption of the sulphur deposits is difficult. Therefore, coulombic efficiency was an imperfect measure of electron loss in such BES. Nevertheless, organic substrates was the only initial electron donor for all the reactions in the BESs in presence of sulphate because the electrogenic elemental sulphur oxidation was absent in the BESs in this study. Therefore, coulombic efficiency was able to assess the electron loss in the BESs in this study.

The measurement of sulphide in BESs is complicated because sulphide can easily escape from the reactors. Since the pH in the BESs in presence of sulphate was between 7 to 7.5, most of the sulphide was present in the soluble form and therefore not released to the atmosphere. Moreover, Nafion cation exchange membrane was used to separate the anodic chamber and cathodic chamber, and therefore sulphide diffusion was unlikely to occur in the BESs in this study (Blázquez et al., 2017; Dutta et al., 2008). In addition, an anti-sulphur oxidation method was used in this study to preserve the sulphide sample in order to avoid the oxidation of sulphur during preservation (Pikaar et al., 2011). In which case, the majority of sulphide was recorded in this study.

Implications

Sulphur cycle in anaerobic system is elusive. This study examined the presence of the major electrogenic steps in sulphur cycle in the acetate+sulphate-fed BESs to illustrate the effect of sulphate on the electrogenic performance of BESs. In particular, the effect of sulphate on the coulombic efficiency of these BESs was minor, compared to the other electron acceptors such as nitrite and carbon dioxide (Parameswaran et al., 2009; Sukkasem et al., 2008). Although electron loss occurred in the BESs with high sulphate availability (15mM) in this study, the sulphate concentration in domestic wastewater is normally much lower than this value. Therefore, the electron loss caused by sulphate was

not major concern in the BESs for domestic wastewater treatment. However, the accumulation of sulphur was a major issue to the BES in long terms because the sulphur accumulation damaged the electrogenic function of anode as the BESs were failed in 3 months (data not shown). Altering anode potential had little effect on the sulphate reduction in the BESs in presence of sulphate. Moreover, no effective reaction was presented in the BESs in presence of sulphate to use sulphur to produce current without producing sulphide. However, sulphide was lethal to *Geobacteraceae* in the anodic microbial communities of these BESs even though it was in trace amount. Therefore, sulphate possibly needs to be removed from the influent of organics-fed BESs. In recent years, many studies have focused on sulphate removal from wastewater by BESs via autotrophic biocathode (Blázquez et al., 2016; Luo et al., 2014, 2017). This method is a type of the biocathode-based microbial synthesis, where renewable energy such as wind was used to split water at anode and thus to provide electrons for cathode reactions. This could be used to pretreat the influent of the organics+sulphate-fed BESs although rationale design is needed to avoid more capital cost.

5.5. Conclusion

This study illustrates the electrogenic constraints in the BESs in the presence of sulphate in the response to the carbon:sulphate ratio and anode potentials. Moreover, the effect of the coexistence of organic degradation and sulphate reduction on the electrogenic performance of BESs was analysed. In particular, the absence of electrogenic elemental sulphur oxidation in the acetate+sulphate-fed BESs was a major electrogenic constraint, and this caused the decrease of the coulombic efficiency of such BESs, which reached lowest value of 67% when the C/S ratio was 1.33. However, this effect was not as decisive as the acetate availabilities to the current production in such BESs because the current production in these BESs was only decreased with the decrease of the availabilities of acetate and reached the lowest value of 0.8mA. To increase anode potential from -250mV to +200mV in the acetate+sulphate-fed BESs increased the current production and the coulombic efficiency from 0.02mA to 2.51mA and from 57.3% to 82.9% respectively, but had little effect on the extent of sulphate reduction. On the other hand, in the BESs in the presence of both organic degradation and sulphate reduction, the negative effect of organic degradation such as fermentation/hydrolysis on electrogenic process was much higher than sulphate reduction. However, the negative effect of sulphate on the microbial electrogenic function of anode was significant because the growth of the major electrogenic species *Geobacteraceae* in the BESs in the presence of sulphate was seriously restrained.

Chapter 6 General conclusion and outlook

Bioelectrochemical systems (BESs) have been designed to recover the energy from wastewater and many of them rely on anodic organic oxidation as driving force. Numbers of studies achieved good electrogenic performance in acetate-fed BESs. However, the electrogenic performance in those BESs fed with wastewater was much worse. This PhD study therefore investigated the effect of complex composition of wastewater on the electrogenic performance of BESs by peeling off this effect into two major parts: the effect of the complex pathway in electron donors and the effect of the presence of an alternative electron acceptor. Glucose and sulphate were used as a model of complex electron donor and alternative electron acceptor respectively. The major electrogenic pathways and the electrogenic constraints in the BESs fed with glucose or sulphate were identified and the relationship between anode potential/carbon:sulphate ratio and such electrogenic constraints was investigated.

In particular, this study identified that the major electrogenic pathway in the glucose-fed BESs was to generate current through acetate and formate via glucose degradation. On the other hand, The major electrogenic pathway in the acetate-fed BESs in the presence of sulphate was through either direct electrogenic acetate oxidation or the sulphide oxidation via reduction of sulphate and sulphur. In fact, many reactions such as acetate production from ethanol/propionate and electrogenic elemental sulphur oxidation can proceed in those individual-fed BESs (Parameswaran *et al.*, 2009, 2011; Zhang *et al.*, 2014; Hari *et al.*, 2016). It is proposed that these reactions can significantly improve the electrogenic performance of the BESs fed with complex composition. However, most of these reactions were absent in BESs fed with complex in real cases and the reason of the absence of these derivative reactions in complex-fed BESs is still unknown. Therefore, systematic studies are needed to investigate the reason of the absence of these derivative reactions in BESs. For instant, the presence of the biotic electrogenic elemental sulphur oxidation is important to the BESs in the presence of sulphate because it can prevent the failure of the electrogenic function of BESs in the long term and electrogenically recover large amounts of electrons from sulphur accumulation. However, this reaction was absent in the BESs in the presence of sulphate in this study. It is known that both pH and anode potential were important factors in the disproportionation of sulphur (Rabaey et al., 2009). Therefore, a study is recommended to investigate whether altering anode potential

and pH can induce biotic electrogenic elemental sulphur oxidation in BESs in presence of sulphate.

Notably, *Desulfovibrionaceae* was the only major sulphate reducer in the anodic microbial communities of the acetate+sulphate-fed BESs. However, *Desulfovibrionaceae* did not use acetate as electron donor to reduce sulphate in anaerobic system (Heidelberg et al., 2004). Likewise, acetate-based sulphate reduction in BESs was not reported so far (Dutta et al., 2009; Rabaey et al., 2005). Notably, it was reported that *Desulfovibrionaceae* has high affinity for hydrogen in sulphate reduction process (Laanbroek et al., 1984). Moreover, major electrogenic bacteria, *Geobacteraceae*, can conduct acetate oxidation via syntrophic process with hydrogen consuming partner *Hydrogenophaga* (Kimura and Okabe, 2013). Although syntrophic processes between *Geobacter sulfurreducens* and *Desulfovibrio desulphuricans* was not observed when using sulphate as electron acceptor and it inferred that high sulphide concentration inhibited acetate degradation (Cord-Ruwisch et al., 1998). However, sulphide accumulation was very low in this study due to the presence of electrogenic sulphide oxidation. Therefore, the syntrophic process for sulphate reduction between *Geobacteraceae* and *Desulfovibrionaceae*, companied with the assist of electrogenic sulphide oxidation, likely occurred in the acetate+sulphate-fed BESs in this study, and hydrogen was proposed as the electron donor for the sulphate reduction in such BESs. In addition, hydrogen can be consumed by other hydrogen consuming processes such as direct electrogenic processes and homoacetagenesis in the BESs in presence of sulphate in this study. Therefore, to understand the electrons transfer pathway of hydrogen in acetate+sulphate-fed BESs can provide further insight on how to control sulphate reduction in BESs. In which case, a study is needed to investigate the fate of hydrogen in the BESs in the presence of sulphate.

The major electrogenic microorganism in both of the glucose-fed BESs and the BESs in the presence of sulphate was *Geobacteraceae*. To understand the electrogenic function of each anodic microorganism is the key to learn the electrogenic pathways in glucose-fed BESs. However, the electrogenic role of the electrogenic microorganisms for these electrogenic pathways in the glucose-fed BESs was not fully identified in this study. Stable isotope probes (SIP) could be an effective method to individually identify the microorganisms for each glucose degradation pathway. However, this analysis requires

large numbers of replicate reactors and anodic biofilms to identify all the major glucose degradation pathways, which was not possible within the scope of the work presented. Therefore, a study is warranted to identify the glucose degradation pathways and corresponding microorganisms in glucose-fed BESs. Importantly, this study infers that the electrons from glucose were significantly lost in biomass synthesis in the glucose-fed BESs. However, there was no actual measurement of these biomass electron sinks in this study. In which case, future work is recommended to evaluate the electron loss in the biomass synthesis in glucose-fed BESs.

This PhD work also concluded that the major electrogenic constraints in the glucose-fed BESs were the low availabilities of acetate/formate and the low abundance of major electrogenic microorganisms *Geobacteraceae*. Moreover, the electrogenic constraints in the BESs in the presence of sulphate were the low availability of acetate and the absence of electrogenic elemental sulphur oxidation. In particular, the current production in BESs with both complex organics such as glucose and alternative electron acceptors such as sulphate was significantly affected by the acetate availability. Moreover, the low acetate availability in the glucose-fed BESs was because of the low acetate production from glucose and glucose degradation intermediates (GDIPs) such as ethanol and propionate. The coulombic efficiency in glucose-fed BESs was affected by the degradation pathways of glucose, formate and ethanol. On the other hand, the overall negative effect of sulphate on the current production of BESs was significantly lower than the effect of fermentation/hydrolysis pathway of complex electron donors. The decrease of the coulombic efficiency in the BESs in presence of sulphate only occurred when sulphate was largely reduced under the feed conditions of 15mM of sulphate and 10mM of acetate. In addition, the low acetate availability and the presence of sulphide and elemental sulphur severely affected the abundance of the major electrogenic microorganisms specifically *Geobacteraceae* in BESs, although the BESs acclimated with sufficient acetate had higher tolerance to the negative effect of sulphate and therefore held higher the abundance of *Geobacteraceae* than other sulphate-fed reactors. This low abundance of *Geobacteraceae* likely caused the lower current production observed in the BESs fed with complex components, compared to acetate-fed ones, even though optimized influent was applied in complex-fed BESs. Energy availability is important for the growth of electrogenic microorganisms. In this study, the energy availability in BESs within only 9

hours was evaluated while the total energy availability for the growth of the major electrogenic microorganism was unknown. This was because that the amount of the electron involved in current production in BESs during the entire growth processes was not measured. The evaluation of this available energy for the growth processes of electrogenic microorganisms has been done in *Geobacter sulfurreducens*-acclimated BESs with sufficient acetate (Wei et al., 2010). Likewise, the total available energy for the growth of electrogenic microorganisms in glucose-fed BESs could be measured by similar method, and in this way, to better understand the microbiology of such systems.

This study demonstrated that anode potentials have little effect on the pathways of glucose degradation and sulphate cycle in BESs, and therefore little affected on the microbial electrogenic constraints in such BESs. In particular, to increase anode potential from -150mV to +200mV in such reactors improved the abundance of *Geobacteraceae* in glucose-fed BESs and thus improved the current production, although coulombic efficiency was only slightly increased. However, the BESs fed with sufficient acetate achieved high abundance of *Geobacteraceae* in despite of the initial acclimation anode potentials. This suggests that altering anode potential was not necessary to the abundance of *Geobacteraceae* in the BESs fed with acetate. On the other hand, alteration of applied anode potential in BESs could barely change the acetate production from glucose degradation and electrogenic sulphur removal. Moreover, altering anode potential in BESs could not restrain unwanted reactions such as sulphate reduction. These results provided instructive information about the electrogenic pathways of complex components in BESs at anode potentials ranging from -250mV to +200mV (in the glucose-fed BESs) or +700mV (in the BESs in the presence of sulphate). This can be used as optimization strategy for the electrogenic performance of the BESs fed with complex composition such as wastewater. Notably, anode potential did not affect the anodic microbial communities in glucose-fed BESs and the peak acetate availability in such BESs did not be improved in this study. Notably, it proposed that several factors such as operation mode and internal resistance other than anode potential are decisive to the anodic microbial communities in BESs. In particular, batch fed mode applied in this study was possibly the factor to result the similar anodic microbial communities in these glucose-fed BESs because only anodic activities-related microorganisms were detained in such conditions while others were periodically washed out. In which case, the microbial diversity in such BESs was possibly

low and this therefore leaded similar anodic microbial communities. Continuous flow mode is also universally applied in wastewater treatment and that can however potentially increase the diversity of anodic microbial communities in BESs. This is because both anodic microorganisms and suspended microorganisms can be detained in BESs with such continuous flow mode. In which case, this mode can induce anodic microbial communities that is more sensitive to the anode potential. However, the effect of anode potential on the continuous flow mode BESs was not investigated in this study. Therefore, the effect of anode potential on the anodic microbial communities in the continuous flow mode BESs needs to be studied.

Other factors such as configuration and internal resistance can also influence the electrogenic performance of BESs. In particular, both H-type reactors and tubular reactors were used in this study. However, the saturated current production of acetate-fed controls was much higher than glucose-fed BESs in the tubular reactors, but they were similar in the H-type reactors. The difference of the internal resistance between these two types of reactors was proposed as the key factor to influence the saturated current production in these reactors. However, the relationship between internal resistance and saturated current production in both acetate-fed controls and glucose-fed BESs was unknown. Understanding this relationship could provide important insight for the design of the BESs reactor when fed with different compositions of influent. DNA-based qPCR was used to evaluate the relationship between the abundance of major electrogenic microorganisms and the current production in this study. However, current production is also related to the gene expression of the electrogenic microorganisms. Therefore, in order to better understand the relationship between internal resistance and the electrogenic function of the anode in BESs fed with different compositions of influent, a study is needed to investigate the relationship between internal resistance and the gene expression in BESs fed with different compositions.

To achieve high electrogenic performance in the BESs fed with complex composition such as wastewater is a great challenge as various factors in such composition can influence the electrogenic performance of BESs. This study proposes that increasing the peak acetate availability and restraining sulphate reduction are particularly important to the BESs fed with complex composition. However, laboratory results show that it was difficult to achieve these two tasks by changing the parameters of BESs such as anode

potentials and the C/S ratio of the influent. In which case, the effect of other parameters such as operation mode on the electrogenic performance of the BESs fed with complex composition needs to be systematically studied. Moreover, it proposed that the high internal resistance in H-type reactors was attributed to the large distance between electrodes. This suggests that improved configuration and design is also important to optimize the electrogenic performance of BESs. Additionally, the deployment of BESs in wastewater treatment should be done rationally, considering the effects of components such as sulphate as this will inevitably affect the electrogenic performance of BESs.

Chapter 7 Reference list

Blázquez, E., Gabriel, D., Baeza, J.A. and Guisasola, A. (2016), "Treatment of high-strength sulfate wastewater using an autotrophic biocathode in view of elemental sulfur recovery", *Water Research*, Vol. 105, pp. 395–405.

Blázquez, E., Gabriel, D., Baeza, J.A. and Guisasola, A. (2017), "Evaluation of key parameters on simultaneous sulfate reduction and sulfide oxidation in an autotrophic biocathode", *Water Research*, Vol. 123, pp. 301–310.

Bond, D.R. and Lovley, D.R. (2003), "Electricity Production by *Geobacter sulfurreducens* Attached to Electrodes Electricity Production by *Geobacter sulfurreducens* Attached to Electrodes", *Applied and Environmental Microbiology*, Vol. 69 No. 3, pp. 1548–1555.

van den Brand, T.P.H., Roest, K., Chen, G.H., Brdjanovic, D. and van Loosdrecht, M.C.M. (2015), "Potential for beneficial application of sulfate reducing bacteria in sulfate containing domestic wastewater treatment", *World Journal of Microbiology and Biotechnology*, Springer Netherlands, Vol. 31 No. 11, pp. 1675–1681.

Call, D. and Logan, B.E. (2008), "Hydrogen production in a single chamber microbial electrolysis cell lacking a membrane", *Environmental Science and Technology*, Vol. 42 No. 9, pp. 3401–3406.

Cao, X., Huang, X., Liang, P., Xiao, K., Zhou, Y., Zhang, X. and Logan, B.E. (2009), "A New Method for Water Desalination Using Microbial Desalination Cells", *Environmental Science & Technology*, Vol. 43 No. 18, pp. 7148–7152.

Chaudhuri, S. and Lovley, D. (2003), "Electricity generation by direct oxidation of glucose in mediatorless microbial fuel cells", *Nature Biotechnology*, Vol. 21 No. 10, p. 1229.

Cheng, S., Hamelers, H.V.M., Logan, B.E., Call, D.F., Cheng, S., Hamelers, H.V.M., Sleutels, T.H.J.A., et al. (2008), "Critical Review Microbial Electrolysis Cells for High Yield Hydrogen Gas Production from Organic Matter", *Environmental Science & Technolgy*, Vol. 42 No. 23, pp. 8630–8640.

Cheng, S., Liu, H. and Logan, B.E. (2006), "Increased performance of single-chamber microbial fuel cells using an improved cathode structure", *Electrochemistry*

Communications, Vol. 8 No. 3, pp. 489–494.

Cheng, S. and Logan, B.E. (2008), "Electricity Generation by *Rhodopseudomonas palustris* DX-1 Electricity Generation by *Rhodopseudomonas palustris*", Vol. 42 No. March 2016, pp. 4146–4151.

Chou, T.Y., Whiteley, C.G. and Lee, D.J. (2014), "Anodic potential on dual-chambered microbial fuel cell with sulphate reducing bacteria biofilm", *International Journal of Hydrogen Energy*, Elsevier Ltd, Vol. 39 No. 33, pp. 19225–19231.

Chou, T.Y., Whiteley, C.G., Lee, D.J. and Liao, Q. (2013), "Control of dual-chambered microbial fuel cell by anodic potential: Implications with sulfate reducing bacteria", *International Journal of Hydrogen Energy*, Elsevier Ltd, Vol. 38 No. 35, pp. 15580–15589.

Chung, K. and Okabe, S. (2009), "Characterization of electrochemical activity of a strain ISO2-3 phylogenetically related to *Aeromonas* sp. isolated from a glucose-fed microbial fuel cell", *Biotechnology and Bioengineering*, Vol. 104 No. 5, pp. 901–910.

Commault, A.S., Lear, G., Packer, M.A. and Weld, R.J. (2013), "Influence of anode potentials on selection of *Geobacter* strains in microbial electrolysis cells", *Bioresource Technology*, Elsevier Ltd, Vol. 139, pp. 226–234.

Cord-Ruwisch, R., Lovley, D.R. and Schink, B. (1998), "Growth of *Geobacter sulfurreducens* with acetate in syntrophic cooperation with hydrogen-oxidizing anaerobic partners", *Applied and Environmental Microbiology*, Vol. 64 No. 6, pp. 2232–2236.

Dar, S.A., Kleerebezem, R., Stams, A.J.M., Kuenen, J.G. and Muyzer, G. (2008), "Competition and coexistence of sulfate-reducing bacteria, acetogens and methanogens in a lab-scale anaerobic bioreactor as affected by changing substrate to sulfate ratio", *Applied Microbiology and Biotechnology*, Vol. 78 No. 6, pp. 1045–1055.

Dennis, P.G., Virdis, B., Vanwonterghem, I., Hassan, A., Hugenholtz, P., Tyson, G.W. and Rabaey, K. (2016), "Anode potential influences the structure and function of anodic electrode and electrolyte-associated microbiomes.", *Scientific Reports*, Vol. 6

No. 1, p. 39114.

Dhar, B.R. and Lee, H.S. (2014), "Evaluation of limiting factors for current density in microbial electrochemical cells (MXCs) treating domestic wastewater", *Biotechnology Reports*, Elsevier B.V., Vol. 4 No. 1, pp. 80–85.

Dolfing, J., Larter, S.R. and Head, I.M. (2008), "Thermodynamic constraints on methanogenic crude oil biodegradation", *ISME Journal*, Vol. 2 No. 4, pp. 442–452.

Dutta, P.K., Keller, J., Yuan, Z., Rozendal, R.A. and Rabaey, K. (2009), "Role of sulfur during acetate oxidation in biological anodes", *Environmental Science and Technology*, Vol. 43 No. 10, pp. 3839–3845.

Dutta, P.K., Rabaey, K., Yuan, Z. and Keller, J. (2008), "Spontaneous electrochemical removal of aqueous sulfide", *Water Research*, Vol. 42 No. 20, pp. 4965–4975.

Escapa, A., Gil-Carrera, L., García, V. and Morán, A. (2012), "Performance of a continuous flow microbial electrolysis cell (MEC) fed with domestic wastewater", *Bioresource Technology*, Elsevier Ltd, Vol. 117, pp. 55–62.

Freguia, S., Rabaey, K., Yuan, Z. and Keller, J. (2007), "Electron and carbon balances in microbial fuel cells reveal temporary bacterial storage behavior during electricity generation", *Environmental Science and Technology*, Vol. 41 No. 8, pp. 2915–2921.

Freguia, S., Rabaey, K., Yuan, Z. and Keller, J. (2008), "Syntrophic Processes Drive the Conversion of Glucose in Microbial Fuel Cell Anodes Syntrophic Processes Drive the Conversion of Glucose in Microbial Fuel Cell Anodes", Vol. 42 No. 21, pp. 7937–7943.

Ge, Z., Li, J., Xiao, L., Tong, Y. and He, Z. (2014), "Recovery of Electrical Energy in Microbial Fuel Cells", *Environmental Science & Technology Letters*, Vol. 1 No. 2, pp. 137–141.

Gildemyn, S., Rozendal, R.A. and Rabaey, K. (2017), "A Gibbs Free Energy-Based Assessment of Microbial Electrocatalysis", *Trends in Biotechnology*, Elsevier Ltd, Vol. 35 No. 5, pp. 393–406.

Gimkiewicz, C. and Harnisch, F. (2013), "Waste Water Derived Electroactive Microbial Biofilms: Growth, Maintenance, and Basic Characterization", JoVE, No. 82, p. e50800.

Ha, P.T., Tae, B. and Chang, I.S. (2008), “Performance and bacterial consortium of microbial fuel cell fed with formate”, *Energy and Fuels*, Vol. 22 No. 1, pp. 164–168.

Hari, A.R., Katuri, K.P., Logan, B.E. and Saikaly, P.E. (2016), “Set anode potentials affect the electron fluxes and microbial community structure in propionate-fed microbial electrolysis cells”, *Scientific Reports*, Nature Publishing Group, Vol. 6 No. 1, p. 38690.

Heidelberg, J.F., Seshadri, R., Haveman, S.A., Hemme, C.L., Paulsen, I.T., Kolonay, J.F., Eisen, J.A., et al. (2004), “The genome sequence of the anaerobic, sulfate-reducing bacterium *Desulfovibrio vulgaris Hildenborough*”, *Nature Biotechnology*, The Author(s), Vol. 22, p. 554.

Heidrich, E.S., Curtis, T.P. and Dolfing, J. (2011), “Determination of the internal chemical energy of wastewater”, *Environmental Science and Technology*, Vol. 45 No. 2, pp. 827–832.

Heidrich, E.S., Edwards, S.R., Dolfing, J., Cotterill, S.E. and Curtis, T.P. (2014), “Performance of a pilot scale microbial electrolysis cell fed on domestic wastewater at ambient temperatures for a 12month period”, *Bioresource Technology*, Elsevier Ltd, Vol. 173, pp. 87–95.

Hoelzle, R.D., Virdis, B. and Batstone, D.J. (2014a), “Regulation Mechanisms in Mixed and Pure Culture Microbial Fermentation”, Vol. 111 No. 11, pp. 2139–2154.

Hoelzle, R.D., Virdis, B. and Batstone, D.J. (2014b), “Regulation mechanisms in mixed and pure culture microbial fermentation”, *Biotechnology and Bioengineering*, Vol. 111 No. 11, pp. 2139–2154.

Holmes, D.E., Bond, D.R. and Lovley, D.R. (2004), “Electron Transfer by *Desulfobulbus propionicus* to Fe (III) and Graphite Electrodes”, *Applied and Environmental Microbiology*, Vol. 70 No. 2, p. 1234.

Holmes, D.E., Finneran, K.T., O’Neil, R.A. and Lovley, D.R. (2002), “Enrichment of Members of the Family *Geobacteraceae* Associated with Stimulation of Dissimilatory Metal Reduction in Uranium-Contaminated Aquifer Sediments”, *Applied and Environmental Microbiology* , Vol. 68 No. 5, pp. 2300–2306.

Ishii, S., Suzuki, S., Norden-Krichmar, T.M., Phan, T., Wanger, G., Nealson, K.H.,

Sekiguchi, Y., et al. (2014), “Microbial population and functional dynamics associated with surface potential and carbon metabolism.”, *The ISME Journal*, Vol. 8 No. 5, pp. 963–978.

Jung, R.K., Zuo, Y., Regan, J.M. and Logan, B.E. (2008), “Analysis of ammonia loss mechanisms in microbial fuel cells treating animal wastewater”, *Biotechnology and Bioengineering*, Vol. 99 No. 5, pp. 1120–1127.

Jung, S. and Regan, J.M. (2011), “Influence of external resistance on electrogenesis, methanogenesis, and anode prokaryotic communities in microbial fuel cells”, *Applied and Environmental Microbiology*, Vol. 77 No. 2, pp. 564–571.

Karra, U., Manickam, S.S., McCutcheon, J.R., Patel, N. and Li, B. (2013), “Power generation and organics removal from wastewater using activated carbon nanofiber (ACNF) microbial fuel cells (MFCs)”, *International Journal of Hydrogen Energy*, Elsevier Ltd, Vol. 38 No. 3, pp. 1588–1597.

Kashima, H. and Regan, J.M. (2015), “Facultative nitrate reduction by electrode-respiring *Geobacter metallireducens* biofilms as a competitive reaction to electrode reduction in a bioelectrochemical system”, *Environmental Science and Technology*, Vol. 49 No. 5, pp. 3195–3202.

Kelly, P.T. and He, Z. (2014), “Nutrients removal and recovery in bioelectrochemical systems: A review”, *Bioresource Technology*, Elsevier Ltd, Vol. 153, pp. 351–360.

Kiely, P., Regan, J. and Logan, B. (2011a), *Kiely PD, Regan JM, Logan BE.. The Electric Picnic: Synergistic Requirements for Exoelectrogenic Microbial Communities. Curr Opin Biotechnol 22: 378-385*.

Kiely, P.D., Regan, J.M. and Logan, B.E. (2011b), “The electric picnic: Synergistic requirements for exoelectrogenic microbial communities”, *Current Opinion in Biotechnology*, Elsevier Ltd, Vol. 22 No. 3, pp. 378–385.

Kim, J.R., Jung, S.H., Regan, J.M. and Logan, B.E. (2007), “Electricity generation and microbial community analysis of alcohol powered microbial fuel cells”, *Bioresource Technology*, Vol. 98 No. 13, pp. 2568–2577.

Kimura, Z. and Okabe, S. (2013), “Acetate oxidation by syntrophic association between *Geobacter sulfurreducens* and a hydrogen-utilizing exoelectrogen”, *The ISME*

Journal, Nature Publishing Group, Vol. 7 No. 8, pp. 1472–1482.

Kokko, M.E., Mäkinen, A.E., Sulonen, M.L.K. and Puhakka, J.A. (2015), "Effects of anode potentials on bioelectrogenic conversion of xylose and microbial community compositions", Vol. 101, pp. 248–252.

Laanbroek, H.J., Geerligs, H.J., Sijtsma, L. and Veldkamp, H. (1984), "Competition for sulfate and ethanol among *Desulfobacter*, *Desulfobulbus*, and *Desulfovibrio* species isolated from intertidal sediments.", *Applied and Environmental Microbiology*, Vol. 47 No. 2, pp. 329–34.

Lee, H.S., Parameswaran, P., Kato-Marcus, A., Torres, C.I. and Rittmann, B.E. (2008), "Evaluation of energy-conversion efficiencies in microbial fuel cells (MFCs) utilizing fermentable and non-fermentable substrates", *Water Research*, Vol. 42 No. 6–7, pp. 1501–1510.

Lee, H.S. and Rittmann, B.E. (2009), "Evaluation of metabolism using stoichiometry in fermentative biohydrogen", *Biotechnology and Bioengineering*, Vol. 102 No. 3, pp. 749–758.

Lee, H.S. and Rittmann, B.E. (2010), "Characterization of energy losses in an upflow single-chamber microbial electrolysis cell", *International Journal of Hydrogen Energy*, Elsevier Ltd, Vol. 35 No. 3, pp. 920–927.

Li, W.-W., Yu, H.-Q. and He, Z. (2013), "Towards sustainable wastewater treatment by using microbial fuel cells-centered technologies", *Energy Environ. Sci.*, Vol. 7 No. 3, pp. 911–924.

Liang, F.Y., Deng, H. and Zhao, F. (2013), "Sulfur pollutants treatment using microbial fuel cells from perspectives of electrochemistry and microbiology", *Fenxi Huaxue/ Chinese Journal of Analytical Chemistry*, Changchun Institute of Applied Chemistry, Chinese Academy of Sciences, Vol. 41 No. 8, pp. 1133–1139.

Liu, H., Cheng, S. a and Logan, B.E. (2005), "Power generation in fed-batch microbial fuel cells as a function of ionic strength, temperature, and reactor configuration", *Environmental Science and Technology*, Vol. 39 No. 14, pp. 5488–5493.

Logan, B.E. (2008), *Microbial Fuel Cells*, John Wiley & Sons.

Logan, B.E. (2010), "Scaling up microbial fuel cells and other bioelectrochemical

systems", *Applied Microbiology and Biotechnology*, Vol. 85 No. 6, pp. 1665–1671.

Logan, B.E., Hamelers, B., Rozendal, R., Schröder, U., Keller, J., Freguia, S., Aelterman, P., et al. (2006), "Microbial fuel cells: Methodology and technology", *Environmental Science and Technology*, Vol. 40 No. 17, pp. 5181–5192.

de los Ángeles Fernandez, M., de los Ángeles Sanromán, M., Marks, S., Makinia, J., Gonzalez del Campo, A., Rodrigo, M. and Fernandez, F.J. (2016), "A grey box model of glucose fermentation and syntrophic oxidation in microbial fuel cells", *Bioresource Technology*, Elsevier Ltd, Vol. 200, pp. 396–404.

Lu, L., Xing, D., Ren, N. and Logan, B.E. (2012), "Syntrophic interactions drive the hydrogen production from glucose at low temperature in microbial electrolysis cells", *Bioresource Technology*, Vol. 124, pp. 68–76.

Luo, H., Fu, S., Liu, G., Zhang, R., Bai, Y. and Luo, X. (2014), "Autotrophic biocathode for high efficient sulfate reduction in microbial electrolysis cells", *Bioresource Technology*, Elsevier Ltd, Vol. 167, pp. 462–468.

Luo, H., Teng, W., Liu, G., Zhang, R. and Lu, Y. (2017), "Sulfate reduction and microbial community of autotrophic biocathode in response to acidity", *Process Biochemistry*, Elsevier Ltd, Vol. 54, pp. 120–127.

Malvankar, N.S., Vargas, M., Nevin, K.P., Franks, A.E., Leang, C., Kim, B.C., Inoue, K., et al. (2011), "Tunable metallic-like conductivity in microbial nanowire networks", *Nature Nanotechnology*, Vol. 6 No. 9, pp. 573–579.

Manning, D.A.C. and Bewsher, A. (1997), "Determination of anions in landfill leachates by ion chromatography", *Journal of Chromatography A*, Vol. 770 No. 1, pp. 203–210.

Marsili, E., Rollefson, J.B., Baron, D.B., Hozalski, R.M. and Bond, D.R. (2008), "Microbial biofilm voltammetry: Direct electrochemical characterization of catalytic electrode-attached biofilms", *Applied and Environmental Microbiology*, Vol. 74 No. 23, pp. 7329–7337.

Methé, B.A., Nelson, K.E., Eisen, J.A., Paulsen, I.T., Nelson, W., Heidelberg, J.F., Wu, D., et al. (2003), "Genome of *Geobacter sulfurreducens*: Metal Reduction in Subsurface Environments", *Science*, Vol. 302 No. 5652, p. 1967-1969.

Milner, E.M., Popescu, D., Curtis, T., Head, I.M., Scott, K. and Yu, E.H. (2016), "Microbial fuel cells with highly active aerobic biocathodes", *Journal of Power Sources*, Elsevier B.V, Vol. 324, pp. 8–16.

Min, B. and Logan, B.E. (2004), "Continuous electricity generation from domestic wastewater and organic substrates in a flat plate microbial fuel cell.", *Environmental Science & Technology*, Vol. 38 No. 21, pp. 5809–5814.

Moscoviz, R., Toledo-Alarcn, J., Trably, E. and Bernet, N. (2016), "Electro-Fermentation: How To Drive Fermentation Using Electrochemical Systems", *Trends in Biotechnology*, Elsevier Ltd, Vol. 34 No. 11, pp. 856–865.

Muyzer, G. and Stams, A.J.M. (2008), "The ecology and biotechnology of sulphate-reducing bacteria", *Nat Rev Micro*, Nature Publishing Group, Vol. 6 No. 6, pp. 441–454.

Nam, J.Y., Tokash, J.C. and Logan, B.E. (2011), "Comparison of microbial electrolysis cells operated with added voltage or by setting the anode potential", *International Journal of Hydrogen Energy*, Elsevier Ltd, Vol. 36 No. 17, pp. 10550–10556.

Omil, F., Lens, P., Visser, A., Hulshoff Pol, L.W. and Lettinga, G. (1998), "Long-term competition between sulphate reducing and methanogenic bacteria in UASB reactors treating volatile fatty acids", *Biotechnology and Bioengineering*, Vol. 57, pp. 676–685.

Parameswaran, P., Torres, C.I., Lee, H.S., Krajmalnik-Brown, R. and Rittmann, B.E. (2009), "Syntrophic interactions among anode respiring bacteria (ARB) and non-ARB in a biofilm anode: Electron balances", *Biotechnology and Bioengineering*, Vol. 103 No. 3, pp. 513–523.

Parameswaran, P., Torres, C.I., Lee, H.S., Rittmann, B.E. and Krajmalnik-Brown, R. (2011), "Hydrogen consumption in microbial electrochemical systems (MXCs): The role of homo-acetogenic bacteria", *Bioresource Technology*, Elsevier Ltd, Vol. 102 No. 1, pp. 263–271.

Parameswaran, P., Zhang, H., Torres, C.I., Rittmann, B.E. and Krajmalnik-Brown, R. (2010), "Microbial community structure in a biofilm anode fed with a fermentable substrate: The significance of hydrogen scavengers", *Biotechnology and*

Bioengineering, Vol. 105 No. 1, pp. 69–78.

Parks, D.H., Tyson, G.W., Hugenholtz, P. and Beiko, R.G. (2014), "STAMP: statistical analysis of taxonomic and functional profiles", *Bioinformatics*, Vol. 30 No. 21, pp. 3123–3124.

Pikaar, I., Rozendal, R.A., Yuan, Z., Keller, J. and Rabaey, K. (2011), "Electrochemical sulfide oxidation from domestic wastewater using mixed metal-coated titanium electrodes", *Water Research*, Vol. 45 No. 17, pp. 5381–5388.

Rabaey, K., Angenent, L., Schroder, U. and Keller, J. (2009), *Bioelectrochemical Systems*, IWA publishing.

Rabaey, K., Clauwaert, P., Aelterman, P. and Verstraete, W. (2005), "Tubular Microbial Fuel Cells for Efficient Electricity Generation", Vol. 39 No. Figure 1, pp. 8077–8082.

Rabaey, K. and Rozendal, R.A. (2010a), "Microbial electrosynthesis — revisiting the electrical route for microbial production", *Nature Reviews Microbiology*, Nature Publishing Group, Vol. 8 No. 10, pp. 706–716.

Rabaey, K. and Rozendal, R.A. (2010b), "Microbial electrosynthesis - revisiting the electrical route for microbial production.", *Nature Reviews. Microbiology*, Nature Publishing Group, Vol. 8 No. 10, pp. 706–16.

Rabaey, K., Van de Sompel, K., Maignien, L., Boon, N., Aelterman, P., Clauwaert, P., De Schamphelaire, L., et al. (2006), "Microbial Fuel Cells for Sulfide", *Environ Sci Technol*, Vol. 40 No. 17, pp. 5218–5224.

Richter, H., Nevin, K.P., Jia, H., Lowy, D.A., Lovley, D.R. and Tender, L.M. (2009), "Cyclic voltammetry of biofilms of wild type and mutant *Geobacter sulfurreducens* on fuel cell anodes indicates possible roles of OmcB, OmcZ, type IV pili, and protons in extracellular electron transfer", *Energy Environ. Sci.*, Vol. 2 No. 5, p. 506.

Rittmann, B.E. and McCarty, P.L. (2012), *Environmental Biotechnology: Principles and Applications*, Tata McGraw-Hill Education.

Rotaru, A.E., Woodard, T.L., Nevin, K.P. and Lovley, D.R. (2015), "Link between capacity for current production and syntrophic growth in *Geobacter* species", *Frontiers in Microbiology*, Vol. 6 No. JUL, pp. 1–8.

Rozendal, R.A., Hamelers, H.V.M., Rabaey, K., Keller, J. and Buisman, C.J.N. (2008), "Towards practical implementation of bioelectrochemical wastewater treatment", *Trends in Biotechnology*, Vol. 26 No. 8, pp. 450–459.

Selembo, P.A., Perez, J.M., Lloyd, W.A. and Logan, B.E. (2009), "High hydrogen production from glycerol or glucose by electrohydrogenesis using microbial electrolysis cells", *International Journal of Hydrogen Energy*, Elsevier Ltd, Vol. 34 No. 13, pp. 5373–5381.

Sleutels, T., Molenaar, S., Heijne, A. and Buisman, C. (2016), "Low Substrate Loading Limits Methanogenesis and Leads to High Coulombic Efficiency in Bioelectrochemical Systems", *Microorganisms*, Vol. 4 No. 1, p. 7.

Sleutels, T.H.J.A., Darus, L., Hamelers, H.V.M. and Buisman, C.J.N. (2011), "Effect of operational parameters on Coulombic efficiency in bioelectrochemical systems", *Bioresource Technology*, Elsevier Ltd, Vol. 102 No. 24, pp. 11172–11176.

Smith, K. and Liu, S. (2017), "Energy for Conventional Water Supply and Wastewater Treatment in Urban China: A Review", *Global Challenges*, Vol. 1600016, p. 1600016.

Speers, A.M. and Reguera, G. (2012), "Electron donors supporting growth and electroactivity of *Geobacter sulfurreducens* anode biofilms", *Applied and Environmental Microbiology*, Vol. 78 No. 2, pp. 437–444.

Srinivasan, V.N. and Butler, C.S. (2017), "Ecological and Transcriptional Responses of Anode-Respiring Communities to Nitrate in a Microbial Fuel Cell", *Environmental Science and Technology*, Vol. 51 No. 9, pp. 5334–5342.

Sukkasem, C., Xu, S., Park, S., Boonsawang, P. and Liu, H. (2008), "Effect of nitrate on the performance of single chamber air cathode microbial fuel cells", *Water Research*, Elsevier Ltd, Vol. 42 No. 19, pp. 4743–4750.

Temudo, M.F., Kleerebezem, R. and van Loosdrecht, M. (2007), "Influence of the pH on (open) mixed culture fermentation of glucose: A chemostat study", *Biotechnology and Bioengineering*, Wiley Subscription Services, Inc., A Wiley Company, Vol. 98 No. 1, pp. 69–79.

Torres, C.I., Kato Marcus, A. and Rittmann, B.E. (2007), "Kinetics of consumption of

fermentation products by anode-respiring bacteria", *Applied Microbiology and Biotechnology*, Vol. 77 No. 3, pp. 689–697.

Torres, C.I., Krajmalnik-Brown, R., Parameswaran, P., Marcus, A.K., Wanger, G., Gorby, Y.A. and Rittmann, B.E. (2009), "Selecting anode-respiring bacteria based on anode potential: Phylogenetic, electrochemical, and microscopic characterization", *Environmental Science and Technology*, Vol. 43 No. 24, pp. 9519–9524.

Torres, C.I., Marcus, A.K., Parameswaran, P. and Rittmann, B.E. (2008), "Kinetic experiments for evaluating the nernst-monod model for anode-respiring bacteria (ARB) in a biofilm anode", *Environmental Science and Technology*, Vol. 42 No. 17, pp. 6593–6597.

Torres, C.I., Marcus, A.K. and Rittmann, B.E. (2008), "Proton transport inside the biofilm limits electrical current generation by anode-respiring bacteria", *Biotechnology and Bioengineering*, Vol. 100 No. 5, pp. 872–881.

Velasquez-Orta, S.B., Yu, E., Katuri, K.P., Head, I.M., Curtis, T.P. and Scott, K. (2011), "Evaluation of hydrolysis and fermentation rates in microbial fuel cells", *Applied Microbiology and Biotechnology*, Vol. 90 No. 2, pp. 789–798.

Verstraete, W. and Rabaey, K. (2006), "Critical Review Microbial Fuel Cells : Methodology and Technology", *Environmental Science & Technology*, Vol. 40 No. 17, pp. 5181–5192.

Wagner, R.C., Call, D.F. and Logan, B.E. (2010), "Optimal set anode potentials vary in bioelectrochemical systems", *Environmental Science and Technology*, Vol. 44 No. 16, pp. 6036–6041.

Wei, J., Liang, P., Cao, X. and Huang, X. (2010), "A new insight into potential regulation on growth and power generation of *Geobacter sulfurreducens* in microbial fuel cells based on energy viewpoint.", *Environmental Science & Technology*, Vol. 44 No. 8, pp. 3187–91.

Zhang, L., Zhou, S., Zhuang, L., Li, W., Zhang, J., Lu, N. and Deng, L. (2008), "Microbial fuel cell based on *Klebsiella pneumoniae* biofilm", *Electrochemistry Communications*, Vol. 10 No. 10, pp. 1641–1643.

Zhang, T., Bain, T.S., Barlett, M.A., Dar, S.A., Snoeyenbos-West, O.L., Nevin, K.P. and Lovley, D.R. (2014), "Sulfur oxidation to sulfate coupled with electron transfer to electrodes by *Desulfuromonas* strain TZ1", *Microbiology (United Kingdom)*, Vol. 160 No. PART 1, pp. 123–129.

Zhao, Z., Zhang, Y., Yu, Q., Dang, Y., Li, Y. and Quan, X. (2016), "Communities stimulated with ethanol to perform direct interspecies electron transfer for syntrophic metabolism of propionate and butyrate", *Water Research*, Elsevier Ltd, Vol. 102, pp. 475–484.

Zheng, Y., Xiao, Y., Yang, Z.H., Wu, S., Xu, H.J., Liang, F.Y. and Zhao, F. (2014), "The bacterial communities of bioelectrochemical systems associated with the sulfate removal under different pHs", *Process Biochemistry*, Elsevier Ltd, Vol. 49 No. 8, pp. 1345–1351.

Zhu, X., Yates, M.D., Hatzell, M.C., Rao, H.A., Saikaly, P.E. and Logan, B.E. (2014), "Microbial Community Composition Is Unaffected by Anode Potential", *Environmental Science & Technology*, Vol. 48 No. 2, pp. 1352–1358.

Chapter 8 Appendix

8.1. Appendix A The calculation of the rate of conversion in a selected glucose-fed test in a glucose-fed BES

The data for calculation was based on Figure 3-1. In which case, the conversion rate of glucose degradation was:

$$\ln(\text{glucose})=-0.5073\text{time}+3.126$$

$$k=-0.5073h^{-1}$$

The conversion rate of ethanol degradation was:

$$\ln(\text{ethanol})=-0.01595+1.998$$

$$k=-0.01595h^{-1}$$

The conversion rate of acetate degradation was:

$$\ln(\text{acetate})=-0.02943\text{time}+2.356$$

$$k=-0.02943h^{-1}$$

The conversion of rate from acetate to electricity was $k \times 75.2\% = 0.02213$

The conversion rate of formate degradation was:

$$\ln(\text{formate})=-0.09501\text{time}+2.244$$

$$k=-0.09501h^{-1}$$

The conversion of rate from acetate to electricity was $k \times 26.9\% = 0.02556$

The conversion rate of glucose to acetate:

$$\ln(\text{acetate})=0.07269\text{time}+1.328$$

$$k=0.07269h^{-1}$$

The conversion rate of glucose to ethanol:

$$\ln(\text{ethanol})=0.06325\text{time}+0.2916$$

$$k=0.06325h^{-1}$$

The conversion rate of glucose to formate:

$$\ln(\text{formate})=0.07916\text{time}+1.096$$

$$k=0.07916h^{-1}$$

The conversion rate of glucose to propionate:

$$\ln(\text{propionate})=0.06325\text{time}+0.2916$$

$$k=0.06325h^{-1}$$

8.2. Appendix B. The calculation of the non-electrogenic electron loss of the degradation of glucose degradation intermediates and products (GDIPs) in the glucose-fed BESs in the glucose-fed tests between 9th hour and 102nd hour

The availabilities of acetate, formate and ethanol at 9th hour and 102nd hour as well as the coulombic efficiency of them in their individual-fed tests in the glucose-fed BESs was as follow:

GDIPs	Availabilities at 9th hour (Cmeq/L)	Availabilities at 102nd hour (Cmeq/L)	Individual coulombic efficiency (%)
Acetate	5.9	0.5	75.2±6.4
Ethanol	5.3	1.0	55.9±21.5
Formate	3.2	0	26.9±2.1

Table 8-1 The individual non-electrogenic electron loss in the glucose-fed BESs

The initial glucose feed was 20Cmeq/L, therefore, the electron loss of the degradation of acetate:

$$[(5.9-0.5) \times(1-0.752)]/20=0.067=6.7\%$$

The electron loss of the degradation of ethanol:

$$[(5.3-1.0) \times(1-0.559)]/20=0.095=9.5\%$$

The electron loss of the degradation of formate:

$$[(3.2-0) \times(1-0.269)]/20=0.117=11.7\%$$

The sum of these electron losses therefore was 6.7%+9.5%+11.7%=27.9%

8.3. Appendix C. Thermodynamic calculation of the ethanol and propionate-based acetogenesis in glucose-fed BESs at anode potential of -150mV.

The calculation was based on the equation:

$$\Delta G = \Delta G^0 + RTln[B]^b/[A]^a \quad (7)$$

At standard condition:(T=25°C, gas was at 1atm, solution was at 1M).

8.3.1. Thermodynamic constraints of hydrogen accumulation

Ethanol-based acetogenesis:

$$C_2H_6O + H_2O \rightarrow C_2H_3O_2^- + H^+ + 2H_2 \quad (8)$$

since ΔG of C_2H_6O = 47.2 KJ/mol, ΔG of H_2O = -157.6 KJ/mol, ΔG of $C_2H_3O_2^-$ = -264.0 KJ/mol, ΔG of H_2 = 81.6 KJ/mol.

Therefore the overall ΔG = (-264.0 + 81.6×2)-(47.2-157.6)= 9.6 KJ/mol

As the $\Delta G_{threshold}$ = 0 is threshold value to trigger this reaction, at standard condition, $RTln[B]^b/[A]^a = 5.71log\ [B]^b/[A]^a$

0 = 9.6 + 5.71×2 log $[H_2]_{threshold}$, therefore $[H_2]_{threshold} = 10^{(-9.6)/(5.71)\times 2}$ = 0.144atm, and $\log[H_2]_{threshold}$ = -0.84.

0 = 9.6 + 5.71×log $[C_2H_3O_2^-]_{threshold}$, therefore $[C_2H_3O_2^-]_{threshold} = 10^{(-9.6)/(5.71)}$ = 0.02M and $\log[C_2H_3O_2^-]_{threshold}$ = -1.68.

Propionate-based acetogenesis:

$$C_3H_5O_2 + 2H_2O \rightarrow C_2H_3O_2^- + H^+ + CO_2 + 3H_2 \quad (9)$$

since ΔG of $C_3H_5O_2$ = -177.9 KJ/mol, ΔG of H_2O = -157.6 KJ/mol, ΔG of $C_2H_3O_2^-$ = -264.0 KJ/mol, ΔG of H_2 = 81.6 KJ/mol, ΔG of CO_2 = -403.1KJ/mol.

Therefore the overall ΔG = (-264.0 + 81.6×3-403.1)-(-177.9-157.6×2)= 70.8 KJ/mol

As the $\Delta G_{threshold}$ = 0 is threshold value to trigger this reaction, at standard condition, $RTln[B]^b/[A]^a = 5.71log\ [B]^b/[A]^a$

0 = 70.8 + 5.71×3 log $[H_2]_{threshold}$, therefore $[H_2]_{threshold} = 10^{(-70.8)/(5.71)\times 3} = 7.36\times10^{-5}$ atm, and $\log[H_2]_{threshold}$ = -4.13.

0 = 70.8 + 5.71×log $[C_2H_3O_2^-]_{threshold}$, therefore $[C_2H_3O_2^-]_{threshold} = 10^{(-70.8)/(5.71)}$ = 4.00×10^{-13}M and $\log[C_2H_3O_2^-]_{threshold}$ = -12.40.

Homoacetogensis:

$$4H_2 + 2\,CO_2 \rightarrow C_2H_3O_2^- + H^+ + 2H_2O \quad (10)$$

since ΔG of H_2 = 81.6 KJ/mol, ΔG of CO_2 = -403.1KJ/mol.l, ΔG of $C_2H_3O_2^-$ = -264.0 KJ/mol, ΔG of H_2O = **-**157.6 KJ/mol.

Therefore the overall ΔG = (-264.0 - 157.6×2)-(81.6×4-403.1×2)= -99.4KJ/mol

As the $\Delta G_{threshold} = 0$ is threshold value to trigger this reaction, at standard condition, $RTln[B]^b/[A]^a = 5.71 log\,[B]^b/[A]^a$

0 = -99.4 - 5.71×4 log $[H_2]_{threshold}$, therefore $[H_2]_{threshold} = 10^{(99.4)/(-5.71)\times4}$ = 4.45×10^{-5}atm, and $\log[H_2]_{threshold}$ = -4.35.

0 = -99.4 + 5.71×log $[C_2H_3O_2^-]_{threshold}$, therefore $[C_2H_3O_2^-]_{threshold} = 10^{(99.4)/(5.71)}$ = 2.56×10^{17}M and $\log[C_2H_3O_2^-]_{threshold}$ = 17.40.

Methanogenesis:

$$4H_2 + CO_2 \rightarrow CH_4 + 2H_2O \quad (11)$$

since ΔG of H_2 = 81.6 KJ/mol, ΔG of CO_2 = -403.1KJ/mol.l, ΔG of CH_4 = 110.7 KJ/mol, ΔG of H_2O = **-**157.6 KJ/mol.

Therefore the overall ΔG = (110.7-157.6×2)-(81.6×4-403.1)= -127.8KJ/mol

As the $\Delta G_{threshold} = 0$ is threshold value to trigger this reaction, at standard condition, $RTln[B]^b/[A]^a = 5.71 log\,[B]^b/[A]^a$

0 = -127.8 - 5.71×4 log $[H_2]_{threshold}$, therefore $[H_2]_{threshold} = 10^{(127.8)/(-5.71)\times4}$ = 2.54×10^{-6}atm, and $\log[H_2]_{threshold}$ = -5.59.

Saturated acetate:

$[C_2H_3O_2^-]_{threshold}$ = 0.0044M, therefore $\log[C_2H_3O_2^-]_{threshold}$ = -2.36.

8.3.2. Thermodynamic constraints of anode potential.

The calculation was based on the equation:

$$\Delta G = \Delta G^0 + RT ln [B]^b/[A]^a \quad (12)$$

$$\Delta G = nEF \quad (13)$$

At standard condition:(T=25°C, R=98.48KJ/V, gas was at 1atm, solution was at 1M).

Propionate based-current production:

$$C_3H_5O_2 + 2H_2O \rightarrow C_2H_3O_2^- + CO_2 + 6e^- \quad (14)$$

Based on the ΔG of each reactant and product, the ΔG of this reaction = -264 +(-403.1)– (-177.9) – (-157.6×2) = -174KJ/mol. Redox potential = ΔG/nF = -174/6/96.48= -0.301V= -301mV.

As the $\Delta G_{threshold} = 0$ is threshold value to trigger this reaction, at standard condition, $RT ln [B]^b/[A]^a = 5.71 log [B]^b/[A]^a$. 0 = -174-5.71× log $[propionate]_{threshold}$, therefore $[propionate]_{threshold} = 10^{(174)/(-5.71)}$, and $log[propionate]_{threshold} = -30.47$.

Ethanol based-current production:

$$C_2H_6O + H_2O \rightarrow C_2H_3O_2^- + 4e^- \quad (15)$$

Based on the ΔG of each reactant and product, the ΔG of this reaction = 264-(-47.2)– (-157.6) = -153.6KJ/mol. Redox potential = ΔG/nF = -153/4/96.48= -0.398V= -398mV.

As the $\Delta G_{threshold} = 0$ is threshold value to trigger this reaction, at standard condition, $RT ln [B]^b/[A]^a = 5.71 log [B]^b/[A]^a$. 0 = -153-5.71× log $[propionate]_{threshold}$, therefore $[propionate]_{threshold} = 10^{(153)/(-5.71)}$, and $log[propionate]_{threshold} = -26.90$.

8.4. Appendix D. The summary of the glucose-fed BESs responds to inocula with additional voltage supply.

	Current production with external resistor of 10 Ω (mA)	Coulombic efficiency when COD<50mg/L (%)
Arctic resource	1.25± 0.11	22.70± 2.85
Howdon activated sludge	1.16 ±0.16	17.60 ±1.51
Tudhoe activated sludge	1.22 ±0.02	21.02± 2.17
Tudhoe settled sewage	1.00 ±0.03	16.93 ±0.23
Tudhoe settled sewage (with fixed anode potential)	1.55±0.07	74.24±5.50

Table 8-2 Summary of electrogenic performance in glucose-fed BESs with different inoculums.

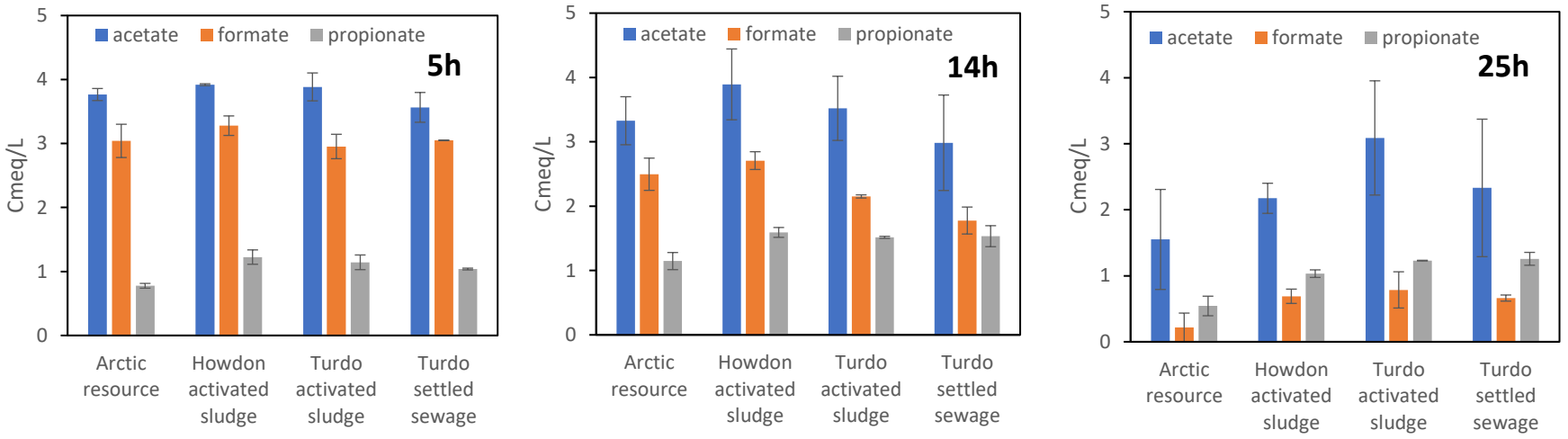

Figure 8-1 Summary of VFAs production at 5hrs, 14hrs, 25hrs and 112 hrs in glucose-fed BESs with different inoculums with additional voltage supply.

8.5. Appendix E. The effect of applied anode potential on the 9 hours input energy in the glucose-fed BESs.

The calculation is based on the equation of:

$$\Delta G = -knF(E_{substrate}^{0'} - E_{anode}) \quad (16)$$

The value of *kn* is based on the value in Table 4-1. Acetate was assumed as the only electrogenic substrates in glucose-fed BESs here. Therefore, $E_{substrate}^{0} = -280$mV. The value of E_{anode} and the calculated value of ΔG is indicated in Table 8-3.

	Acetate-fed controls acclimated at			**Glucose-fed BESs acclimated at**		
	+200	**0**	**-150**	**+200**	**0**	**-150**
9 hours applied anode potential (mV vs SHE)						
+200	333.5±9.3	324.2±13.9	310.3±4.6	226.9±32.4	236.2±32.4	134.3±9.3
0	186.4±5.4	183.7±5.4	186.4±2.7	151.3±8.1	127.0±24.3	81.0±11.0
-150	86.5±1.3	86.5±2.5	87.8±2.5	32.6±2.5	37.6±6.3	25.1±6.3

Table 8-3 Summary of 9 hours energy involved in electrogenic processes in glucose-fed BESs and acetate-fed controls at anode potential of -150mV, 0mV, +200mV (J)

8.6. Appendix F. The polarization curves of the glucose-fed BESs at -150mV, 0mV and +200mV.

The polarization curves in the glucose-fed BESs fed with either glucose and acetate+formate was built The anode potential in the glucose-fed BESs was stepwise altered once stable current production was obtained. The current production in the BESs acclimated at 0mV and +200mV was generally higher than the BESs acclimated -150mV (Figure 8-2).

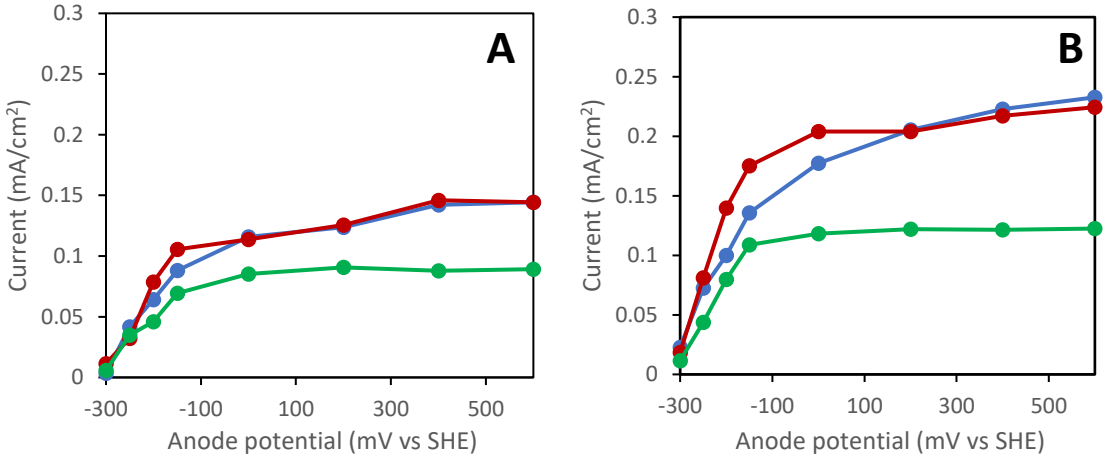

Figure 8-2 Polarization curves of the glucose-fed BESs acclimated at 200mV (blue lines), 0mV (red lines) and -150mV (green lines) in 20Cmeq glucose-fed cycles(A) and 10Cmeq acetate+10Cmmol formate-fed cycles (B).

8.7. Appendix G. The relationship between current production and the *Geobacteraceae* numbers in the glucose-fed BESs and acetate-fed controls.

The current production and the abundance of *Geobacteraceae* in the glucose and acetate-fed controls at -150mV, 0mV and +200mV were shown below. The current production from glucose and the abundance of *Geobacteraceae* in glucose-fed BESs was generally lower than the acetate-fed controls. However, the current production in the glucose-fed BESs at 0mV and +200mV increased to the similar level as the acetate-fed controls when acetate+formate was fed (Figure 8-3).

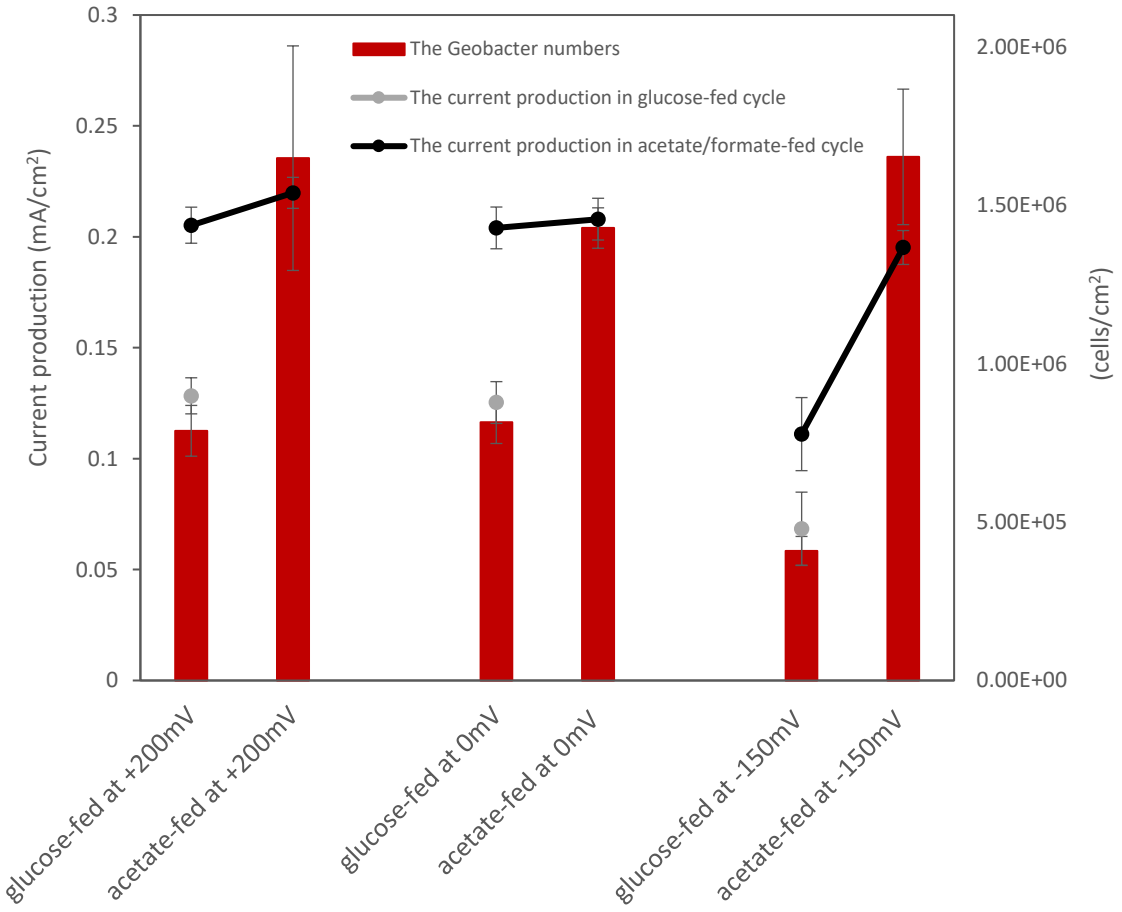

Figure 8-3 The relationship between current production and the abundance of *Geobacteraceae* in the glucose and acetate-fed BESs.

8.8. Appendix H. The detailed current production and the carbon removal, sulphate removal and sulphide accumulation in the tests of acetate+sulphate-fed BES

The summary of the acetate+sulphate-fed BESs with increased sulphate from 0e⁻mmol/L to 240e⁻mmol/L and the current production in the acetate-fed BESs with increased equivalent conductivity of NaCl corresponding to Figure 5-1A and Figure 5-1B.

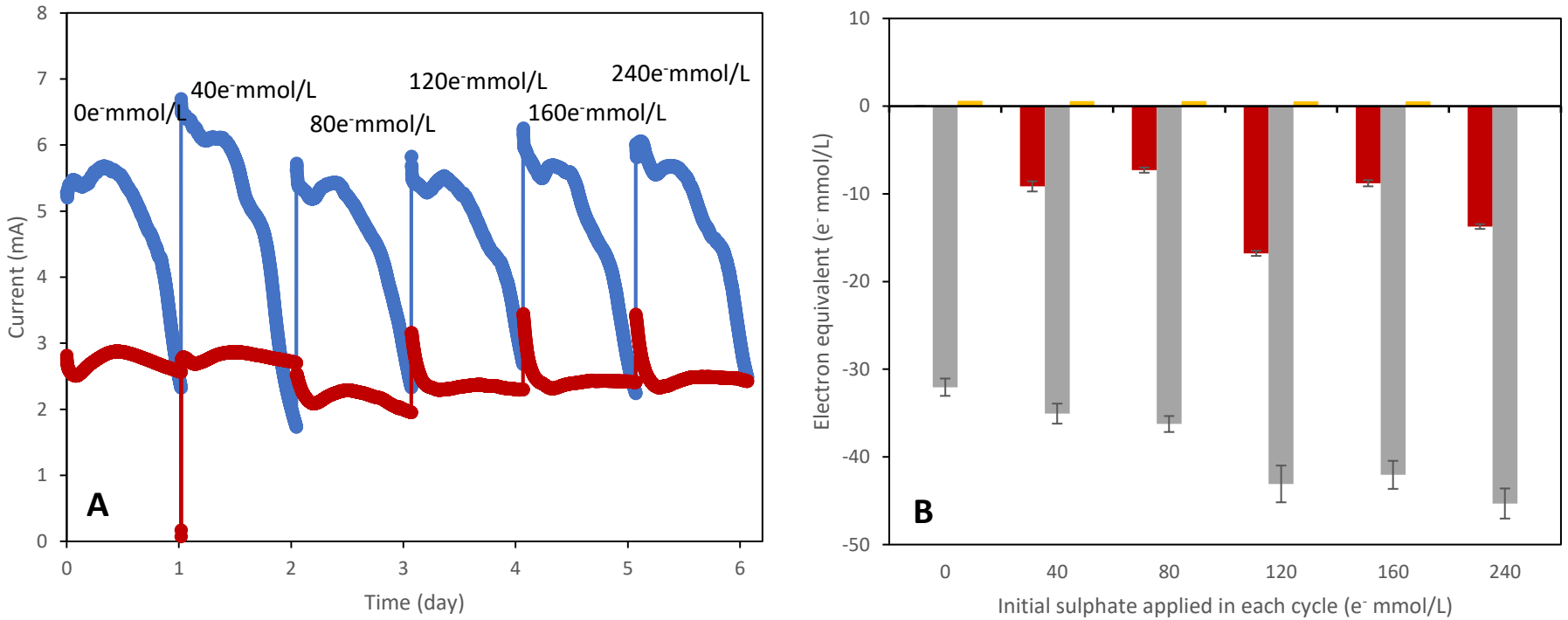

Figure 8-4 The current production in stepwise increased applied sulphate/NaCl in the acetate+sulphate-fed BESs (red line) and the acetate-fed BESs (blue line) (A). The carbon removal (grey), sulphate removal (red) and sulphide accumulation (yellow) in the acetate+sulphate-fed BESs (B).

The summary of the acetate+sulphate-fed BESs and the acetate-fed controls with increased acetate from 0e⁻mmol/L and 80e⁻mmol/L corresponding to Figure 5-2A and Figure 5-2B.

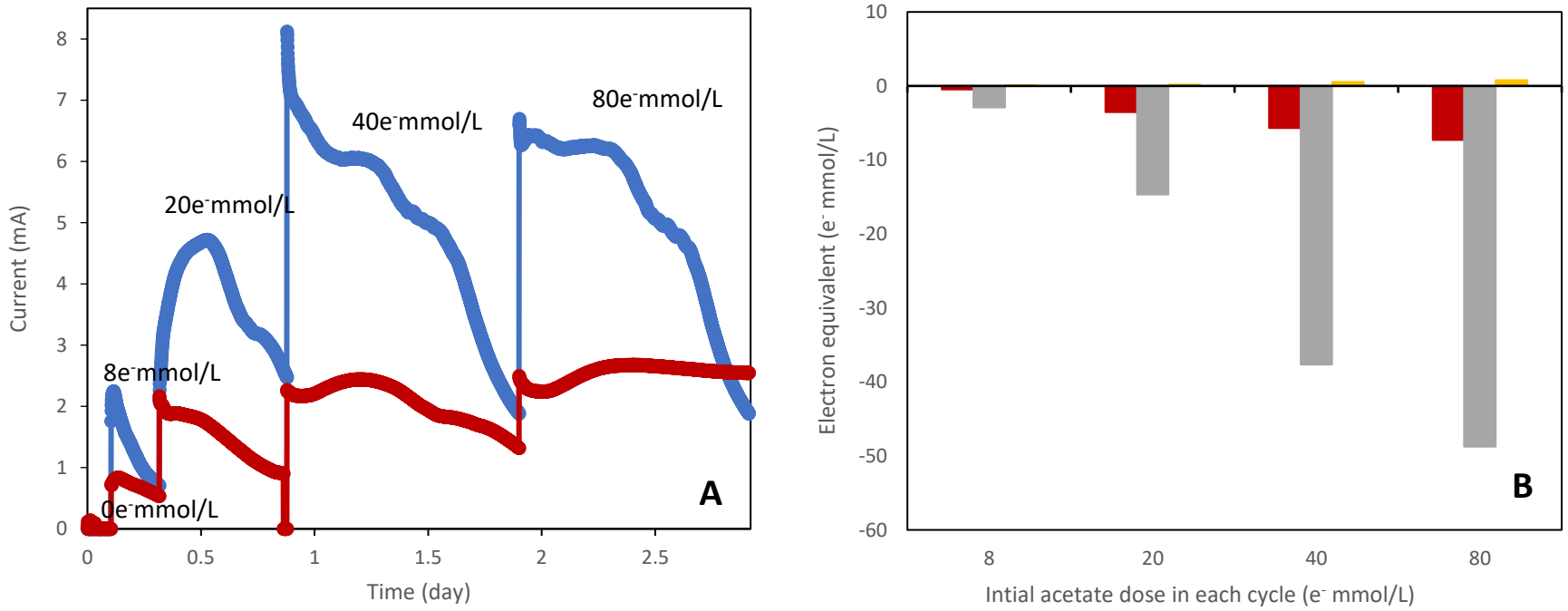

Figure 8-5 The current production in stepwise increased applied acetate cycles in the acetate+sulphate-fed BESs (red line) and the acetate-fed controls (blue line) (A). The carbon removal (grey), sulphate removal (red) and sulphide accumulation (yellow) in the acetate-fed controls (B).

8.9. Appendix I. The summary of the anodic microbial communities in the BESs fed with sulphate and the corresponding controls.

The selected OTU table of the anodic microbial communities in the BESs acclimated with sulphate and the corresponding controls was listed below. Only 37 microorganism with the highest relative abundance was shown here.

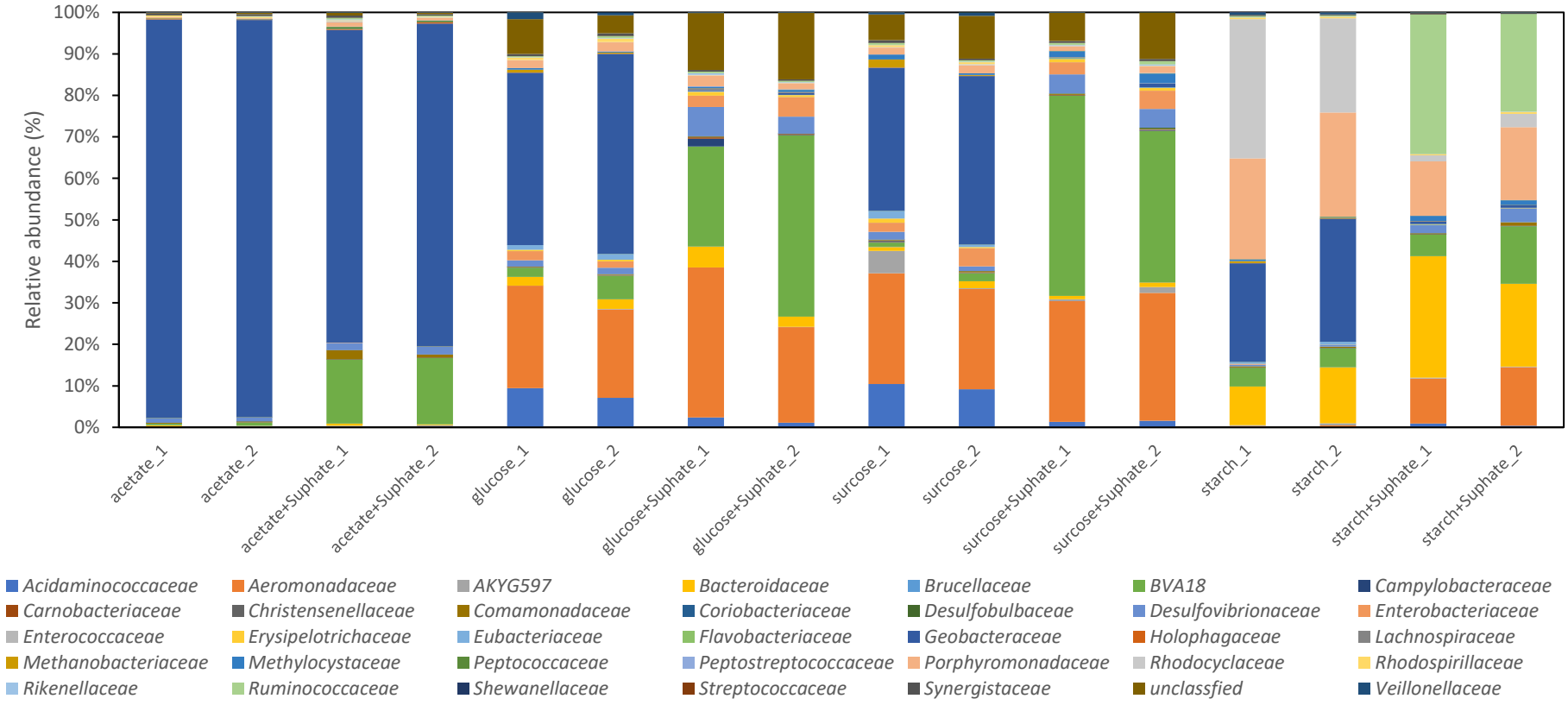

Figure 8-6 The taxonomy of anodic microbial communities at family level in the sulphate-fed BESs and the corresponding controls.

8.10. Appendix J. The calculation of the current loss in the BESs in the presence of sulphate

	Test A (mA)	Test B (mA)	Test C (mA)
Acetate-fed BESs	6.21	6.21	6.21
Acetate+sulphate-fed BESs	2.87	2.89	2.87
Glucose-fed BESs	1.44	1.65	2.29
Glucose+sulphate-fed BESs	1.08	1.20	1.97
Sucrose-fed BESs	1.65	2.85	2.59
Sucrose+sulphate-fed BESs	0.89	1.02	1.56
Starch-fed BESs	0.82	0.89	2.34
Starch+sulphate-fed BESs	0.46	0.41	0.67

Table 8-4 The current production in the tests in the BESs in the presence of sulphate with different feeds.

Current loss caused by the effect of sulphate on electrogenic processes

In acetate+sulphate-fed BESs: 2.89mA-2.87mA=0.02mA

In glucose+sulphate-fed BESs: 1.20mA-1.08mA=0.12mA

In sucrose+sulphate-fed BESs: 1.02mA-0.89mA=0.13mA

In starch+sulphate-fed BESs: 0.41mA-0.46mA=-0.05mA

Current loss caused by the effect of the degradation of complex organics on electrogenic processes

In glucose-fed BESs: 2.29mA-1.44mA=-0.85mA

In glucose+sulphate-fed BESs: 1.97mA-1.08mA=0.89mA

In sucrose-fed BESs: 2.59mA-1.65mA=0.94mA

In sucrose+sulphate-fed BESs: 1.56mA-0.89mA=0.67mA

In starch-fed BESs: 2.34mA-0.82mA=1.52mA

In starch+sulphate-fed BESs: 0.67mA-0.46mA=0.21mA

Current loss caused by the effect of sulphate on anodic biofilm:

In acetate+sulphate-fed BESs: 6.21mA-2.87mA=3.34mA

In glucose+sulphate-fed BESs: 2.29mA-1.97mA=0.32mA

In sucrose+sulphate-fed BESs: 2.59mA-1.56mA=1.03mA

In starch+sulphate-fed BESs: 2.34mA-0.67mA=1.67mA

Current loss caused by the effect of the degradation of complex organics on anodic biofilm

In glucose-fed BESs: 6.21mA-2.29mA=3.91mA

In glucose+sulphate-fed BESs: 6.21mA-1.97mA-0.32mA=3.91mA

In sucrose-fed BESs: 6.21mA-2.59mA=3.62mA

In sucrose+sulphate-fed BESs: 6.21mA-1.56mA-1.02mA=3.62mA

In starch-fed BESs: 6.21mA-2.34mA=3.86mA

In starch+sulphate-fed BESs: 6.21mA-0.67mA-1.67mA=3.86mA

8.11. Appendix K. The electron equivalent of organics

Molecules	Degradation reaction	Electron equivalent per carbon
Glucose	$C_6H_{12}O_6 + 6H_2O = 6CO_2 + 24H^+ + 24e^-$	24/6=4
Pyruvate	$C_3H_4O_3 + 3H_2O = 3CO_2 + 10H^+ + 10e^-$	10/3=3.33
Propionate	$C_3H_6O_2 + 4H_2O = 3CO_2 + 14H^+ + 14e^-$	14/3=4.67
Ethanol	$C_2H_6O + 3H_2O = 2CO_2 + 12H^+ + 12e^-$	12/2=6
Acetate	$C_2H_4O_2 + 2H_2O = 2CO_2 + 8H^+ + 8e^-$	8/2=4
formate	$CH_2O_2 = CO_2 + 2H^+ + 2e^-$	2/1=2

Table 8-5 The electron equivalent of glucose and degradation intermediates and products

8.12. Appendix L. The recipe of trace element solution and vitamin solution

The recipe of trace element solution and vitamin solution (Table 8-6) was according to (Gimkiewicz and Harnisch, 2013).

Trace element solution (mg/L)		Vitamin solution (mg/L)	
Nitriloacetic acid	1500.0	Biotin	2.0
$MgSO_4•7H_2O$	3000.0	Folic acid	2.0
$MnSO_4•2H_2O$	500.0	Pyridoxine hydrochloride	10.0
NaCl	1000.0	Thiamine hydrochloride	5.0
$FeSO_4•7H_2O$	100.0	Riboflavin	5.0
$CoSO_4$	100.0	Nicotinic acid	5.0
$CaCl_2•2H_2O$	100.0	DL-Calcium pantothonate	5.0
$ZnSO_4$	130.0	Vitamin B12	0.1
$CuSO_4•H_2O$	10.0	p-Aminobenzoic acid	5.0
$AlK(SO_4)_2$	10.0	Lipoic acid	5.0
H_3BO_3	10.0		
$Na_2MoO_4•2H_2O$	10.0		

Table 8-6 The recipe of trace element solution and vitamin solution.